Master Thesis

Evaluation of Mature Gas Fields in the Detfurth Formation in Northern Germany for the Possibility of Deploying Wellhead Compression to Extend Economical Natural Gas Production

Written by:
Antonia Thurmaier, BSc
1035315

Advisor:
Univ.-Prof. Dipl.-Ing. Dr. mont. Herbert Hofstätter
Dipl.-Ing. Jürgen Mahr, Wintershall Holding GmbH

Leoben, 13.03.2017

EIDESSTATTLICHE ERKLÄRUNG

Ich erkläre an Eides statt, dass ich die vorliegende Diplomarbeit selbständig und ohne fremde Hilfe verfasst, andere als die angegebenen Quellen und Hilfsmittel nicht benutzt und die den benutzten Quellen wörtlich und inhaltlich entnommenen Stellen als solche erkenntlich gemacht habe.

AFFIDAVIT

I hereby declare that the content of this work is my own composition and has not been submitted previously for any higher degree. All extracts have been distinguished using quoted references and all sources of information have been acknowledged.

Danksagung / Acknowledgement

First of all, I want to thank my advisor from Wintershall Jürgen Mahr. He supported me with information, ideas and he always had an open ear for the challenges that occurred throughout my thesis.

In this sense I thank Wintershall Germany and Alexander Steigerwald for the possibility to write my thesis at the operational gas department. Many thanks to Matthias Schäfer, who was the one in charge to make my thesis possible in the first place. I was provided with information, got insights into the operational business, and my colleagues Wolfgang Jelinek, Torben Sander, Boris Roggelin, Anna Langholf and Ines Felstehausen provided help and guidance when needed.

I would also like to thank my professor Herbert Hofstätter, who provided knowledge and professional support. Especially appreciated is the fact, that he believed in my work and gave me the freedom to develop my own approach.

This is also the time to thank my family. My parents Rosi and Klaudius, my siblings Verena and Alexander, as well as my grandparents Wilma, Josef, Hedwig and Karl, who have always and unconditionally believed in me and the professional path I would ascend. Especially in times when I did not believe in myself anymore it was your unconditional love and support that kept me going.

Last but not least, I thank my boyfriend Stephan for his never ending patience and support.

Kurzfassung

Der Großteil der europäischen Gasfelder befindet sich bereits in ihrer letzten Produktionsstufe, der Tail-End Phase. Bei maturen Gasfeldern treten eine Vielzahl von Problemen auf, wobei die Flüssigkeitsbeladung, das so genannte „Liquid Loading“, eine der größten Herausforderungen darstellt. Darunter versteht man den Prozess, wenn Flüssigkeiten die normalerweise fortlaufend aus der Gasbohrung ausgetragen werden, sich am Fuße des Bohrlochs ansammeln, weil die Geschwindigkeit des produzierten Gases zu niedrig ist um sie kontinuierlich zu Tage zu fördern. Die Folgen reichen von einer Einschränkung in der Produktion bis zu einem kompletten Einschluss des Bohrlochs, im schlimmsten Fall auch des gesamten Reservoirs.

Diese Arbeit beschäftigt sich mit funktionellen Methoden zur Bestimmung von Liquid Loading auch schon in frühen Stadien, wo es oft noch schwer zu erkennen ist. Zusätzlich wurden Möglichkeiten aufgezeigt, zukünftig auftretendes Liquid Loading vorhersagen zu können. Einige etablierte Systeme zur Vorbeugung wurden vorgestellt und die physikalischen Grundlagen der verschiedenen Anwendungen diskutiert.

Es wurden praktische Anwendungsbeispiele aufgezählt, gefolgt von Einschränkungen der Systeme, sowie Vor- und Nachteilen. Diese Arbeit konzentriert sich auf die Anwendung von Bohrlochkopf-Kompression – Wellhead Compression, die eine etablierte Methode zur Entwässerung von Gasbohrungen ist. Eine Verringerung des Bohrlochkopfdrucks erhöht nicht nur die Gasproduktion, sondern verhindert auch das Auftreten von Liquid Loading und erhöht letztendlich auch die förderbaren Gasreserven.

Um Wellhead Compression in den norddeutschen Gasfeldern der Detfurth Formation wirtschaftlich effizient einsetzen zu können, wurde ein Bewertungssystem für mögliche Bohrungskandidaten aufgestellt. Screening - Kriterien wurden eingeführt, um potenzielle Bohrungen objektiv zu evaluieren und so einen idealen Kandidaten für den Feldversuch von Wellhead Compression zu identifizieren.

Die theoretischen Prinzipien der Kompression wurden skizziert und die verschiedenen Kompressortypen, die üblicherweise für Wellhead Compression verwendet werden, wurden beschrieben. Um den idealen Kompressor für die Anforderungen der norddeutschen Gasbohrungen in der Detfurth Formation zu finden, wurde eine Marktanalyse durchgeführt. Zusätzlich zur technischen Bewertung wurde die Wirtschaftlichkeit der Kompressoren analysiert, um zu überprüfen ob die Systeme auch ökonomisch umsetzbar sind.

Abschließend wurden die HSE- relevanten Aspekte im Zusammenhang mit der Anwendung von Wellhead Compression, einschließlich Umwelt-, Anlagensicherheits- und Reputationsaspekten, diskutiert. Am Ende wurde eine Empfehlung für den weiteren Einsatz der Wellhead Compression in den maturen Gasfeldern der Wintershall in Norddeutschland ausgearbeitet.

Abstract

Most gas fields in Europe are already in their last stage of production, the so-called tail-end phase. Several problems arise as the fields mature, liquid loading being one of the main challenges. It explains the process of liquids accumulating at the bottom of the wellbore, leading to a loss in production, potentially resulting in the death of the well or even the reservoir.

This thesis discusses functional methods to identify liquid loading in gas wells even during its early stages, when it is often difficult to recognize. Practical techniques were introduced, which allow one to forecast future liquid loading scenarios, along with the theoretical principles behind them. A variety of techniques to prevent liquid loading was presented. The physical tenets of the diverse systems were discussed.

Furthermore, the practical application principles were introduced, followed by restrictions of the systems, identifying advantages and disadvantages along the way. This thesis focusses on the application of wellhead compression, which is an established gas well deliquification method. Lowering the wellhead pressure does not only increase the gas production, but also prevents the occurrence of liquid loading, potentially enhancing the recoverable gas reserves.

A screening of possible well candidates was conducted to evaluate an eventual future application of wellhead compression for the gas fields of Wintershall in the Detfurth formation in northern Germany. Several screening criteria were introduced to rank the potential well candidates objectively in order to identify an ideal trial well for wellhead compression. The theoretical principles of compression were outlined and the different compressor types commonly used for wellhead compression were described. A market analysis was conducted to explore various compressor systems in order to find an ideal fit for the gas wells. In addition to the technical evaluation, an economic analysis was carried out to verify whether the systems are commercially feasible or not.

Finally, the HSE- relevant aspects related to applying wellhead compression, including environment, plant safety and reputation aspects, were discussed. At the end a recommendation for further deployment of wellhead compression in Wintershall’s mature gas fields in northern Germany was drafted.

Table of content

Page

1 Introduction

Wintershall Holding GmbH Germany operates gas fields in northern Germany, producing sweet gas from the Detfurth formation, which were mainly discovered between 1950 and 1970. By now, most of them show low productivity, hence tail-end production. These low production rates cause liquid loading of the wells, which is the accumulation of fluids at the bottom of the wellbore.

This process is critical for the life of the well, because if liquid cannot be produced to surface, a fluid column builds up at the bottom of the wellbore, and when the pressure of this column overcomes the acting reservoir pressure, the well is eventually killed.

To overcome this liquid loading problem in order to extend the economically feasible life of the wells in the fields Düste, Staffhorst and Barrien, the concept of wellhead compression will be applied. It is the aim of this thesis to screen existing wellhead compression systems and explore their potential application in the gas fields of Wintershal

2 Theory

2.1 Gas Reservoirs

Gas reservoirs hold a mixture of hydrocarbons which only exist in gaseous state at initial reservoir pressure**.** [1] They can be divided into three groups: dry gas, wet gas and retrograde-condensate gas.

Dry and wet gas are produced from single phase gas reservoirs. During production the pressure declines along the path A-A_1 (Figure 1) but the reservoir maintains its gaseous state throughout its life. The production conditions for dry gas are typically outside the two-phase envelope, so no liquid is produced at all. [2] During the production of wet gas, the pressure and temperature conditions within the wellbore fall below the dew point line and liquids form in the tubing or in surface facilities (Figure 1, path A-A_2).

Retrograde-condensate gas is originally in a single-phase gaseous state in the reservoir. As the reservoir pressure decreases and drops under the dew point line (Figure 1, point B_1), condensed liquid forms in the reservoir, which adheres to the walls of the pore spaces of the rock and becomes immobile. Retrograde condensation continues until point B_2, where the maximum liquid volume is reached. Decreasing the reservoir pressure further, some of the liquid that developed in the reservoir vaporizes again until the abandonment pressure (Figure 1, point B_3) is reached. [3]

Gas reservoirs are produced by gas expansion, depletion drive, aquifer water drive or a combination of them. The recovery efficiencies for depletion drive reservoirs can reach 80 to 90%, whereas the recovery efficiency for water drive gas reservoirs is in the range of 50 to 60%, due to bypassed gas. [4]

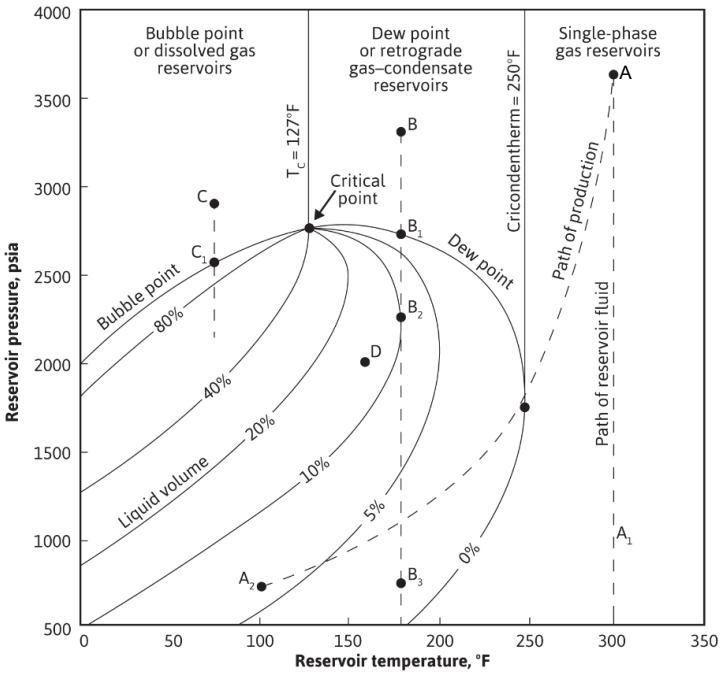

Figure 1: Pressure- temperature phase diagram of a reservoir fluid [3],

2.2 Material Balance

The material balance equation is used to predict the gas in place in gas reservoirs. It is based on the principle of conservation of mass and results in a zero-dimensional equation describing the cumulative production as a function of the average reservoir pressure and the fluid properties. The term “zero-dimensional” indicates, that the reservoir fluids are assumed to be in equilibrium, exhibiting constant PVT properties and a constant average pressure throughout the reservoir, in an environment of uniform fluid saturation. Furthermore, it does not include the geometry of the reservoir, the drainage area, nor the position and orientation of wells. [5]

For gas reservoirs, the following equation can be written as:

$$Cumulative\ fluid\ production = gas\ expansion + formation\ expansion + water\ influx \quad (1)$$

Where the cumulative fluid production includes the produced gas and water:

$$Cumulative\ fluid\ production = G_P * B_g + W_p * B_w \quad (2)$$

Where

G_P, W_P produced gas, water, [Sm^3]

B_g, B_w formation volume factor for gas and water, [m^3/Sm^3]

The right side of the equation states the principle drive mechanisms of the gas reservoir, which are calculated as follows:

$$Gas\ expansion = initial\ gas\ in\ place - remaining\ gas = G_i - \frac{G_i * B_{gi}}{B_g} \quad (3)$$

Where

G_i initial gas in place, [Sm^3]

B_g, B_{gi} formation volume factor for gas at given pressure or at initial pressure, [m^3/Sm^3]

The formation expansion illustrates the expansion of the pores and can be expressed as:

$$Formation\ expansion = c_f * (PV) = c_f * \frac{G_i * B_{gi}}{1 - S_w} * \Delta p \quad (4)$$

Where

c_f formation compressibility, [1/Pa]

PV pore volume, [m^3]

S_w water saturation, [ ]

Δp change in pressure, [kPa]

$$Water\ influx = W_e * B_w \tag{5}$$

Where

W_e cumulative water influx, [Sm^3]

Combining the terms, the generalized form of the material balance equation can be derived as:

$$G_P * B_g + W_p * B_w = G_i * \left[B_g - B_{gi}\right] + \frac{G_i * B_{gi}}{1 - S_w} * \left[c_w * S_{wc} + c_f\right] * \Delta p + W_e * B_w \tag{6}$$

Where

c_w water compressibility, [1/Pa]

S_{wc} connate water saturation, [ ]

Assuming that the gas is only produced due to volumetric expansion, the equation can be simplified and rewritten as:

$$G_P * B_g = G_i * \left[B_g - B_{gi}\right] \tag{7}$$

Substituting B_g with

$$B_g = 0{,}350958 * \frac{z * T}{p} \tag{8}$$

Where

z compressibility factor, [ ]

T temperature, [°K]

p pressure, [kPa]

The following equation can be rearranged as:

$$G_p = G_i * \left[1 - \frac{\frac{p}{z}}{\frac{p_i}{z_i}}\right] \tag{9}$$

or,

$$\frac{p}{z} = \frac{p_i}{z_i} * \left[1 - \frac{G_p}{G_i}\right] \tag{10}$$

Plotting the production data over pressure vs. compressibility factor, the following diagram (

Figure 2) is attained. The initial gas in place can be estimated through a linear extrapolation of the available data points. Additionally, the maximum recoverable gas that can be produced having a fixed abandonment pressure can be calculated. Although this method is popular to use when it is known, that the main drive mechanism of the gas reservoir is volumetric expansion; when other mechanisms are occurring, this plot does not show any sensitivity to the simultaneous occurrence of other drive mechanisms. [6]

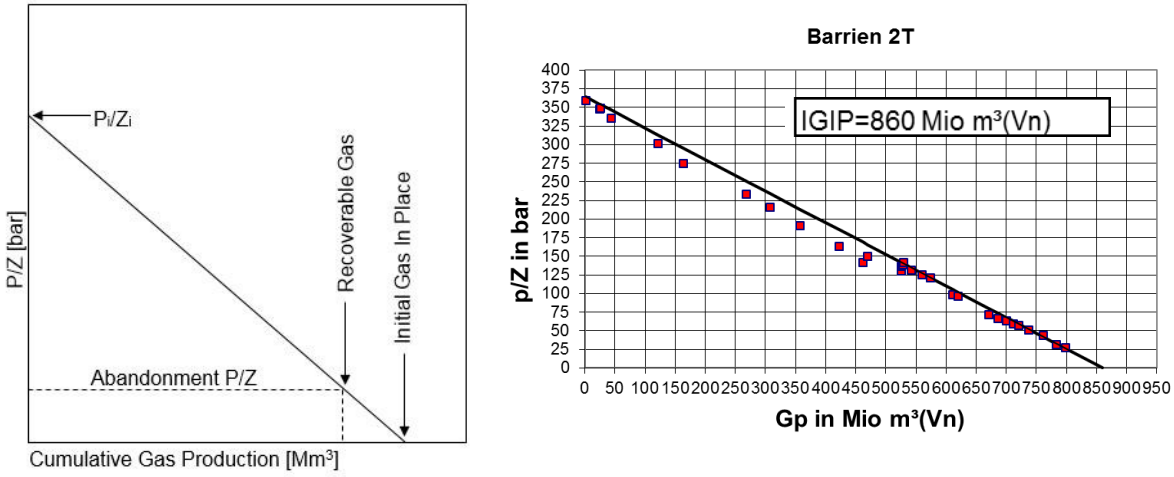

Figure 2: Plot of p/Z versus cumulative produced gas: left the schematic diagram, on the right the p/Z plot of the gas field Barrien 2T (for the location in the field see Appendix A). Vn stands for standard conditions (1 atm and 15,5°C)

2.3 Production Phases of a Field

The production phases of a gas field can be broken down into three stages, the build-up, plateau and decline phase, which includes the tail-end production (Figure 3).

The build-up phase includes the time of development, the first gas and the time after, when the production rate increases significantly. Initially the flowrates of the wells in a gas reservoir are only restricted by the surface equipment used. The produced gas is under such high pressure at surface that it does not require additional compression before being fed into the high pressure natural gas network.

The plateau phase starts, when the production rate settles at a constant level. To keep this phase up as long as possible, additional wells are drilled to maintain this production rate. During the phase, centralized compressor stations are installed to produce and transport the gas at economical and efficient conditions.

The third phase is the decline phase, which terminates in the tail-end production, where the production rate decreases gradually until the economic limit is reached. During this phase the reservoir pressure declines, resulting in a reduction of the flowrate, hence also the gas velocity. One problem in this phase is that the centralized compressor stations require a certain entry

pressure, given by a fixed compression ratio, which might not be achievable by all the wells which feed the compressor. It is the main challenge to elongate the tail-end production phase and keep the production rate above the economic limit for as long as possible. [7] One possible solution is the installation of wellhead compression systems, which are locally mounted, providing an additional compression stage and increasing the production rate.

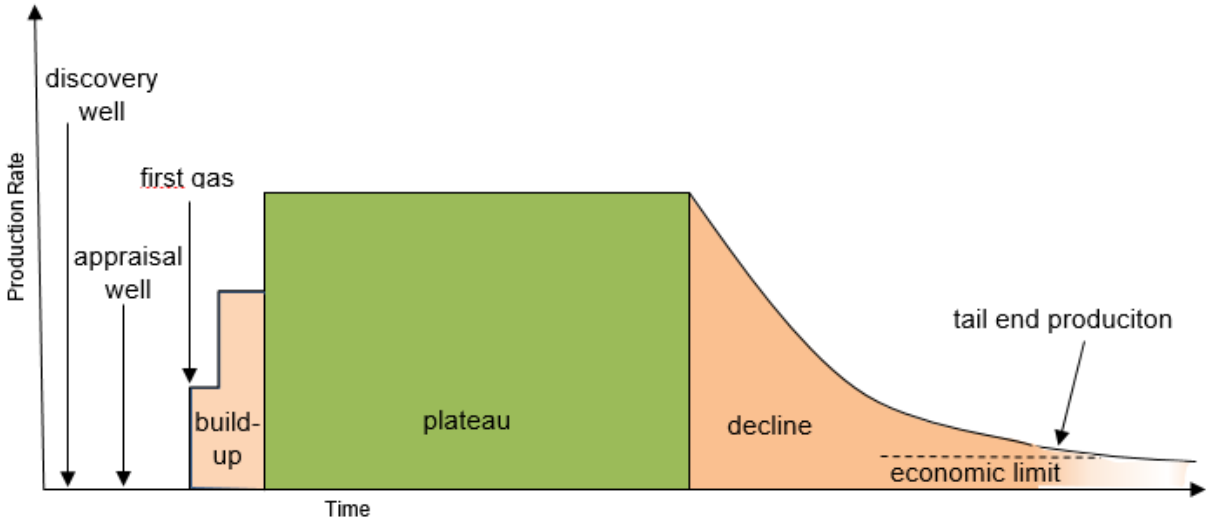

Figure 3: Generalized life cycle of a well

2.4 Multiphase Flow

In gas wells, multiphase flow describes the simultaneous flow of multiple phases with different densities. [8] In order to understand the principle behind liquid loading, it is essential to comprehend how gas and liquid behave when flowing upwards together in the production tubing. For vertical upward two-phase flow, there are four flow regimes to be distinguished by the decreasing gas rate. So at any given time, one or more flow regimes are present. [9]

Annular - Mist Flow: at high gas rates, gas is the continuous phase. The liquid is mostly present as mist, and as a thin layer on the inner tubing wall. The pressure gradient in this flow regime is determined through the gas.

Slug - Annular Transition: decreasing the gas rate, the flow changes from continuous gas phase to continuous liquid phase. Liquids may still be transported as mist, but the pressure gradient is already significantly influenced by the liquid.

Slug Flow: the gas forms bubbles that combine to large slugs in the continuous liquid phase. When the flowrate is too low, the liquid film around the slugs falls downwards. In this flow regime the pressure gradient is affected by gas and liquid flow.

Bubble Flow: the tubing is almost completely filled with liquid. The free gas is present as small bubbles ascending in the liquid. The pressure gradient is entirely determined by the liquid; the bubbles merely reduce the density, but insignificantly.

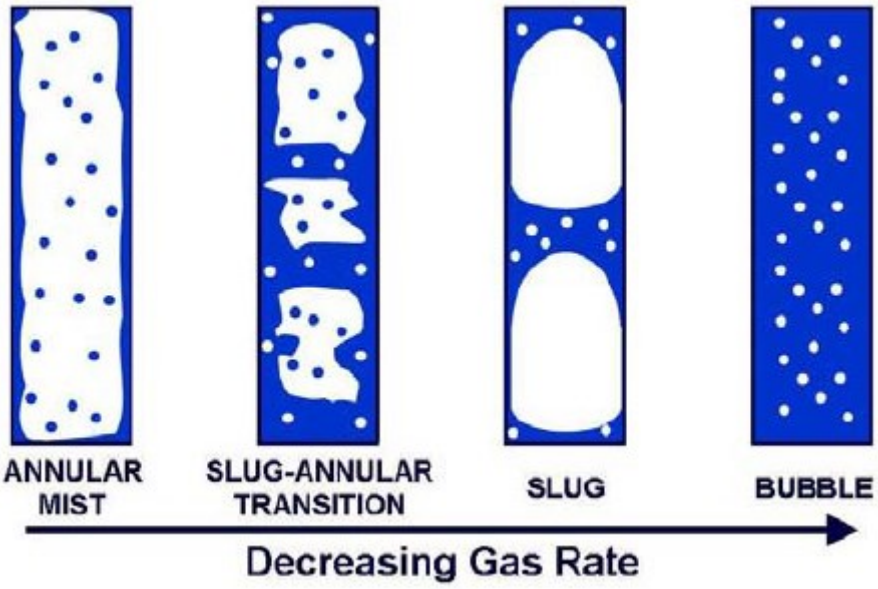

Figure 4: The different flow regimes of a vertical flowing gas well [9]

2.5 Critical Gas Velocity

The critical velocity of gas in the production tubing is defined as the minimum velocity which is needed to move liquid upwards. [9]

$$v_{actual,gas} \geq v_{critical,gas} \rightarrow no\ liquid\ loading\ occurs \tag{11}$$

Literature shows different approaches regarding the methods to predict this velocity adequately. There are two fundamental models used: the liquid droplet fallback model and the liquid film reversal model. Turner was the first to address this topic and evaluated the two flow models using a large database of field data. [10] He came to the conclusion, that the droplet model yielded a better model to predict the critical velocity.

All models discussed below enumerate the critical velocity, hence flowrate -based on the conditions at the wellhead, which might not be representative of the liquid loading scenario of the whole well [11]. If information concerning the in-situ conditions of the well downhole is available, a profile of the critical velocity should be created along the entire well path. [12] [9] Sutton identifies the wellbore geometry and conditions (pressure, temperature) and the fluid properties (density of gas and liquid, surface tension) as the main factors influencing the critical velocity. He also proposes to use the Turner model for all pressure applications [12]. It is stated that one should utilize the wellhead conditions to calculate the critical velocity for high-pressure applications above 70 bar and the bottomhole-conditions for wellhead pressures below 70 bar.

This might in fact prove to be challenging to accomplish, because bottomhole-conditions are not always measured.

2.5.1 Liquid Droplet Fallback Model

The droplet fallback model was first introduced by Turner [10]. His model assumes free flowing liquid in the wellbore in the form of droplets, which are suspended in the gas stream. He developed it by correlating his model with field data from nearly vertical wells.

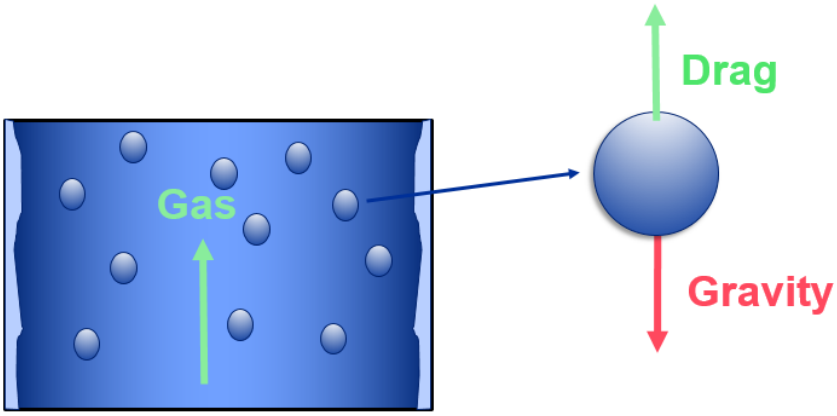

Figure 5. Liquid droplet transported in a vertical gas well [9]

For his model, Turner used fluid flow equations developed by Hinze who stated, that “liquid drops moving relative to a gas are subjected to forces that try to shatter the drop, while the surface tension of the liquid acts to hold the drop together.” [13] Therefore, a droplet is affected by two forces: gravitational (F_G) and drag (F_D). While the gravitational force is pulling the droplet down, the drag force generated by the upward flowing gas pushes the droplet upwards. If the velocity of the gas is above the critical velocity the droplets are continuously carried to surface. If not, they fall down and accumulate at the bottom of the wellbore.

$$F_G = \frac{g}{g_c} * (\rho_l - \rho_g) * \frac{\pi * d^3}{6} \tag{12}$$

$$F_D = \frac{1}{2 * g_c} * \rho_g * C_D * A_D * (v_t - v_D)^2 \tag{13}$$

Where

g	gravitational constant, (32,17 ft/s^2) ‘
g_c	gravitational conversion constant, (32,17 lbm*ft/lbf*s^2)
ρ_l, ρ_g	density of liquid or gas, [lbm/ft^3]
d	diameter of droplet, [in]
C_D	drag coefficient, [ ]
A_D	area droplet, [in^2]

v_t critical velocity, [ft/s]
v_D droplet velocity, [ft/s]

According to this theory, at the critical velocity the droplet has a velocity of zero, meaning these two forces are equal to each other.

$$\frac{g}{g_c} * (\rho_l - \rho_g) * \frac{\pi * d^3}{6} = \frac{1}{2 * g_c} * \rho_g * C_d * A_d * (v_C - v_d)^2 \quad (14)$$

After transforming the equation, the critical velocity can be calculated:

$$v_t = \sqrt{\frac{4 * g * (\rho_l - \rho_g) * d}{3 * \rho_g * C_D}} \quad (15)$$

Hinze proved, that the droplet diameter is dependent on the gas velocity and can be expressed in terms of the dimensionless Weber number:

$$N_{WE} = \frac{v_t^2 * \rho_g * d}{\rho_l * \sigma} \quad (16)$$

Where
N_{WE} Weber number, [ ]
σ surface tension, [dynes/cm]

Hinze also showed, that the droplet shatters when N_{WE} is greater than 30; thus solving the equation for a value of 30 for the largest droplet diameter gives:

$$d = 30 * \frac{g_C * \sigma}{\rho_g * v_t^2} \quad (17)$$

Turner assumed a drag coefficient C_D of 0.44 valid for turbulent conditions. Substituting the droplet diameter found from the Weber number, the drag coefficient and converting surface tension from 1 lbf/ft to 0.00006852 dyne/cm gives the equation below:

$$v_t = 1{,}59 * \frac{\sigma^{\frac{1}{4}} * (\rho_l - \rho_g)^{\frac{1}{4}}}{\rho_g^{\frac{1}{2}}} \quad (18)$$

Assumptions			
ρ_l	Water Density	67	lb/ft³
γ_G	Gas Gravity	0,6	
T	Temperature	120	°F
M	Molecular Mass Air	28,97	g/mol
R	Universal Gas Constant	10,73	psi*ft³/(lb*mol*°R)
ρ	Surface Tension	60	dynes/cm

Using the real gas law, the gas density is given by:

$$\rho_G = 2{,}715 * \gamma_G * \frac{p}{(460 + T) * Z} = 0{,}0031 * p \tag{19}$$

Where

Z Z – factor, [ ]

With using this correlations and values, the equations form as:

$$v_{t,condensate} = \frac{3{,}37 * (45 - 0{,}0031 * p)^{\frac{1}{4}}}{(0{,}0031 * p)^{\frac{1}{2}}} \tag{20}$$

$$v_{t,water} = \frac{4{,}43 * (67 - 0{,}0031 * p)^{\frac{1}{4}}}{(0{,}0031 * p)^{\frac{1}{2}}} \tag{21}$$

Where

p pressure, [psi]

Turner decided to adjust the constants of the equations by 20% to match the compared field data optimally. The adjusted final equations for the critical velocity are displayed below. In the case that water as well as condensate is produced, Turner recommends to use the critical velocity of water, because it has a higher density, hence requires a higher velocity.

$$v_{t,condensate} = \frac{4{,}04 * (45 - 0{,}0031 * p)^{\frac{1}{4}}}{(0{,}0031 * p)^{\frac{1}{2}}} \tag{22}$$

$$v_{t,water} = \frac{5{,}32 * (67 - 0{,}0031 * p)^{\frac{1}{4}}}{(0{,}0031 * p)^{\frac{1}{2}}} \tag{23}$$

From the critical velocity, the critical gas flowrate can be calculated:

$$q_t = \frac{C * p * v_t * A}{T * Z} \tag{24}$$

Where

C constant, dependant on liquid (water or condensate)

q_t critical flowrate, [Mio scf/d]

A flow area, [in^2]

With

$$A = \frac{\pi * d_{ti}^2}{4 * 144} \tag{25}$$

Where

d_{ti} tubing inside diameter, [in^2]

Even though the critical velocity is the controlling factor, the critical gas flowrates required for transporting water or condensate can be calculated for a more practical approach. Similar as for the critical velocity above, when both, condensate and water are present, the higher flowrate, the water correlation, should be used.

$$q_{t,condensate} = \frac{0{,}067 * p * d_{ti}^2 * (45 - 0{,}0031 * p)^{\frac{1}{4}}}{(T + 460) * Z * (0.0031 * p)^{\frac{1}{2}}} \tag{26}$$

$$q_{t,water} = \frac{0{,}089 * p * d_{ti}^2 * (67 - 0{,}0031 * p)^{\frac{1}{4}}}{(T + 460) * Z * (0{,}0031 * p)^{\frac{1}{2}}} \tag{27}$$

The Turner droplet model is reliable for wells with a wellhead flowing pressure above 70 bar (1000 psi). To be also able to predict the critical flowrate for lower surface pressures, Coleman established a similar relationship. [14] To adjust and verify the new model, he extensively tested it on actual field data. The Coleman model basically uses equations identical to the Turner droplet model, with the same default values and the only difference being, that the 20% adjustment was undone. He assumed that surface tension, gas density and temperature do not have a significant effect on the critical velocity, stating that the main parameters determining this value are the diameter of the wellbore and the pressure.

$$v_{t,condensate} = \frac{3{,}37 * (45 - 0{,}0031 * p)^{\frac{1}{4}}}{(0{,}0031 * p)^{\frac{1}{2}}} \tag{28}$$

$$v_{t,water} = \frac{4{,}43 * (67 - 0{,}0031 * p)^{\frac{1}{4}}}{(0{,}0031 * p)^{\frac{1}{2}}} \tag{29}$$

$$q_{t,condensate} = \frac{0{,}056 * p * d_{ti}^2 * (45 - 0{,}0031 * p)^{\frac{1}{4}}}{(T + 460) * Z * (0{,}0031 * p)^{\frac{1}{2}}} \tag{30}$$

$$q_{t,water} = \frac{0{,}074 * p * d_{ti}^2 * (67 - 0{,}0031 * p)^{\frac{1}{4}}}{(T + 460) * Z * (0{,}0031 * p)^{\frac{1}{2}}} \tag{31}$$

Turner and Coleman assume, that the liquid droplets in the wellbore are perfect spheres, whereas in reality, the free falling droplets are deformed. Li's model took the basic equations of the Turner model as well as the deformation of the droplets into account. [15]

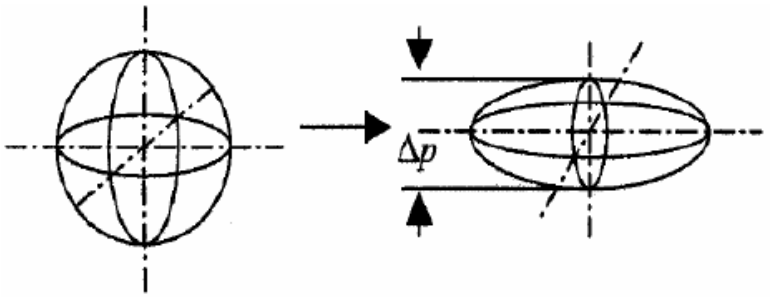

Figure 6: Change of shape when liquid drop enters a high velocity gas stream [15]

The deformed, flattened droplet has a higher effective area, and therefore needs a lower critical velocity and rate to be lifted to surface.

$$v_{t,water} = \frac{2{,}5 * (67 - 0{,}0031 * p)^{\frac{1}{4}}}{(0{,}0031 * p)^{\frac{1}{2}}} \tag{32}$$

$$q_{t,water} = \frac{0{,}042 * p * d_{ti}^2 * (67 - 0{,}0031 * p)^{\frac{1}{4}}}{(T + 460) * Z * (0{,}0031 * p)^{\frac{1}{2}}} \tag{33}$$

Using the conversion factors below, the critical velocity and critical flowrate can be computed in SI units.

Critical velocity:	1 [ft/s] → 0,305 [m/s]
Critical flowrate :	1 [Mio scf/d] → 0,028 [Mio m^3/d]

2.5.2 Liquid Film Model

The second approach to predict the critical velocity assumes, that the fluid is transported as a liquid film along the pipe walls. If the actual gas velocity is higher than the critical velocity, the liquid velocity profile in the film is headed upwards, in the same direction as the gas flow [11]. When the velocity of the gas is lower than its critical velocity, parts of the velocity field change its direction. In the middle section of the well the fluid film still travels upwards, but further from the centre and close to the pipe wall, the velocity field of the fluid points downwards, initiating the loading of the well (Figure 7).

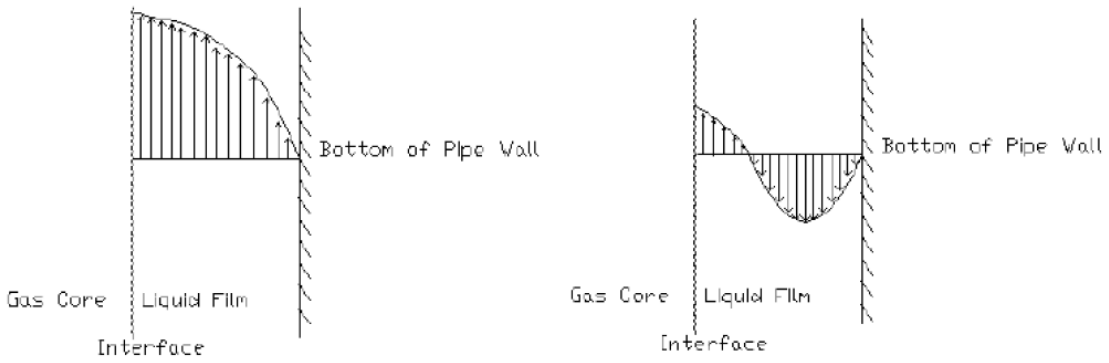

Figure 7: Velocity profile of the liquid film at different gas flowrate s [16]

While the droplet fallback model is applicable for wells which are nearly vertical, Yuan et al investigated and concluded, that the reverse liquid film model should be used for deviated wells. He also stated, that the critical velocity reaches its maximum at a deviation of 30 to 60°, and decreases thereafter until the horizontal is reached (Figure 8).

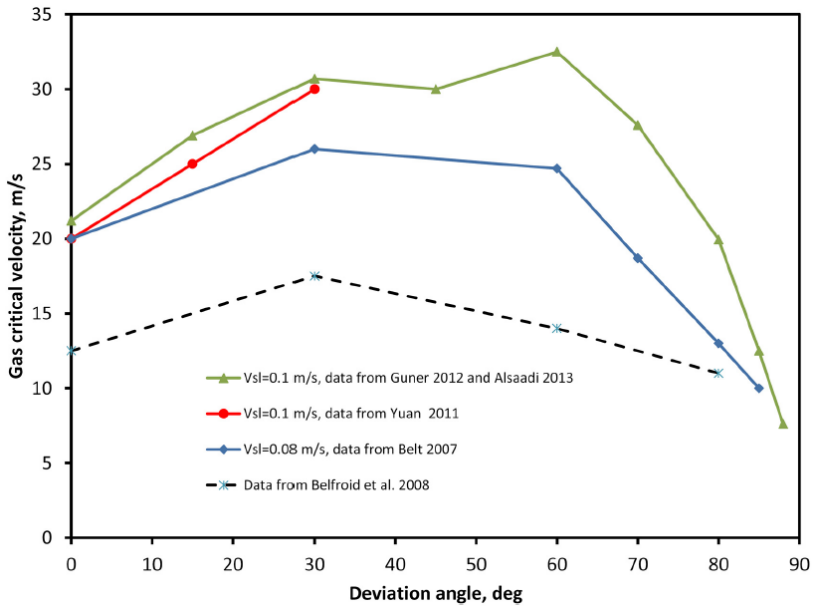

Figure 8: Comparison of critical gas velocities for different well deviation angles which are based on the reverse liquid film model [11]

3 Liquid Loading

Liquid loading of gas wells explains the process by which the flowrate and hence velocity of the gas becomes too low to carry the produced liquid to surface, resulting in liquid accumulation at the bottom of the wellbore. The liquid column causes an additional hydrostatic backpressure against the formation, which lowers the available transport energy. [14] [17]

The existing liquid phase, in the form of free formation water, condensed water or condensed hydrocarbons, has different origins. Free water might come in contact with the well from a water carrying layer below the produced gas zone, or from an aquifer which supports the reservoir. Condensed water as well as condensed hydrocarbons appear when the temperature and pressure conditions in the well drop below the dew point line (see Figure 1). [9]

Figure 9 shows the different stages of liquid loading in a gas well. At Figure 9 (a), the gas flowrate (q_g) exceeds the critical flowrate (q_t), so the produced fluid is transported to surface by the gas in a steady-state annular mist flow behaviour.

As the gas velocity, and hence flowrate decreases over time due to a depleting reservoir pressure, q_g will eventually fall below q_t. Starting at that point (Figure 9 (b)), the liquid carried out along with the gas will not be produced to surface anymore, but drops and accumulates in the wellbore as an aerated column, which causes the pressure gradient to increase in this region.

The accumulated column acts as a downhole choke, which decreases the effective flowrate for the gas phase. Due to the fact, that the gas velocity is indirectly proportional to the flow area, the velocity of the gas increases. The narrowed flow area leads to a larger pressure drop across the arisen fluid column. The pressure drop will increase until the downstream pressure is able to push the liquid up the wellbore, identifiable on surface as slug flow. A well cycles between loading liquid and blowing up the liquid slug as long as the reservoir pressure can overcome the required blow up pressure.

As soon as the hydrostatic pressure of the liquid column is overcoming the reservoir pressure, the gas well starts to load-up completely (Figure 9 (c)). The flow regime shifts from slug flow to bubble flow and the bottomhole pressure in the well increases due to the arisen liquid column. A significantly reduced amount of free gas still makes it through the liquid column and rises in the production tubing, but now lacks the ability to carry liquid with it. As the pressure gradient in the tubing increases, the additional back pressure acting on the formation grows accordingly. As soon as this pressure balances out with the reservoir driving forces, the well is not able to produce gas anymore and eventually dies. [14]

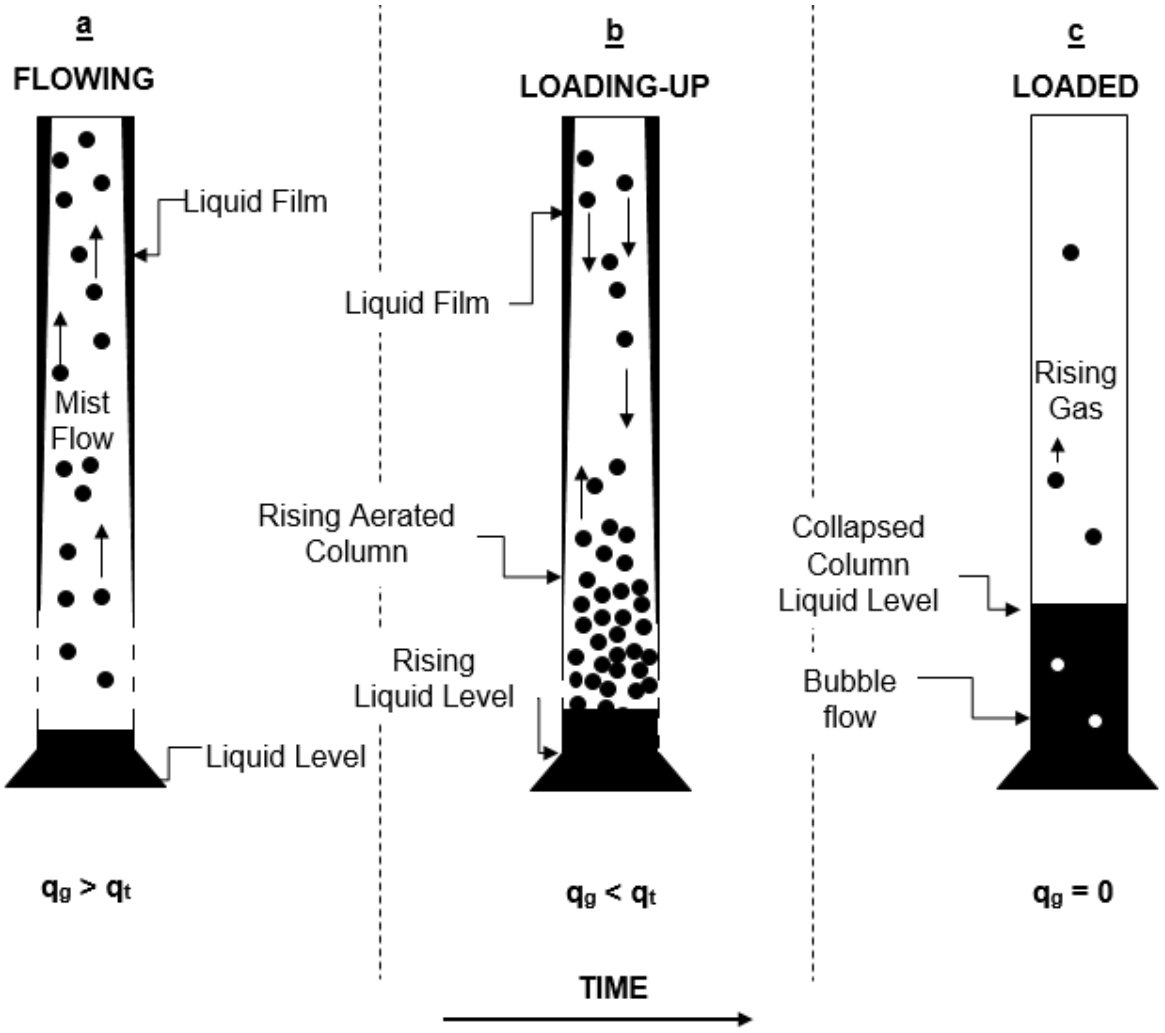

Figure 9: Stages of gas well load-up

3.1 How to Recognize Liquid Loading

Typically, during the life of a gas well, the volume of liquids present in the wellbore increases, while the volume of produced gas decreases. Therefore, the velocity of the gas is also reduced, as is its ability to transport fluid to the surface, thus leading to an accumulation of liquids in the wellbore, which results in a variety of problems. Additional factors which contribute to liquid loading include a high drawdown, high wellhead pressure, poorly designed completions, low GLR (gas liquid ratio), leaks and channeling and a change in the flow regime. The consequences might include permanent damage to the reservoir, a decrease in the gas production or even the eventual death of the well. [9]

Liquid loading is not always entirely observable, because a loaded well may still produce gas for a long time. However, if liquid loading can be recognized at early stages and reduced or even prevented, an economically sufficient production rate can be restored. Typical symptoms that indicate liquid loading are discussed below. [18]

3.1.1 Detect and Monitor Flow Regime on Surface

Careful monitoring of flow parameters and the flow regime at the wellhead is a common method to detect liquid loading. When liquids are loading at the bottom of the wellbore and the velocity of gas drops below the critical value concerning the transport of liquids to surface, typically a slug flow regime occurs. [9] Slug flow can be detected at the free-water-knock-out separator by monitoring the liquid level (Figure 10). Because of the intermitted production of water torrents, the curve shows peaks and the level rises significantly. The liquid level can be monitored and controlled through a variety of technologies including ultrasonic or laser level transmitters.

The monitoring of wellhead pressure and flowrate can also indicate the occurrence of liquid loading. When both values decrease at the same time, liquid loading might be present. When there is no liquid (free or condensed water, condensate) produced with the gas, it is also a strong indication that the well is loaded.

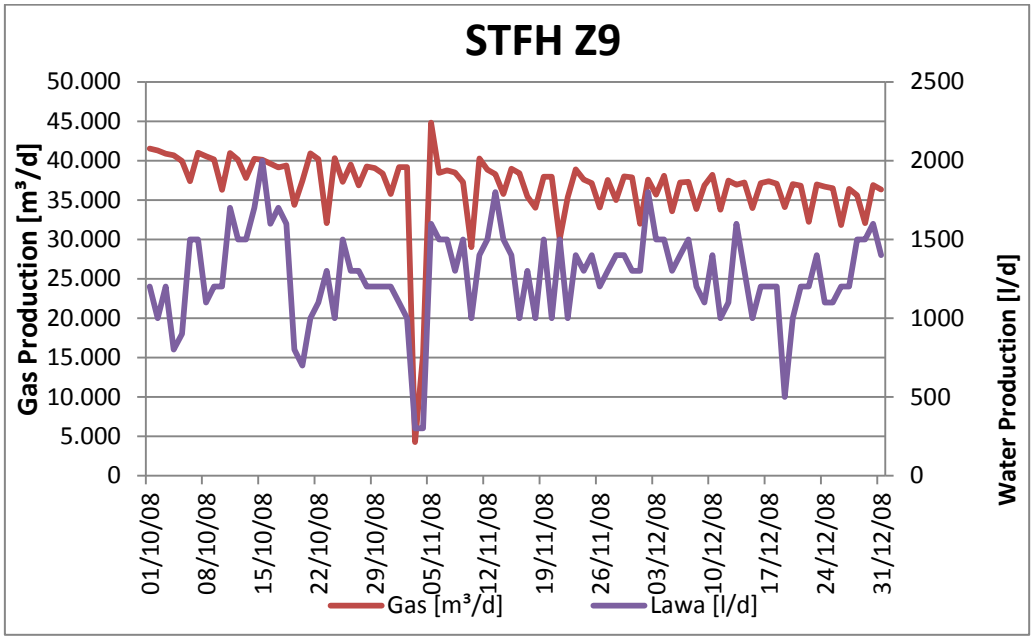

Figure 10: Gas and water production of well Staffhorst Z9. The figure shows, that the gas production decreases over time and a strong fluctuation of produced liquid with the gas, which indicates slug flow.

3.1.2 Decline Curve Analysis

An accurate analysis of the decline curve of a gas well can be a useful tool to reveal downhole flow problems, because any changes in the overall predicted shape of well decline curves may be an indication of liquid loading. Normally the average production decline curve is a smooth, exponential curve as the reservoir depletes over time (Figure 11). Fluctuations of the produced gas as shown in Figure 10, or steeper slopes compared to the actual decline curve might indicate liquid loading, causing the reservoir to deplete much earlier than forecasted. [9]

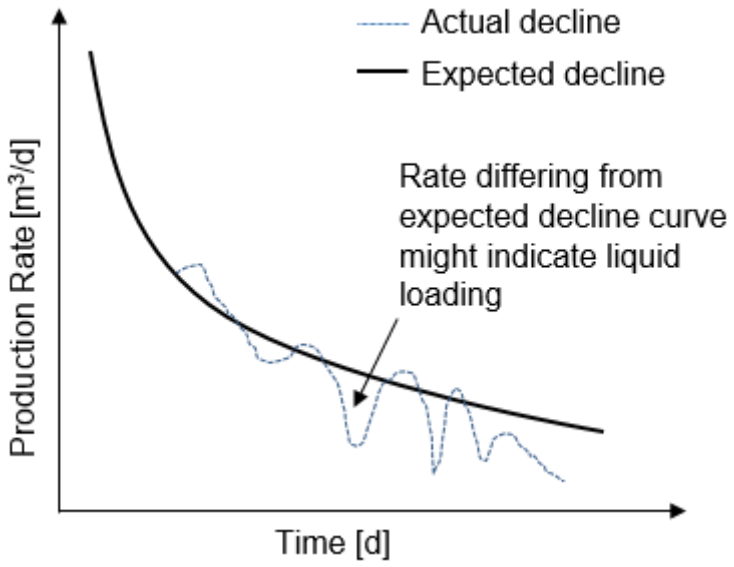

Figure 11: Decline curve analysis schematic [9]

3.1.3 Pressure Survey Investigating Liquid Level

One of the most precise ways to determine the liquid level inside a tubing are flowing or static well pressure surveys. Mounted downhole gauges measure the pressure and the corresponding measured depth of the well either during flow or shut-in condition of the well. The data is used to calculate the pressure gradient, which is a direct function of the density of the medium and the depth (Figure 12, Figure 13). Because gas has a significantly lower density compared to water or condensate, the liquid level can be estimated accurately by spotting the sharp bend in the gradient curve. When the liquid level lies above the perforations, the well suffers from liquid loading. [9]

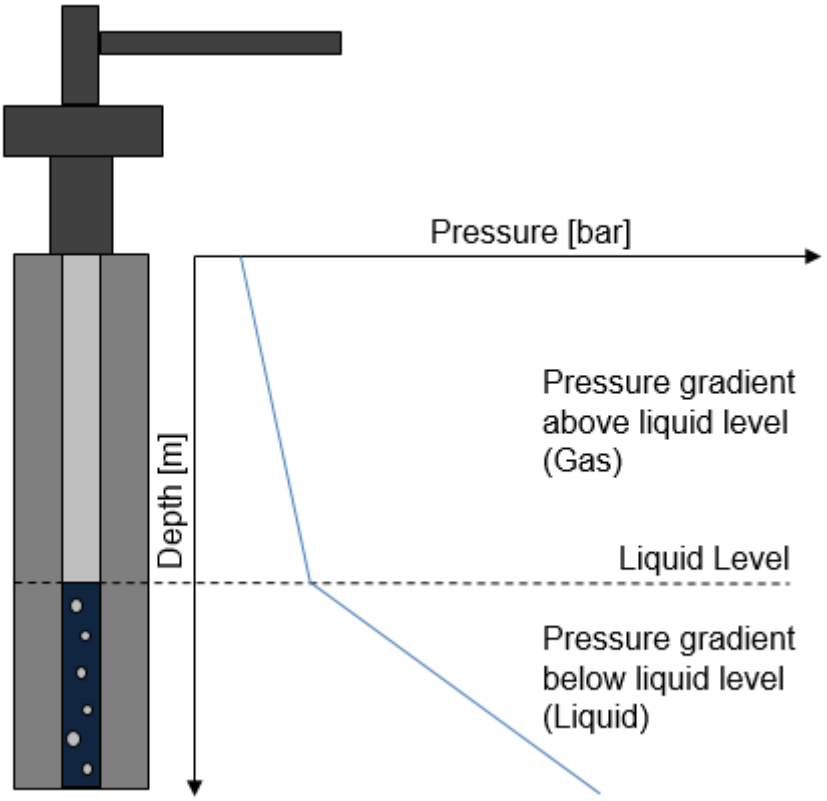

Figure 12: Schematic pressure survey

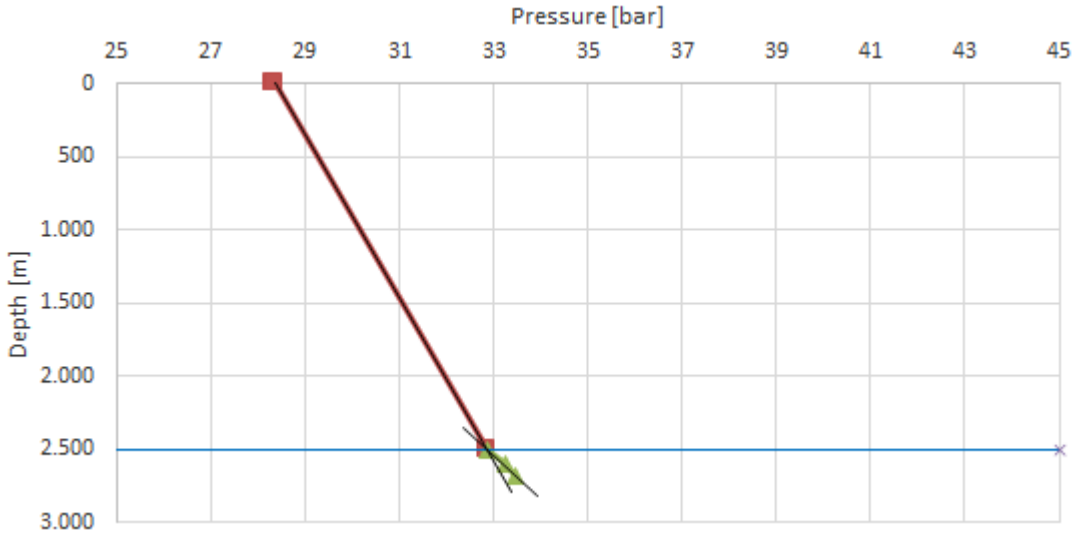

Figure 13: Static pressure survey of Staffhorst Z4 showing the gas water contact (GWC) at about 2500 m depth (MD). The shut – in pressure measured at the wellhead was 28,3 bar, the highest measured pressure in 2680 m MD was 33,4 bar.

3.2 Forecasting Liquid Loading with Nodal Analysis

Nodal analysis proofs to be a valuable tool to identify liquid loading. Typically, gas has to flow against many flow restrictions to reach the surface separator. Nodal analysis divides the system into two sub-systems at a so-called “Nodal point”.

The Nodal point is commonly set at the top depth of the perforations. The inflow system covers the gas flow from the reservoir to the Nodal point, while the outflow system includes the pressure losses from the Nodal point to a set surface pressure point, often the separator. [9]

Figure 14 shows a typical example of a nodal analysis result. The intersection between the inflow and outflow curve determines the operating point, hence the achievable flowrate of the system. Both curves are calculated using single or multiphase flow correlations to obtain the pressure losses associated with each component of the system.

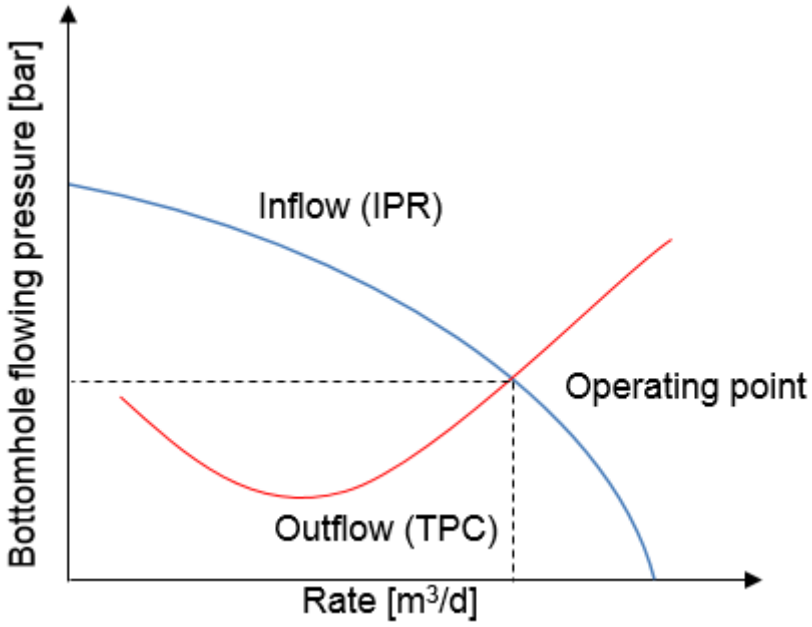

Figure 14: System Nodal Analysis

3.2.1 Inflow Curve

The reservoir inflow performance rate (IPR), also called deliverability curve, connects the production rate with the bottomhole flowing pressure (p_{wf}). The pressure differential forms between the reservoir and the Nodal point, where pressure losses appear due to the reservoir matrix, perforations, completion and tubing. Figure 15 shows the typical form of an IPR curve, which is unique for every well. The absolute open flow (AOF) shows the maximum possible flowrate, but due to the fact that p_{wf} can never be zero, it is only a theoretical, calculated value. In fact does p_{wf} hinge from the wellhead pressure (p_{wh}), which is controlled by operational decisions, e.g. choke management.

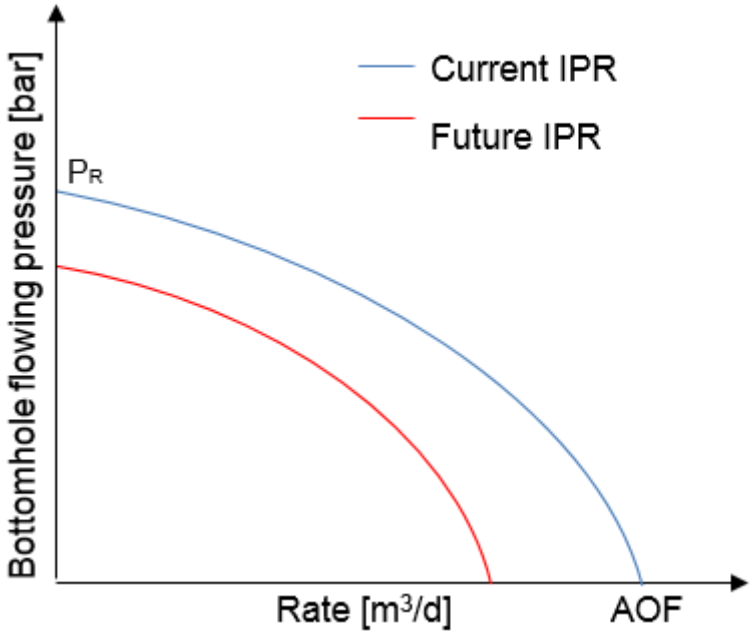

Figure 15: Typical IPR curve

The simplified, commonly used mathematical relationship to calculate the IPR curve is known as “gas well backpressure equation”, which assumes radial flow of the gas in a well perfectly centered within the well drainage area without rate dependent skin.

$$q = C * (\overline{p_r^2} - p_{wf}^2)^n \tag{34}$$

Where

q gas flowrate , [m^3/d]

C performance coefficient, calculated from effective permeability, stratigraphic reservoir thickness, gas viscosity, gas compressibility factor, temperature, reservoir drainage radius, wellbore radius and total skin

$\overline{p_r}$ average reservoir pressure, [kPa]

p_{wf} well flowing pressure, [kPa]

n deliverability exponent, 0,5 < n < 1, where n=0,5 stands for non-Darcy flow (high turbulences) and n=1 indicates Darcy flow in the reservoir (no turbulence loss) [8], [ ]

3.2.2 Outflow Curve

The outflow curve, also “Tubing Performance Curve” (TPC), vertical lift performance (VLP) or “J-curve”, displays the relationship between the pressure drop inside the tubing and the flowrate. The pressure drop consists of the surface pressure, the friction losses, and the hydrostatic head. [9]

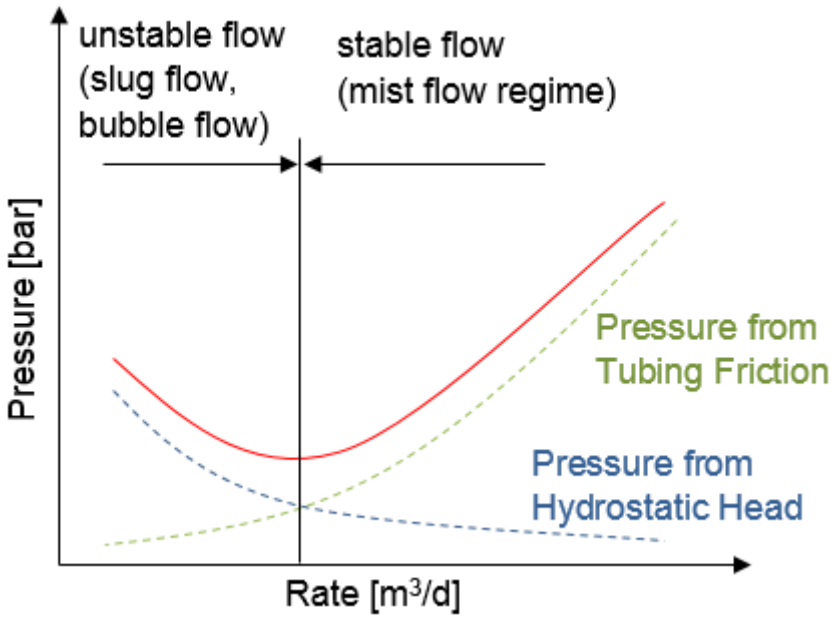

Figure 16: Tubing Performance Curve

When there is no flow and no additional surface pressure, the acting pressure only consists of the hydrostatic head, since there is no friction loss without flow. At low flowrates, the hydrostatic head governs the TPC because of a large ratio of liquid. As the flowrate increases, the impact of the hydrostatic head decreases, whereas the friction losses increase, giving the curve its typical “J”-shape (see Figure 16). As the flowrate increases further, the friction losses govern the TPC curve and the hydrostatic head does not have a major impact on the pressure, because the rate is high enough to carry the liquid to the surface.

To the left of the minimum of the TPC curve, the flow regime is unstable: liquid accumulation leads to lower flow velocities resulting in a slug flow or even a bubble flow regime. To the right of the minimum is the stable area, where the gas velocity is high enough to carry the liquid to the surface, a mist flow regime can be detected.

The friction losses are a function of the flow velocity and the tubing inside diameter. Tubings with a smaller diameter are associated with higher friction losses at the same velocity (Figure 17).

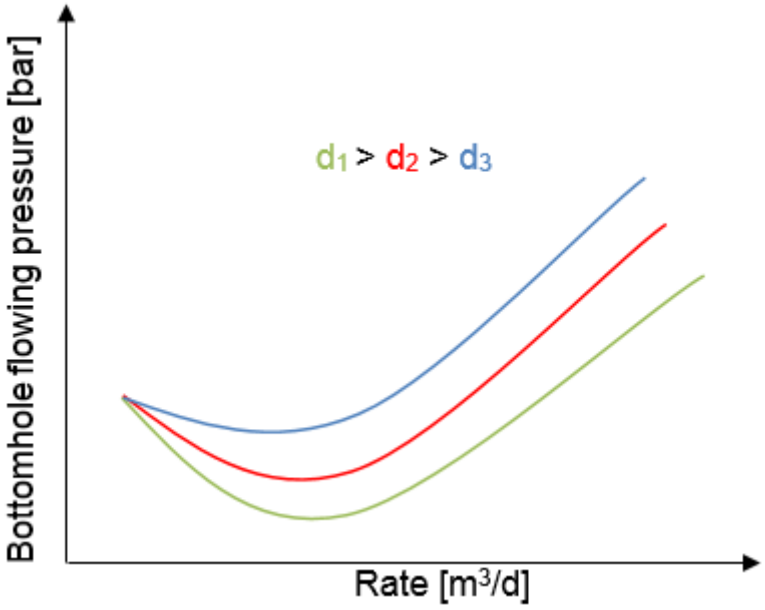

Figure 17: Effect of tubing diameter on TPC

To analyze the flow regime, the TPC curve can also be used by itself, especially when there is no current data available displaying the reservoir performance. The result is obviously quite inaccurate, but it is a useful approach to predict and determine liquid loading problems.

However, if reservoir performance data is present, the intersection of TPC and IPR allows an accurate determination of the operating point, hence finding the optimum pressure and flowrate. [9]

3.2.3 Methodology determining liquid loading using Nodal analysis

When the critical rate calculated by Turner is plotted on the IPR-TPC curve (Figure 18), one can evaluate, whether liquid loading is likely to appear or not. When the intercept of TURNER with the IPR curve is plotted left of the IPR- TPC intersection (TPC 2), the production rate is sufficient to produce liquid to surface. In the other case, the intercept of Turner-IPR lies right of the crossing point IPR-TPC (TPC 1), so the actual flowrate of the gas lies below the critical rate, hence liquid loading will occur. [19]

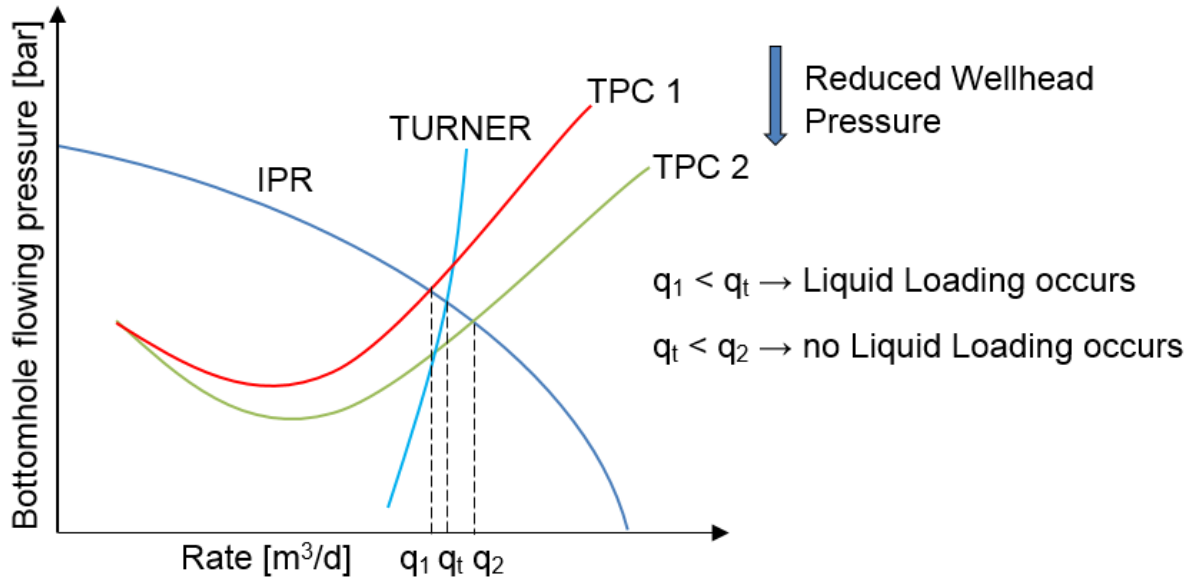

Figure 18: IPR and TPC overlap with the critical rate based on TURNER

There are three main factors influencing the TPC: the gas - liquid ratio, the tubing inside diameter and the wellhead pressure. Since the gas - liquid ratio cannot be changed, either tubing size or wellhead pressure have to be altered.

Reducing the tubing inside diameter results in a decreased production rate, because the friction losses inside the tubing increase. Additionally, the Turner rate shifts to the left, because the area for flow is directly proportional to the critical Turner rate.

When the wellhead pressure is reduced, the TPC ideally shifts downwards (Figure 18, TPC 1 to TPC 2), moving the operational point to the right, hence overcoming the Turner rate. However, a reduction of the wellhead pressure may not necessarily increase the flowrate when the well is tubing- or reservoir-limited.

In tubing-limited wells, the effect of the reduction of wellhead pressure is repealed by additional friction losses of the tubing. When the well is reservoir-limited, the bottomhole pressure is already low, an area where the IPR curve is steeper and an additional reduction would not lead to significantly higher production rates. [5]

4 Prevention of Liquid Loading

Due to the variety of different factors influencing the occurrence of liquid loading, not every prevention technique is applicable for every case.

Following considerations should be taken into account whilst identifying the best prevention method:

- Liquid:
  - Type of liquid produced (condensate, water or both)
- Reservoir:
  - dry or wet gas
  - presence of aquifer interconnected to reservoir
  - high or low permeability
  - reservoir pressure
  - volume of reserves remaining
- Well:
  - Configuration (borehole geometry, deviation, completion)
  - Flow condition (production rate, flow regime)
  - Integrity of production tubing
- Economics:
  - Capital Expenditure costs
  - Operating costs
- Infrastructure

There are numerous deliquification methods one can apply when the natural flow of the gas well becomes ineffective. In general, they can be categorized as systems which sustain the natural flow of the wellbore, systems which assist lifting the liquid or the use of pumps.

4.1 Sustain Natural Flow

To achieve continuous well production, it is essential to predict liquid loading accurately, so the production rate can be kept above the critical rate. Methods to compute these rates were discussed in chapter 0.

4.1.1 Alternate Flow/ Shut-in Periods

This method is based on manually or automatically induced shut-ins, which result in a temporary pressure increase. During the shut-in, pressure builds up at the near wellbore region, which eventually leads to a point, where the well unloads itself once it is opened again. Alternate shut-ins are cost effective; they do not need any downhole modification nor an

external energy source. However, the production downtime results in a revenue loss and it is not an effective method for low reservoir pressures, because the lengths of shut-in increase with continuous depletion of the reservoir and eventually the build-up pressure will not be high enough anymore to carry the liquid up the wellbore. [20]

Whitson et al. explained that cyclic shut-in can be applied for fields with various permeabilites (10^{-3}-10^{2}mD), their models have a constant bottomhole pressure of around 10bar. [21] Their approach only needs a wellhead device, which shuts the well automatically when a specified "liquid-loading" rate, defined by the critical velocity, is reached, and which re-opens the well after a short shut-in period. Thus, the well is never allowed to produce below the critical gas rate. They demonstrated that the shut-in time should be as short as possible, typically around an hour. Their observations also showed that multiple shut-in times do not mandatorily lead to lost production.

4.1.2 Alteration of Tubing

The aim of installing a tubing with a smaller diameter (velocity string) is to decrease the effective flow area and thereby increase the velocity of the fluid travelling upwards. This method does not need an additional energy source, and the evaluation of the right tubing size can be carried out effortlessly with an analysis of the tubing performance curve (see 3.2.2 Outflow Curve). Despite the above, the workover operation for installation might be expensive and sometimes it is not effective for already depleted wells. [20]

Higher friction losses due to the decreased tubing diameter must be taken into account, which may lead to a different choice of material (plastic instead of steel pipes). [22]

A practical application of coiled tubing velocity strings was carried out at the Amistad field in Ecuador. Six wells, completed with tubing having an ID of 2,991" were first shut-in, then freely produced until the production stopped due to liquid loading. After the water was removed, a coiled tubing (ID 1,5") string was inserted. The flowrates were determined based on Turner's equation and for over 12 months the flowrate exceeded the initial flowrate by 48% without any occurrence of liquid loading. Even though the production rate decreased down to an additional 10% to the initial flowrate after 26 months, the well still produced above its critical flowrate, therefore no liquid loading occurred. [23]

Another approach to prevent liquid loading suggests to keep the temperature losses in the well as low as possible. By the mitigation of heat loss several desirable effects can be achieved:

- higher fluid temperatures at the wellhead
- less pressure losses
- higher gas stream velocities along the entire tubing

As a result, the gas flowrate can be kept above the critical rate for longer time periods. Schwaiger et al did extensive simulations analyzing parameters such as pressure, temperature and velocities when conventional steel tubings were used, and compared the results to steel tubings with varying insulation thicknesses and GFK tubings. He showed, that the use of insulation for steel tubings or the deployment of GFK tubings clearly improves the conditions for the removal of liquids from the wellbore. [24]

Figure 19 below shows the effect of insulation at different gas production rates. The insulation has only minor effects on the bottomhole flowing pressure, but major consequences on the temperature at the wellhead. With increasing thickness of the insulation (from 0 to 1") the temperature at the wellhead rises.

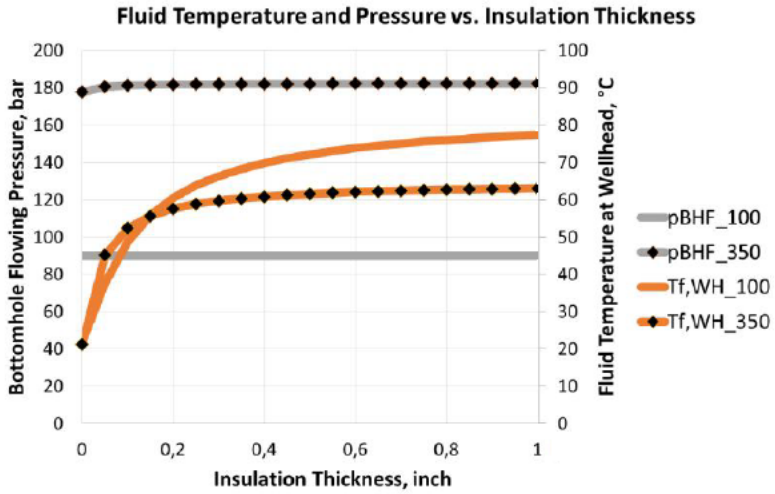

Figure 19: Bottom flowing pressure (p_{BHF}) and wellhead fluid temperature ($T_{f,WH}$) vs. insulation thickness at gas rates of 100.000Sm^3/d (100) and 350.000Sm^3/d (350) respectively. [24]

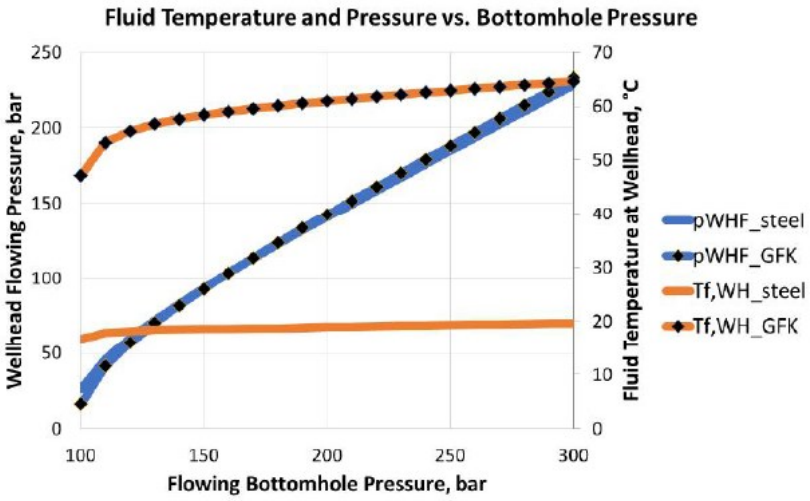

Figure 20: Wellhead flowing pressure and fluid temperature at wellhead vs. flowing bottomhole pressure comparing conventional steel tubing (conductivity = 16 $\frac{W}{m°K}$) with GFK tubing (conductivity = 0,045 $\frac{W}{m°K}$) without additional insulation. [24]

Figure 20 above shows that while the choice of tubing does not show changes in pressure, it effects the temperature. When GFK tubings are used, heat is preserved throughout the wellbore, allowing a three times higher fluid temperature at the wellhead compared to the use of conventional steel tubings.

4.2 Assisted Lift

4.2.1 Wellhead Compression

Because wellhead compression is the main topic of this thesis, the subject is analyzed more thoroughly in a separate paragraph. (Chapter 5).

4.2.2 Gas Lift

The objective of gas lift is to inject high pressured gas at the lowest possible point into the well through gas lift valves in the production tubing. The injected gas decreases the hydrostatic head because of a density reduction of the fluid in the wellbore. Leading to an increased gas velocity, the accumulated liquids at the bottom of the wellbore will be transported to the surface. The gas lift can be carried out either continuously or intermittently, though intermitted lifting proves to be more economically when used for low productivity gas wells. Gas lift is a flexible method to prevent liquid loading applicable for various GLR and well deviations, although it

comes with high implementation and operating costs and shows a lower efficiency compared to pump systems. [9] [20]

At the Box Church Field in Texas, a field test was conducted using continuous gas lift to avoid the appearance of liquid loading. The trial included four wells where a gas lift with 10 1” side-pocket mandrels was used. Continuous gas lift was chosen, because once the wells are unloaded, the system adds energy to keep the velocity at a sufficient level to hinder the occurrence of future liquid loading. The implemented gas lift proved to be unexpectedly successful, resulting in a gas production increment of approximately 30% compared to the production before the installation. [27]

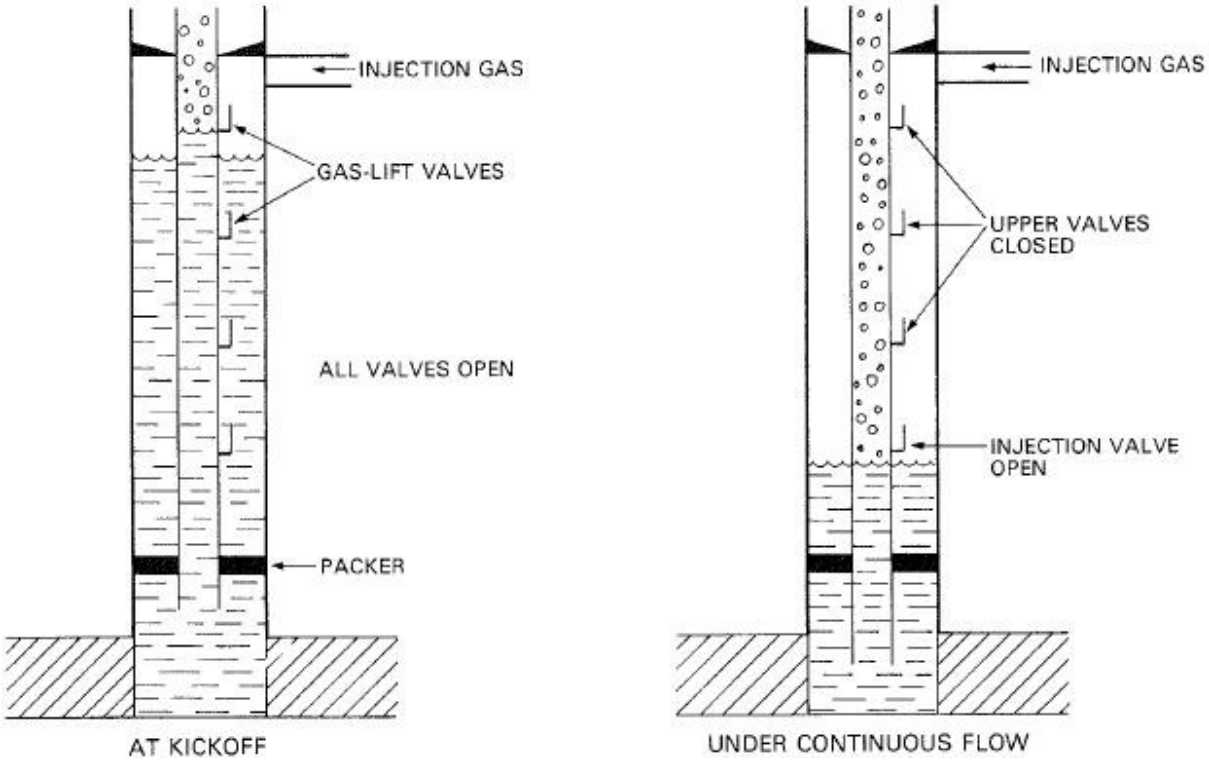

Figure 21: Schematic of a continuous gas lift installation. During the continuous injection of gas, the liquid level in the annulus lowers until it reaches it operating injection point. The design of the valves allows to close the upper valves and keep only the lowest valve open for gas injection. This installation increases the efficiency considerably compared to the case, when all valves would be opened the whole time. [26]

4.2.3 Plunger Lift

Plunger lift is an alteration of the alternate flow method, addressing the problem of “slippage” (liquid fallback). It uses free moving pistons or plungers which act as a solid interphase between the liquid and the lift gas. Only one downhole installation is necessary: a bumper spring seat installed on a seating nipple in the tubing.

When the well is open, the plunger rests in its surface position, gas is produced, and liquid accumulates on the top of the standing valve in the wellbore (Figure 22, 1). Once the production rate is lower than the set critical rate of the well, it shuts in, and the plunger drops to its bottom position (Figure 22, 2). Pressure builds up from the accumulated gas at the near wellbore region (Figure 22, 3). After the well is opened again, the liquid gets pushed up by the plunger, which is supported by the gas (Figure 22, 4). The plunger remains at surface as long as there is a sufficient gas flowrate (Figure 22, 5). When the velocity decreases, liquid starts to accumulate at the bottom of the wellbore. The well is shut in again, the plunger falls to the downhole resting position under the liquid and the cycle repeats, controlled by a plunger-lift controller positioned above the wellhead.

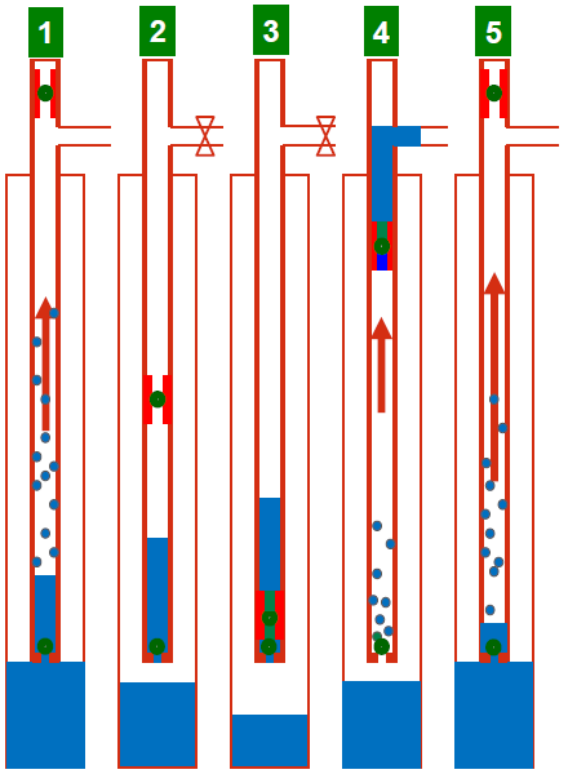

Figure 22: Schematics of the Working Principle of a Plunger Lift System [25]

Plunger lift works well with high gas-liquid ratios (GLR) and with large, uniform sized tubings. The system has relatively low initial installation and operation costs and does not require any external power to operate. However, the system cannot be applied for deviated wells with a non-uniform tubing size or highly depleted reservoirs. [20]

A combination of plunger lift and wellhead compression has been used successfully in the Western Canadian Sedimentary Basin. The combo faced a number of operational challenges, for instance that the compressor was not supplied with intake gas during the shut-in period of the well. This challenge was accomplished with a different plunger design, which can travel down the well even when there is gas flowing upwards, as well as with the use of variable speed drives which slow down the compressor without the necessity to turn it off completely. [22]

4.2.4 Foaming

The application of surfactants, so called foaming agents creates an emulsion of gas and liquid, where gas bubbles are surrounded by a liquid film (Figure 23). The foam has a reduced density and lower surface tension, leading to a significantly decreased critical velocity.

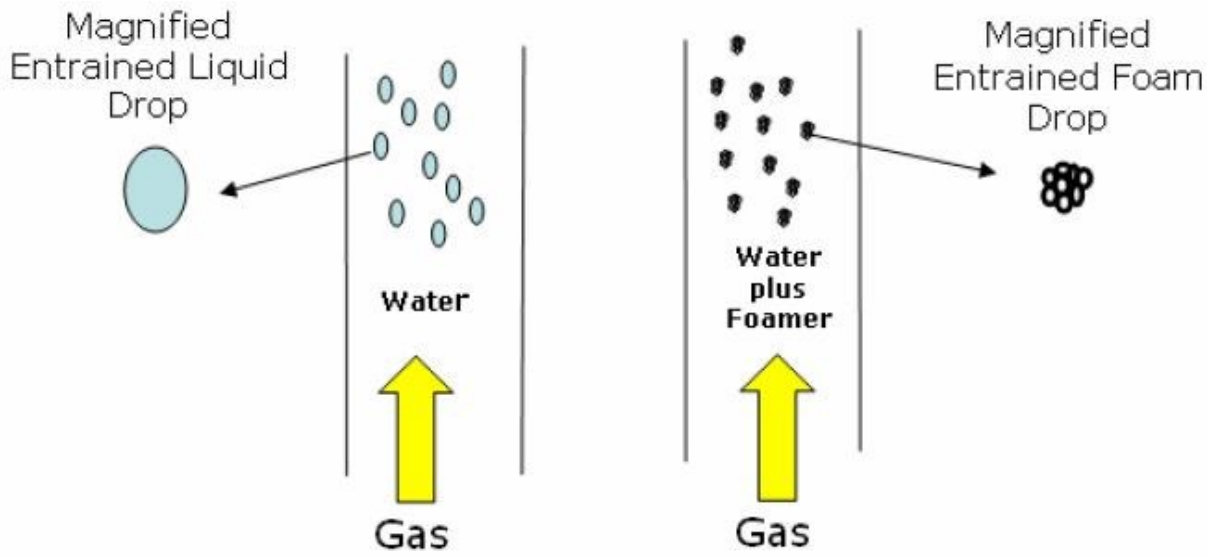

Figure 23: When the foaming agent is added to the liquid (right side), its overall density becomes lower than the one of the original liquid (left side), which directly leads to a lower critical velocity. [28]

The foaming agents are brought into the reservoir either in form of solid sticks, liquid batches or continuously during production. Batches of surfactants can be injected from the surface inside the tubing or the annulus, when there are no packers. Usually small amounts of brine are pumped into the wellbore after the batch, so it reaches the bottom easier. [25]

When surfactants are injected continuously, it is carried out either via a chemical injection line (CIL) or a capillary system. The difference between the CIL and the capillary system is the position where the line is mounted. Whereas capillary strings are “microtubing” systems which are installed inside the production tubing, CILs are installed in the tubing-casing annulus with a valve into the production tubing.

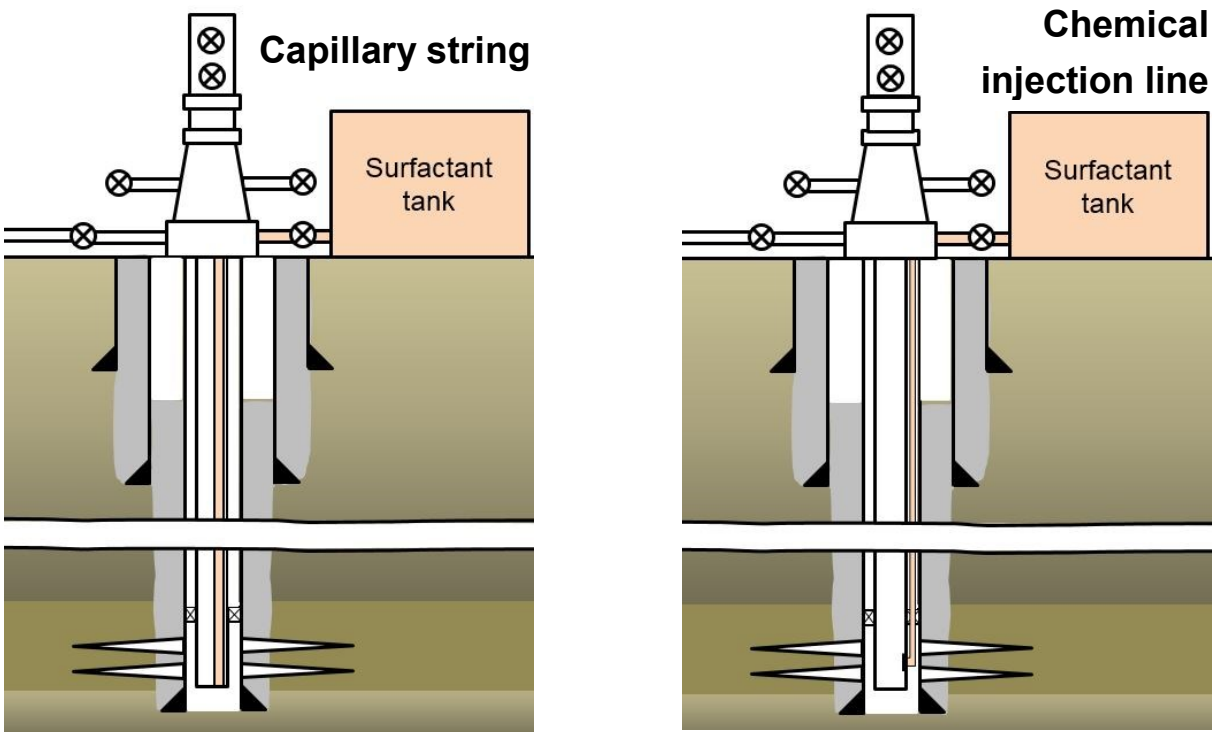

Figure 24: The different ways to continuously bring surfactants into a set point in the tubing. The left picture shows the capillary string, which is entered through the wellhead and inside the production tubing. The CIL is installed outside the tubing, and the surfactants are brought into the production tubing through a valve to the desired depth.

The installation of capillary systems can be carried out under flowing conditions using a capillary coiled tubing unit. The main advantages compared with batches are that the foaming agent can be brought into the wellbore in a continuous manner to the preferred depth and neither shut-in time nor workover is necessary for its installation.

Foaming is preferable to prevent liquid loading when the well has a high water cut. The system does not require any downhole modifications, has low initial costs and it uses the well's energy. Disadvantageous is that foaming agents do not work efficiently in the presence of condensates, because they are non-polar, compared to polar water molecules, which build relatively high film strengths, resulting in a high foam stability. Additionally, the application in wells with long horizontal sections are limited, and it is challenging to select the right composition and concentration of the agent, as a wrong choice may lead to a foam-locked well or no sufficient response at all. [9]

Batch foaming has been successfully used in an offshore gas condensate field in the Central North Sea to reduce liquid loading of 10 existing mature wells. First the well was shut in and the foam agent (2 bbl) was pumped into the tubing. The agent had 24 hours to reach the loaded zone and mix with the accumulated liquid downhole, followed by a flowing back period to generate foam. The well was finally reopened to unload as much liquid as possible in a low - pressure system and returned to normal high-pressure production mode afterwards. The trials

proved to be very successful, the shut-in time of the wells due to liquid loading had been effectively decreased. [26]

4.2.5 Swabbing

The objective of swabbing is to mechanically lift the accumulated liquid with swab cups from the bottom of the wellbore to surface. The system consists of swab cups which are operated via wireline, and the aim is to remove as much liquid as possible to ensure that the reservoir's energy can overcome the fluid head so the well is able to flow on its own again. It is used to revive already dead wells, or wells where the liquid level is so high, that compression or cycling might not work. Even though it provides continuous flow again, it is only a temporal solution because it must be carried out repeatedly which ultimately makes it an expensive method to prevent liquid loading. [20]

Figure 25: A variety of swab cubs. The aim is, that the cup dives into the liquid and pushes it upwards when the cups are retrieved to surface via wireline.

4.3 Pumps

For deliquification purposes sucker rod pumps (SRP), progressive cavity pumps (PCP) and electrical submersible pumps (ESP) can be used to generate a pressure drawdown in the wellbore. Pumps are particularly prone to gas locking, so they are restricted to a narrow range of operation possibilities and additional modifications are needed to utilize them properly. That includes the installation below the perforations when there is enough space, or alternatively the installation of special downhole separators. However, the use of pumps is limited in gas applications because of tremendous implementation and equipment costs, the wear and tear of equipment, their restricted ability to handle heat, the required maintenance and the concomitant decreased reliability. [9] [27]

5 Wellhead Compression

The aim of wellhead compression is to lower the wellhead pressure in order to increase the gas rate. A higher flowrate improves the ability of the well to remove liquids which accumulated in the wellbore because of a non-sufficient gas velocity. Additionally, the producible reserves increase due to the lower flowing bottomhole pressure (Figure 26). Wellhead compression is commonly carried out by compressors with low to medium throughputs and medium to high compression ratios. [5]

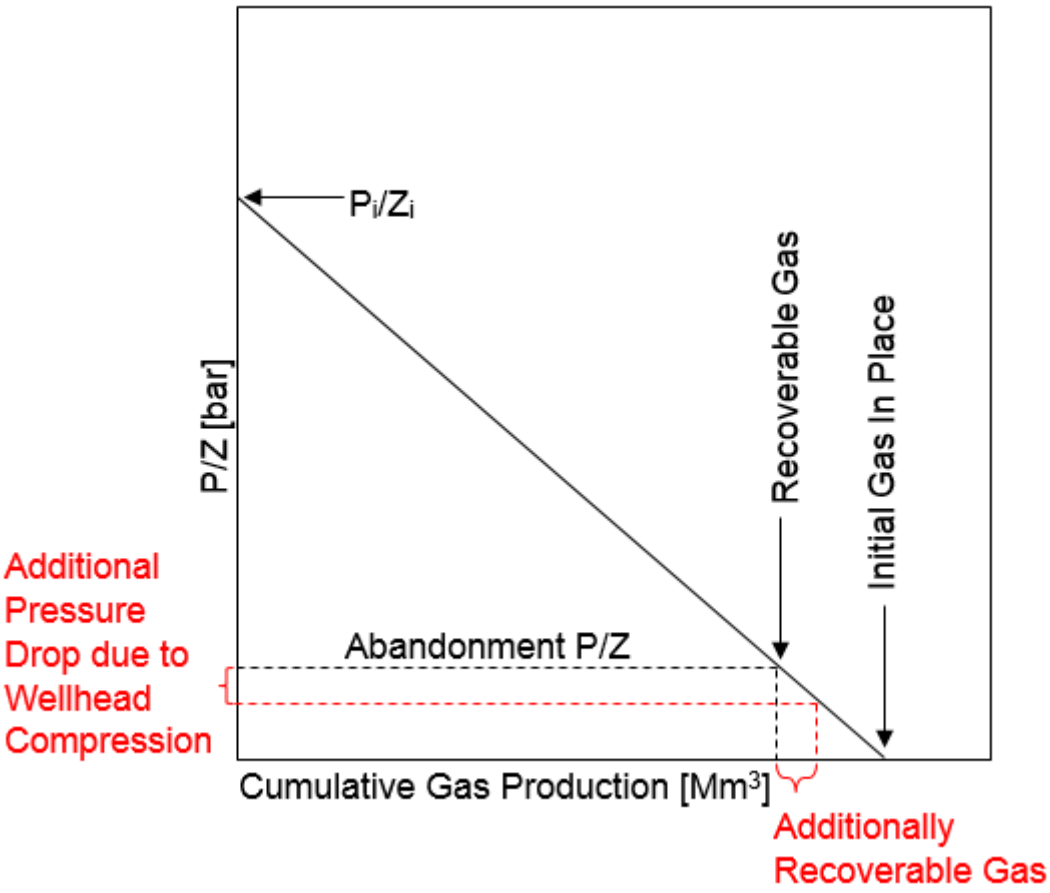

Figure 26: Schematic of a P/Z Plot [6]

Wellhead compression is an assisted lift deliquification method which can be used solitarily or in combination with other liquid loading prevention methods. Especially when there are known problems, such as the presence of downhole restrictions such as chokes or differing tubing inside diameters, methods which do not need any downhole equipment, like wellhead compression, are to be favoured.

Compression can be carried out in a centralized manner, meaning that one compressor lowers the wellhead pressure of several wells, or locally at each wellhead. When wells show similar or comparable pressure and flow regimes, centralized compression may be considered. However, due to unavoidable pressure losses in the lines to the compressor it has to be

carefully evaluated whether or not the centralized system will provide the required pressure differential.

On the advantageous side, wellhead compression does not need any downhole equipment and it provides a continuous, steady flow. [28]

Detrimental are the high capital expenditures and constant operational expenditures of a compression system.

Examples of successful wellhead compression are broadly documented, e.g. in the Lobo Wilcox wells in south Texas, operated by ConocoPhilips. Initially, they evaluated their wells ranked by their cumulative production, their production rate and whether it was below the unloading rate and their sensitivity to a change in wellhead pressure. They chose single stage reciprocating compressors which were powered by gas engines, mainly because of their small footprint and their flexibility to move them fast and easy. Their 21 low-cost wellhead compressors were used to boost the overall production by almost 60% over the following two years. The lessons learned are that unloading the well for the first time after the compressor's installation required significant efforts, using shut-in periods as well as foaming agents.

5.1 Working Principle of Compressors

Compressors are similar in design and operation to pumps. Where compressors are movers of compressible fluids (i.e. gases), pumps are movers of basically incompressible fluids (i.e. liquids). [30]

Compressors are widely used in the petroleum industry, ranging from flash gas compressors over gas lift compressors, reinjection compressors, booster-, vapor-recovery to casing head compressors. [31]

The theory of compression is based on the laws of thermodynamics. For gas, a compressible fluid, there are three possible compression types: isothermal, adiabatic and polytropic. The types are classified by analyzing whether heat transfer or friction losses occur during the compression. [5]

When isothermal compression is carried out, the temperature is constant. That can only be accomplished when the compression is done so slowly that even though heat is transferred, the temperature remains the same.

$$p * V = constant \tag{35}$$

Where

p	pressure [kPa]
V	volume [m^3]

Adiabatic compression is described as a completely reversible process, where no heat transfer is allowed at all. This means that energy is only transferred as work, and no heat is transferred to the surroundings.

$$p * V^k = constant \tag{36}$$

Where

k specific heat ratio [ ]

In practice it may be hard to achieve adiabatic compression, because any compression will cause some heat transfer and friction losses, which is represented by polytropic compression.

$$p * V^{n_p} = constant \tag{37}$$

Where

n_p polytropic index [ ]

1<n<k when the compression is between an isothermal and an adiabatic process and n>k if the compression is below an adiabatic process.

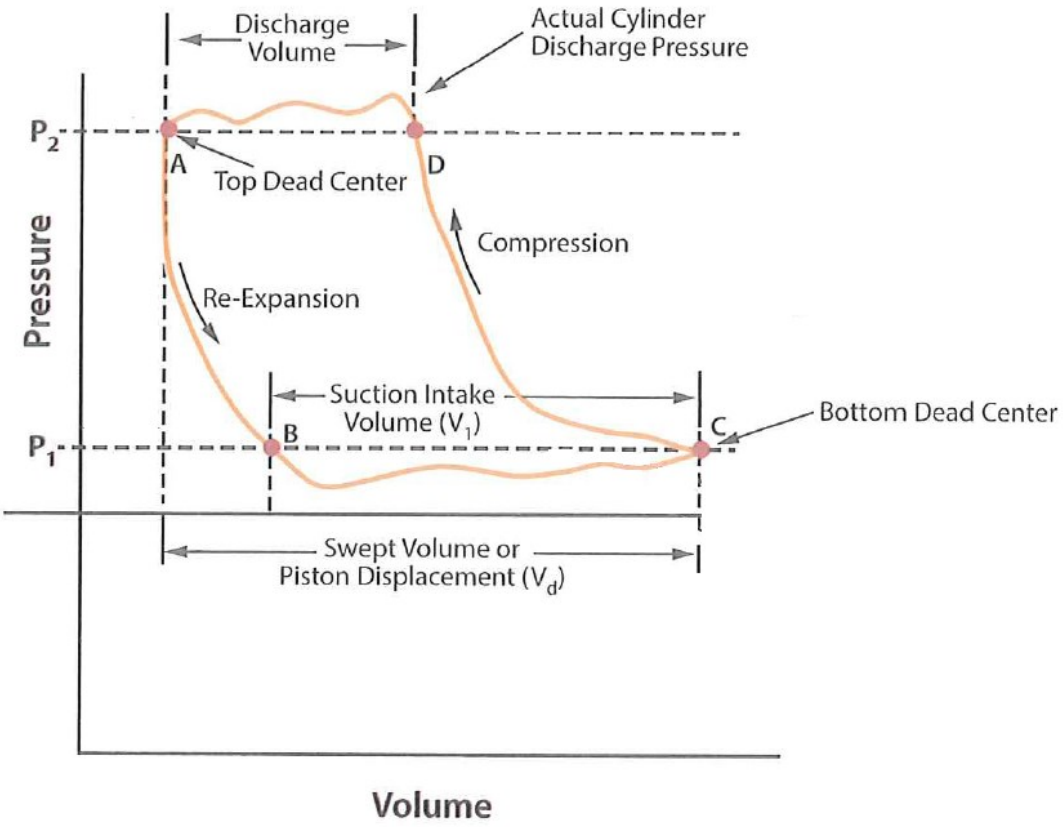

Figure 27: Theoretical compression cycle of a reciprocating compressor, consisting of four different stages [32]

B → C: at the suction pressure (p_1) a certain volume of gas ($V_C \rightarrow V_B$) is taken into the compressor

C → D: the gas gets compressed ($p_1 \rightarrow p_2$), and depending on whether the process is isothermal, polytropic or adiabatic, a different compressed end point volume is reached. The volume difference evolves due to different temperatures at given pressures: the higher the temperature, the higher the volume, explained by the ideal gas law.

D → A: the compressed gas gets discharged at compression pressure p_2

A → B: not 100% of the gas gets discharged, so some gas remains at the end of the discharge step; the pressure decreases, the remaining gas expands and the next cycle commences.

5.2 Classification of Compressors

Further division of compressors is based on the process of how the compaction is carried out; there are two general groups: positive displacement and dynamic compressors (Figure 28). Positive displacement compressors, including rotary and reciprocating types, increase its pressure by reducing the volume of gas. The principle of dynamic compressors (subdivided into axial flow and centrifugal) is the acceleration and deceleration of gas, meaning that kinetic energy is converted into a pressure rise. [33]

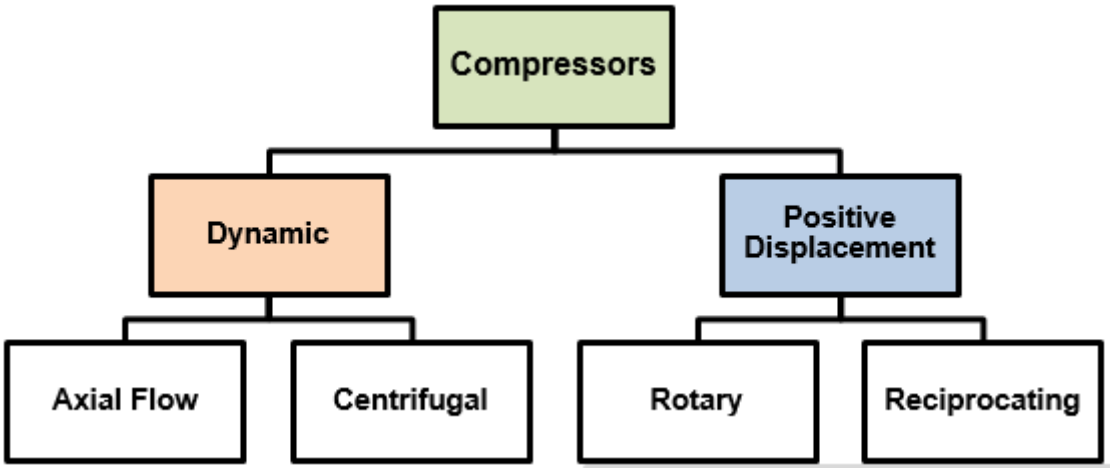

Figure 28: Classification of compressors

Figure 29 shows the field of application for compressors divided by their respective volumetric flowrate and the compression ratio (= absolute outlet pressure/absolute inlet pressure) they can achieve. The graphic shows that positive displacement compressors are well suited for handling high compression ratios with low flowrate s. Dynamic compressors on the other hand can handle large volumetric flowrates, but achieve merely moderate compression ratios.

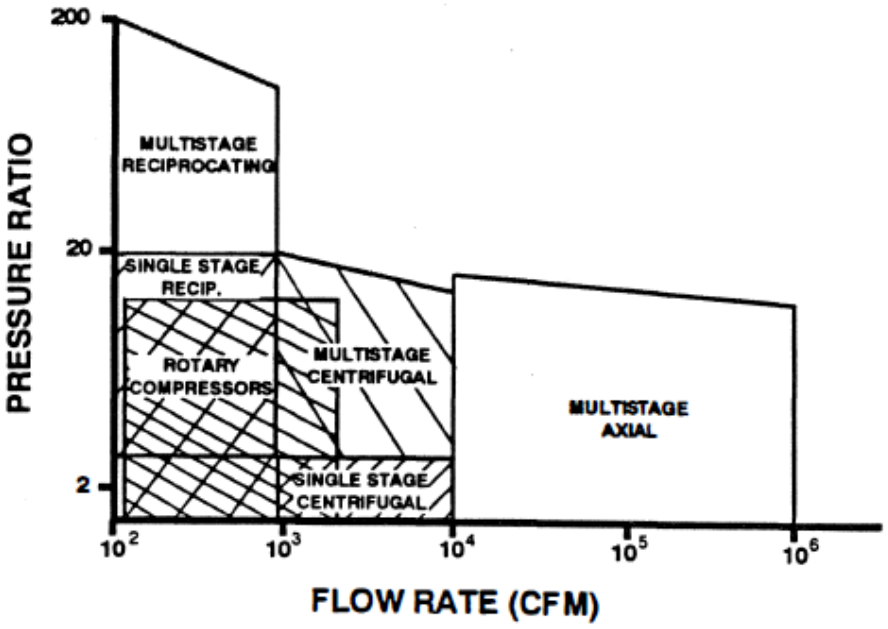

Figure 29: Application ranges of various compressor types [34]

The main components of a compressor are the driven unit, its drive, the transmission devices and the auxiliary equipment. The driven unit carries out the compression work of the fluid using different physical principles. The most widely used drivers are turbines (steam or gas), motors (induction, synchronous or various speed), and engines (internal combustion, diesel or gas). The transmission devices include the gears, clutches and couplings, and the auxiliary equipment contains the lube and seal as well as the cooling systems. [35]

Due to the fact that wellhead compression is carried out almost exclusively with different types of positive displacement compressors, they are discussed in detail below.

5.2.1 Rotary Compressors

Rotary compressors can be further divided into straight lobe and helical lobe (screw) compressors. It is noteworthy that rotary screw compressors have become increasingly popular in the gas industry. [33]

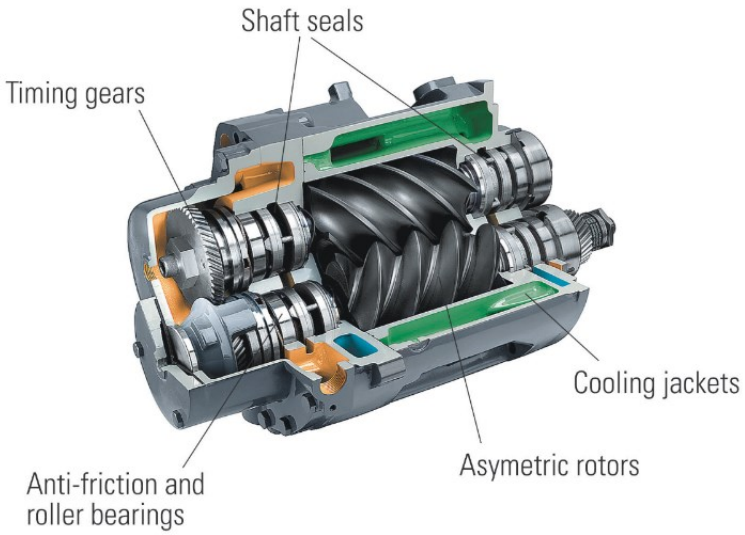

Figure 30: Helical lobe compressor (screw compressor) [35]

Rotary screw compressors consist of identically synchronized, asymmetric twin rotors, bearings, cooling and gears. An external timing gear prevents the rotor contact and minimizes the meshing rotor clearance to optimize the efficiency. The gas is compressed by a positive displacement in the ever-diminishing space between the two rotors, operating either oil-free or oil-flooded (Figure 30). Oil-flooded systems provide a liquid seal around the rotors and absorb the heat of the compression, allowing significantly higher pressure ratios in one stage than those achievable with oil-free systems. Disadvantageous is the fact the oil has to be removed after the compression process and cooled before being used again. [34]

Rotary screw compressors consist of few wearing parts, so the system provides a very high reliability, thus low maintenance. Compared to reciprocating compressors, rotary systems have a smaller footprint, weight and show only minimal vibrations due to a smooth flowrate. However, they have a low efficiency (typically between 65 to 75%) and can only be operated in a limited pressure range. [33]

The most common drives used are gas engines or electrical motors.

5.2.2 Reciprocating compressors

These compressors consist of pistons, which move reciprocatingly within a cylinder and connection rods which link the piston to the crankshaft (Figure 31). The driver rotates the crankshaft, which converts the rotary movement into the reciprocating motion of the pistons. The fluid enters through the suction valve, gets compressed and exits through the discharge valve.

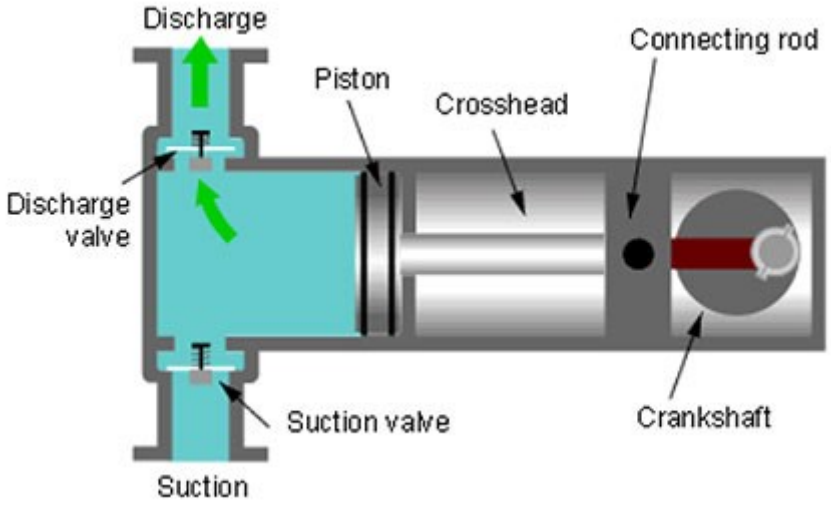

Figure 31: Scheme of a reciprocating compressor [36]

There are single and double stage compressors available on the market, which are differentiated whether the process of compression is carried out in one or two stages. Double acting reciprocating compressors use the forward and backstroke of the piston to compress fluid, increasing the performed work on the fluid over time, saving energy. They have an overall higher efficiency compared to rotary screw compressors (typically between 72 to 90%).

High pressure ratios through multistaging and variable capacities are the main advantages of the reciprocating compressor; however, they have many moving parts which leads to high maintenance efforts and additionally they suffer from pulsation during operation.

5.3 Wellhead Compression Systems Available on the Market

For this thesis three different compressor systems were analysed and compared with each other:

1. reciprocating compressor
2. rotary screw compressor
3. GasJack (see chapter 6.1)

1. The reciprocating single- stage acting compressor is equipped with eight cylinders and powered by a gas engine drive with 8,8l. The scope of supply includes the compressor, its gas engine drive, a scrubber to remove liquids from the produced gas prior compression, an air cooler, and the control panel; all mounted on a mobile skid. (Figure 32)

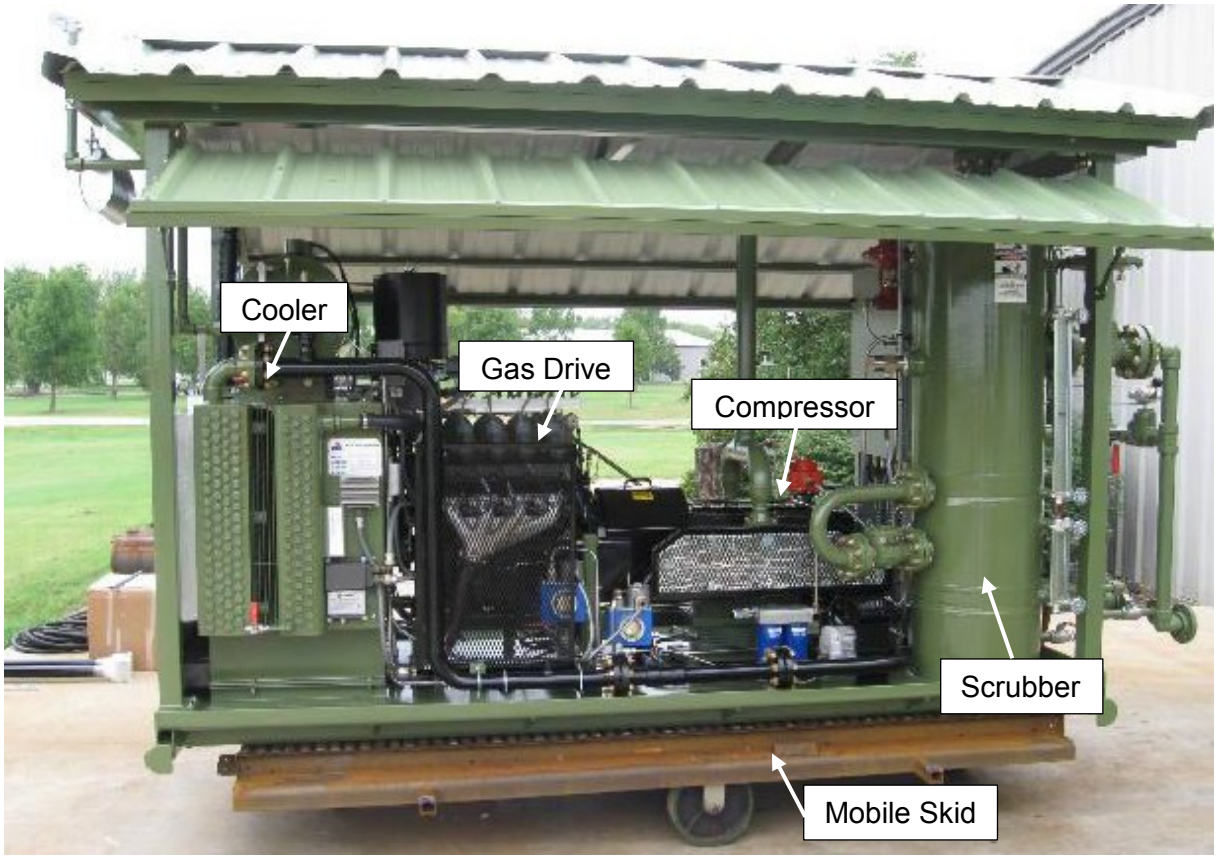

Figure 32: Reciprocating Compressor assembly

2. The rotary compressor consists of a single-stage oil-flooded screw compressor which is driven by a 90kW electric motor (Figure 33). The scope of supply consists of an inlet knock-out vessel, the compressor and its electrical drive, a compressor oil system, a gas cooling system, a filter system and piping. The screw system is assembled in a sound- silencing package enclosure.

Figure 33: Screw compressor, which is installed in a container

3. The GasJack is not build like a “usual” compressor with a compression and drive unit which are connected by a clutch: the GasJack combines both components in one single housing of a modified Ford-V8 motor. The motor is modified, that four cylinders serve as the drive unit, fuelled by wet gas, and the other side functions as the compression element. (Figure 34)

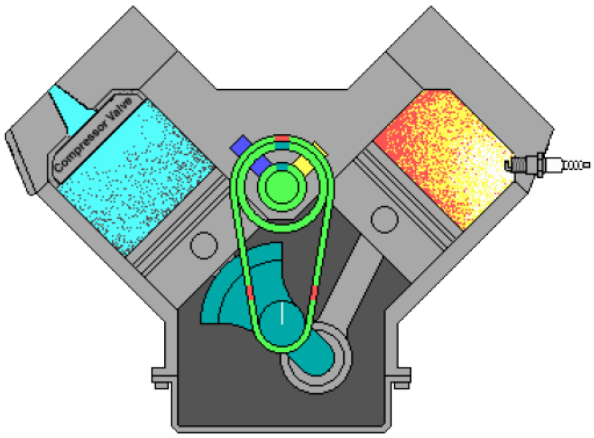

Figure 34: Schematic of the GasJack [38]: The right cylinder represents the drive unit, which provides power due to combustion of gas for the compression system. Over the cross head, connection rod and crank shaft, the reciprocating motion is transmitted to the cylinder on the left, which carries out the compression.

Figure 35: CSI Compressco GasJack system, and how it is utilized in the US [38]

The GasJack package includes the compressor, two separation units, a control unit for the fuel gas, a pressure control valve and a cooling unit.

Table 1: Technical Specification of the analyzed compressors

Type	Suction Pressure [bar] min	Suction Pressure [bar] max	Discharge pressure [bar] min	Discharge pressure [bar] max	Drive	Fuel Consum-ption [m^3/day]	Power Consum-ption [kWh/day]	Dimensions L x W x H [m]	Weight [kg]
Reciprocating Compressor	1	4	4	18	Gas	ca. 550		5,4 x 2,2 x 2,1	3650
Screw Compressor	2	13	10	21	Electrical		2160	6,0 x 2,4 x 2,6	12000
GasJack	1	4	5	31	Gas	ca. 300		3,1 x 2,4 x 2,6	5000

From the technical point of view, all systems could be considered for wellhead compression in Wintershall. An economic analysis of the deployment of the analysed compressors is carried out in chapter 8.2.

6 Application of Wellhead Compression Systems in Wintershall

6.1 Experience of Wellhead Compression in Wintershall Germany

In 2012 Wintershall Germany conducted a technology project using wellhead compression to enhance the economic production of selected gas wells as many have suffered regularly from liquid loading.

Staffhorst Z9 was chosen as a trial well, because back in 2012, the production site of Staffhorst was constantly manned, hence potential problems or failures could promptly addressed by the staff.

The utilized compressor model named “GasJack” was built by the American company Compressco. The major advantage of this integrated system is its low price.

To match the requirements of German authorities, the compressor had to be certified and positively inspected by European TÜV. In the US, the GasJacks are mounted on a skit without any housing, which is not permitted in Germany due to noise emissions (Figure 36). To meet the standards, a container- normally used for offshore operations- was installed, housing the compressor and its equipment. The added container bore the risk that due to non-sufficient ventilation inside, Ex-zones could arise. To deal with this issue, the container was equipped with an additional ventilation system and Ex- zone- compatible- sensors which measure the concentrations of methane and carbon monoxide.

Figure 36: GasJack housed by offshore container

The installation of the GasJack system was simple, as the compressor only has two line connections (suction and pressure line) and no power connection was necessary, because the system powers its own 24V battery. To achieve the intended wellhead pressure of 3bar, two GasJack modules were connected parallel with a manifold.

The advantages of the GasJack were obvious: the system is cost effective, robust and easy to maintain. It solely needs two line connections, and it uses the produced wet gas as fuel after it is separated from the water at the free water knock out vessel (FWKO). Because of the innovative construction, the required amount of spare parts is also significantly lower compared to conventional compression systems.

The operation result was fair to middling, because the starting process of the compression proved to be complicated. Even though the system specifications assured, that the GasJacks would work with gas at a calorific value as low as 6,74kWh/m^3, the system became unsteady and prone to disfunctions with gas at a significantly higher calorific value.

Additionally, the required maintenance became a problem too. With the widespread use of wellhead compression systems for mature gas fields in the US comes the vast availability of sufficient service; this service infrastructure is missing in Europe. So when maintenance or repairs which called for specialist knowledge had to be conducted, technicians had to be flown in from the US. Even more time was lost because the various components and the flow of the gas were not labelled properly. That not only increased the operational costs, but also the down-time of the GasJacks.

The design of the container bore additional difficulties during repair and maintenance work: because of the container's harshly limited space originally designed for offshore applications, the mechanics had problems reaching certain spots. The appearing vibrations of the compressor in the container led to the disfunction of parts, occasionally even screws started to unscrew themselves.

Because of neighbours directly bordering the production site, the allowable noise emission was critical. It became a serious problem in summer, when the temperatures within the container were too high to operate the compressor properly, so the doors had to be opened to provide the necessary cooling. A gabion wall was then constructed to curb the additional noise pollution.

During the trials, problems regarding the integrity of the completion appeared. A well inspection executed with a borehole camera revealed several leaks in the tubing. That led to a lower production and several problems, because the fluids that entered the tubing partially escaped into the annulus instead of being produced to surface.

Even though the gas production was increased by the installation of the GasJack system, the technology project was terminated, because the negative effects outweighed the benefits of the installation.

To ensure, that future projects do not suffer from the same problems, the lessons learned from the project are as follows:

- Wells for wellhead compression
    - Check whether the integrity of the production tubing of the well is given

- Housing container:
    - When designing the housing container, take into account that all components should be reachable with relative ease for repairing purposes
    - Label all relevant components, so they can be identified properly by all operators
    - Assure, that a proper ventilation system is installed. It should be capable of regulating the temperature so that the housing container can be closed at all times during operation.
    - Provide a manual that is complete and simple to follow for all operators

6.2 Evaluated Reservoirs

A gradual screening of the wells was carried out to find the most suitable and promising candidates for testing the feasibility of wellhead compression.

The wells of the gas reservoirs Barrien, Düste and Staffhorst were evaluated using the software Microsoft Excel as well as the Petroleum Experts Integrated Production Modelling (IPM) toolkit, including MBAL™, PROSPER™ and GAP™.

6.2.1 Barrien

The field Barrien started its production back in 1965, with about 14.995 Mio m^3 of gas initially in place. The reservoir consists of sandstone from the middle Triassic (middle Buntsandstein), the Detfurth formation. Overall, 11 wells have been drilled, of which 7 wells are currently producing and 5 are investigated in this thesis (see Appendix A for the locations of the wells within the reservoir). At the end of 2015 a total of 12718 Mio m^3 have been produced, translating into a recovery factor of 84%.

The wells under investigation are Barrien T2, T3, T5, T9 and T12.

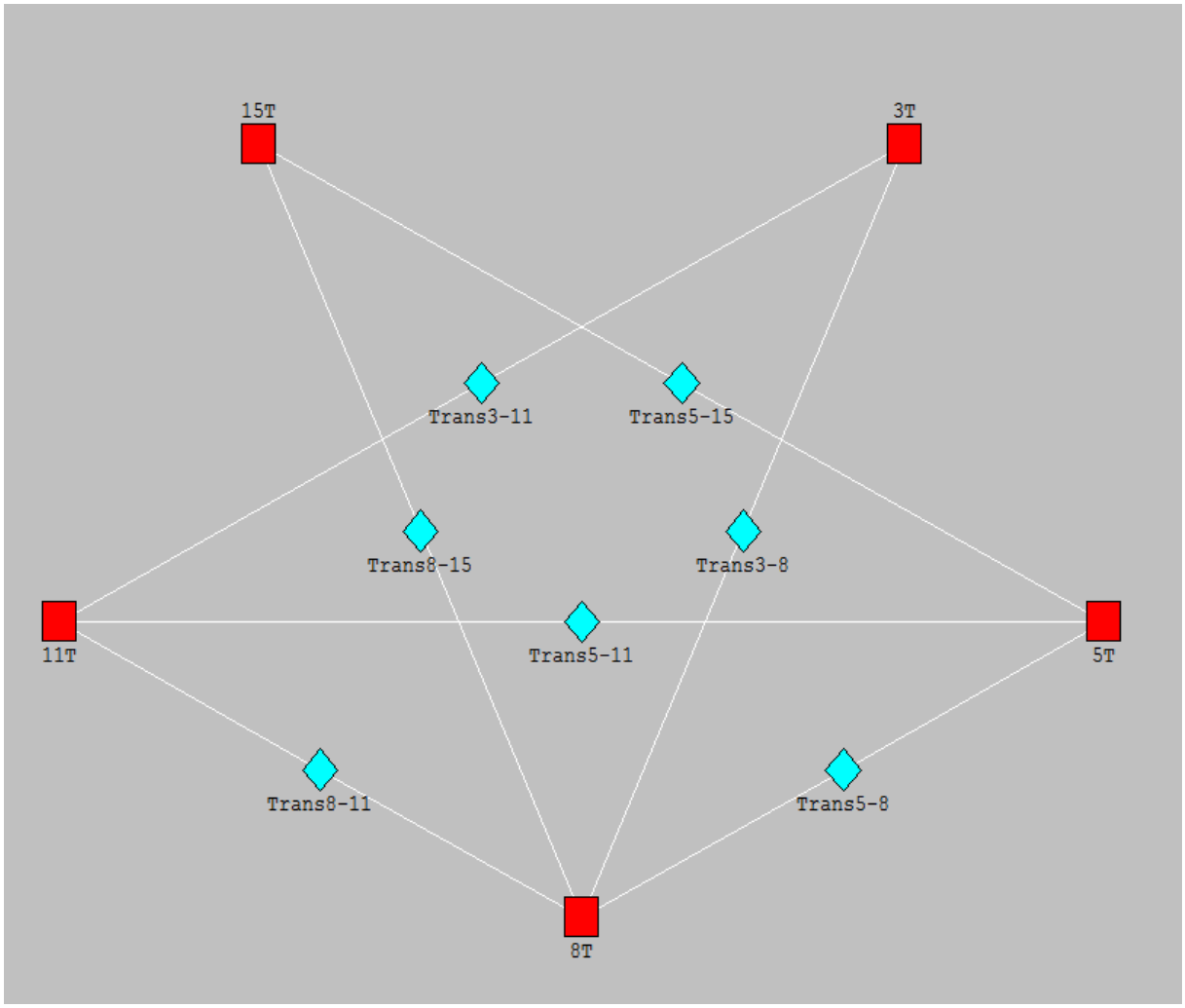

Figure 37: MBAL™ model for the southern part of the reservoir Barrien

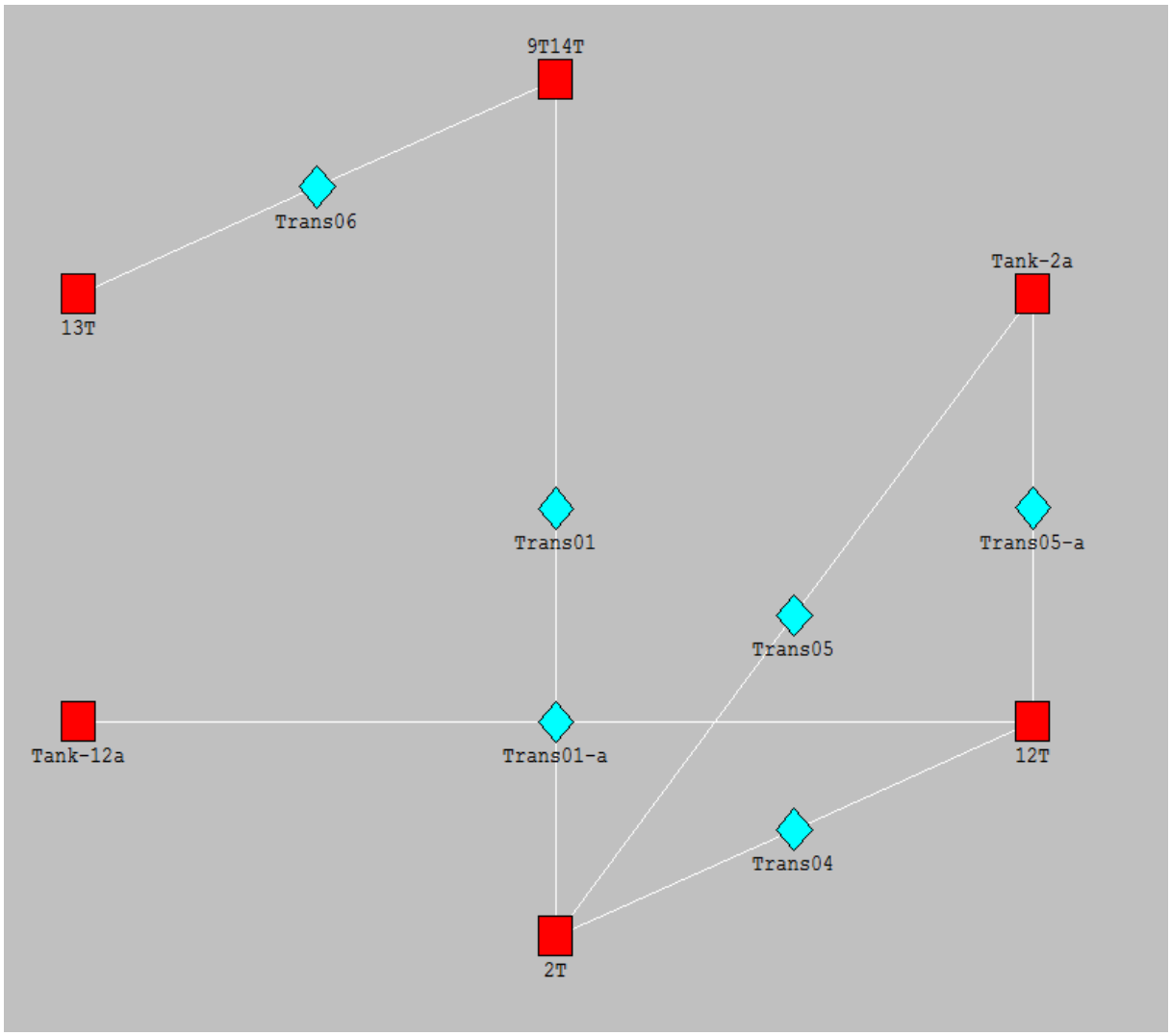

Figure 38: MBAL™ model for the northern part of the reservoir Barrien

As shown in Figure 37 and Figure 38, the MBAL™ model Barrien consists of 11 main tanks, which communicate with each other. The model was prepared to be further analyzed with GAP™. For the GAP™ model not only the MBAL™ reservoir model was provided, but also the trajectory and completion design modeled in PROSPER™ were included. In GAP™ a history match was conducted in order to carry out trustworthy production predictions.

6.2.2 Staffhorst

The reservoir Staffhorst was explored in 1964, where sweet and sour gas were produced from two horizons. This thesis investigates two wells (Z4 and Z9) which are both producing sweet gas from the lower Triassic (Buntsandstein) sandstone (see Appendix A for the location of the wells within the reservoir). The initial gas in place was forecasted with 1.900 Mio m^3, at the end of 2015 a total of 1.523 Mio m^3 have been produced, translating into a recovery factor of 80%. The wells Staffhorst Z4 and Z9, which both produce sweet gas were investigated for the use of wellhead compression.

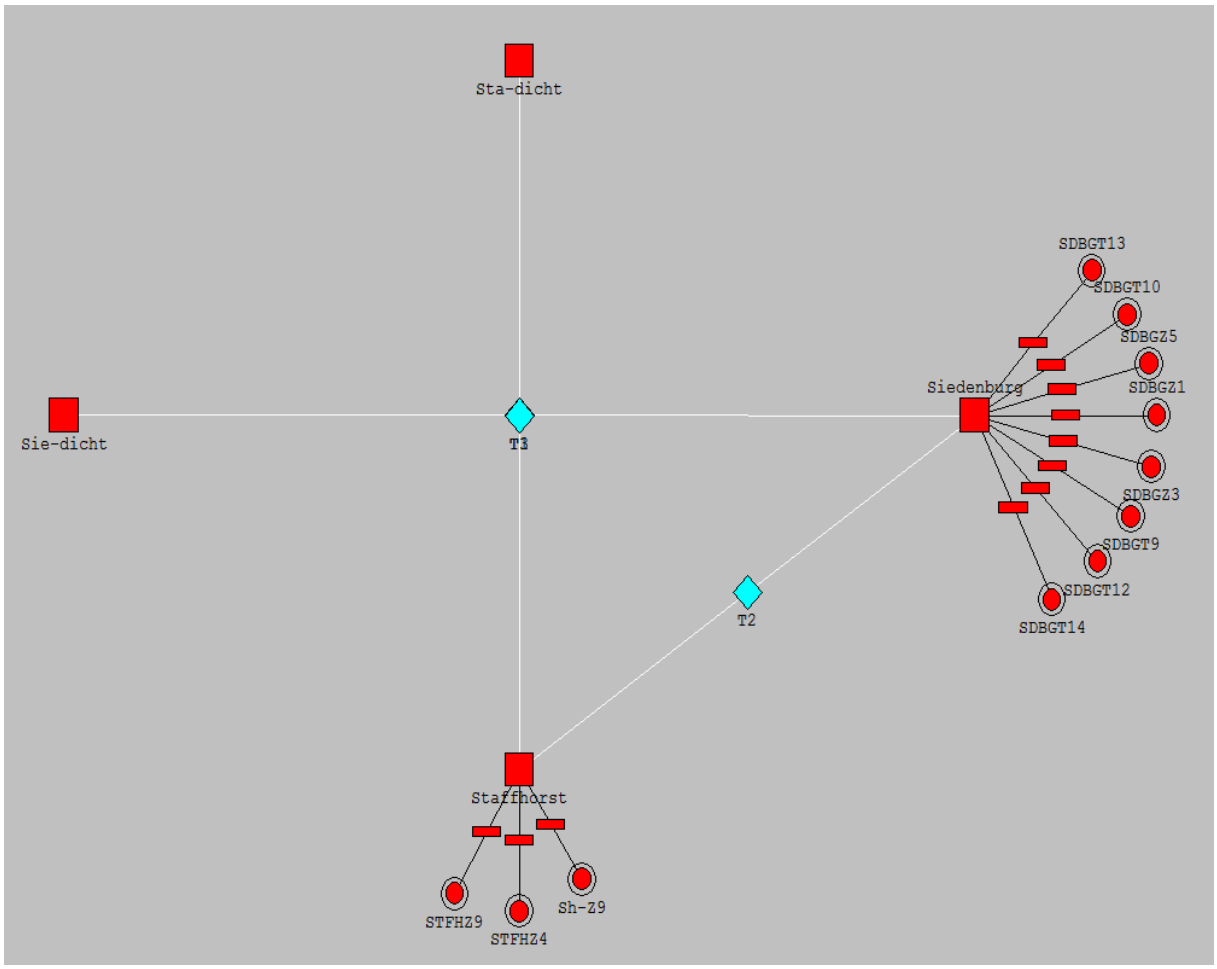

Figure 39: MBAL™ model for the reservoir Staffhorst

6.2.3 Düste

The reservoir Düste was discovered in 1961, currently 5 wells are producing. The reservoir consists of Triassic (Buntsandstein) sandstone, the Detfurth formation (see Appendix A for the location of the wells within the formation). An initial gas in place of 1.520 Mio m^3 was predicted, and by the end of 2015 1.253 Mio m^3 had been produced, so the recovery factor is around 82%. This thesis evaluates the wells T1, T3, T4, Z7 and Z8.

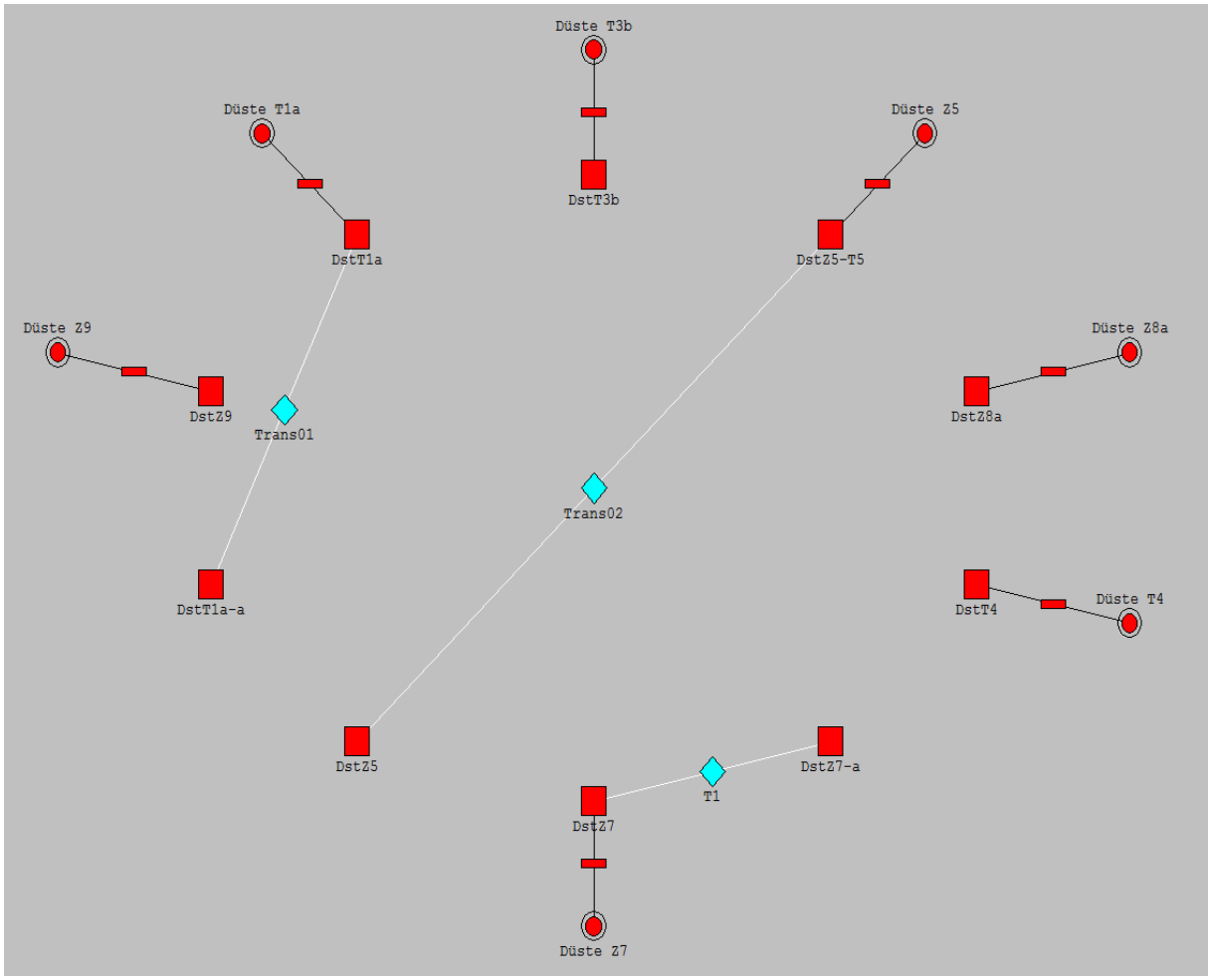

Figure 40: MBAL™ model of the reservoir Düs

7 Health, Safety and Environment

The work of a petroleum engineer does not just concern the exploration of reservoirs and the production of oil and gas. At all times the protection of people and the environment and the concern for safety have to be the main focus of all actions taken. To be certain that all possible hazards and their prevention measures are discussed, a general-production-facility hazard tree can be used. [41] In a first step, a hazard tree identifies all possible hazards and describes when they will occur. The main aim is to eliminate the hazard, but if it cannot be eliminated for any given reason, its likelihood to appear will be reduced as much as possible. The main factors of a hazard tree are pollution of the environment, fire/explosion and injury of people and business reputation.

The general approach to minimize risks can be explained by the hierarchy of control measures, the so-called TOP system. [39] It includes the reduction and minimization of risks by technical, organizational and personal measures. Technical measures include modifications of the machines used, for example the use of a special materials or the constructive modification of the machine to reduce the risk of hazards when it is used. Organizational measures are for instance that only qualified specialists are allowed to do the work. The third step, the personal measures include for example the use of personal protective equipment (PPE).

7.1 Environmental Safety and Business Reputation

The integrity of the environment proves to be a main factor, especially because the work of the oil and gas industry is continuously in the critical focus of the public eye. When gas is produced from the reservoir, a number of side products are unavoidably produced along with it. By-products may be sand or water from different origins.

Especially the reservoir water bears certain risks for the environment, because it is typically highly saline. Salts, and so called naturally occurring radioactive material (NORM) might dissolve and precipitate inside the tubing, or it might lead to a restriction of the flow path, plugging and corrosion when the materials were chosen poorly. [40] As a result, material failures might lead to severe consequences harming the environment, so that the use of a sufficient corrosion monitoring system becomes necessary. On the surface, the produced products have to be processed according to industry standards and the countries' regulations, always providing a minimum risk for the environment and the people, who are in contact with it.

When wellhead compression is successfully used to increase the production of gas, more water will be produced inevitably. In Wintershall the produced water coming from the FWKO is stored in tanks from where tank trucks transport it to the storage tanks of the water injection wells. When the amount of produced water increases, the frequency of the truck transports from the production well to the injection well increases correspondingly. There the water is reinjected into a former produced formation, according to German legal guidelines. An internal

study was conducted in 2015, addressing the disposal capacities of the produced water of the sweet gas wells, which are disposed to five different injection wells. The study shows, that even if the amount of produced water increases significantly, the initial reservoir pressure, which is the upper limit for a disposal injection layer, will not be reached, so the additional water can be treated. [41]

Noise emission bears another harm to the environment and the people. The first time a wellhead compression system was tested at Wintershall, it bore a big problem, because neighbours complained about the noise emission which arose due to a misconstruction of the compressors' housing container. Especially because most wells of the field Barrien are within a 250m distance to residential areas, where noise immission reference values are 50dB(A) for the day time and 35dB(A) during night time. [42] To minimize the risk of occurring noise emission, technical measures have to be taken, such as a different construction design, different materials used, or similar.

Flaring can be a technical measure when emergency situations occur, or for the disposal reasons of sour gas. Nevertheless, it bears another source of emission. Even though in most countries flaring is already only permitted for short test periods, its application should be limited as much as possible.

7.2 Fire and Explosion Prevention

When gas is produced, there are defined areas on the production site, which bear a certain risk of explosion.

According to an EC regulation, methane is rated as a highly explosive gas. [43] Per definition, a gas explosion is a process of combustion where a premixed gas phase fuel and an oxidizer causes a rapid increase in pressure. [47] Figure 41 shows the relationship between methane (fuel), oxygen and passive agents, which in air is mostly nitrogen. The triangle shows, that under normal conditions (21% of oxygen in air), the explosive limits for methane are between 4 Vol.-% (lower explosive limit) and 17 Vol.-% (upper explosive limit).

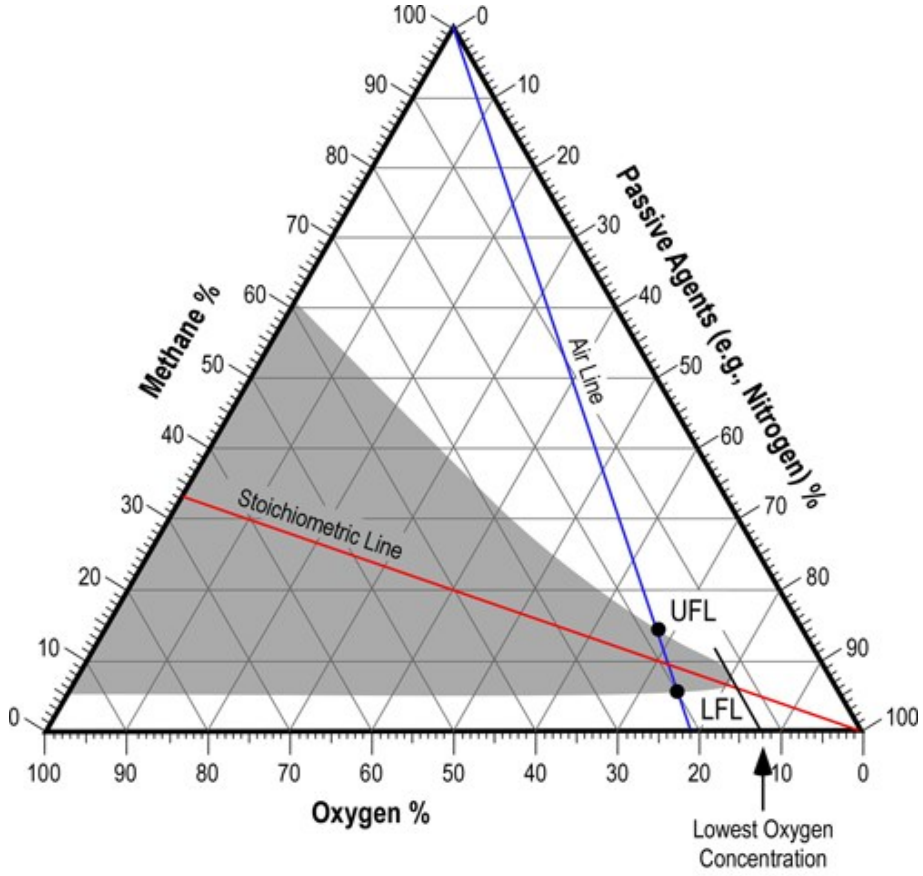

Figure 41: Methane Flammability Diagram [47]

Due to operational processes it cannot be ruled out completely that natural gas does not occur outside its production facilities; so it has to be guaranteed, that no point in time will allow an explosive atmosphere to evolve.

Generally, there are three different classes of explosive zones (Ex-zones), divided by the likelihood of the occurrence of an explosive atmosphere.

Zone 0 describes an area, where an explosive atmosphere is constantly present, or present over long periods of time. In zone 1, an explosive atmosphere develops occasionally under normal conditions. Zone 2 is an area where an explosive atmosphere either occurs for short durations, or is unlikely to occur at all.

For every gas production site, Wintershall has conducted a specific risk assessment to evaluate the occurring explosive zones. In general, there is an Ex-zone 1 within the cellar and around the absorber, and an Ex-zone 2 1m around the cellar. Further Ex-zones are set for individual production settings according to specific risk assessments (see Appendix D).

When a decentralized wellhead compression system is installed, which is mounted directly next to the wellhead, parts of the system lie within Ex-zones. For compressors which are used for gases lighter than air and which are mounted outdoors, DGUV prescribes an Ex-zone 2 for the connection points of the compressor which has the form of a rounded, truncated cone with

a radius of 1m at bottom and 3m at top at a maximum height of 3m (Figure 42) [48]

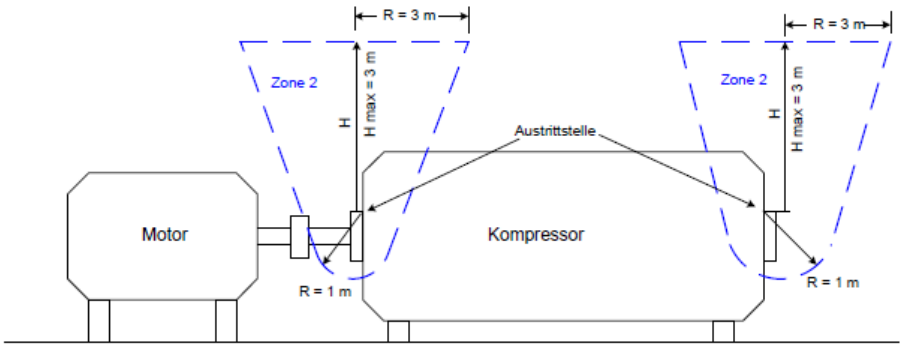

Figure 42: Ex zones for a technically tight compressor mounted outdoors) [48]

Explosion protection measures include a correct classification of explosion-hazard areas, technical as well as organizational actions and a regular control of the introduced arrangements. Basically, the explosion protection can be divided into three main steps: primary, secondary and tertiary stage. [46]

The goal of primary explosion protection is to prevent the creation of an explosive atmosphere. This practically means that the explosion protection is given when the installations and pipes are sealed tight, which has to be checked before commissioning and after repairs were carried out.

Secondary explosion protection tries to exclude the presence of effective ignition sources, through using special commissioned equipment, which requires certain certification in order to allow its usage in Ex-zones.

The third explosion protection includes constructional arrangements, which limit the impact of an explosion to a safe level, e.g. flame arresters which make sure that there is no flashback in case of an adjacent fire.

7.3 Health and Safety Prevention

The use of a wellhead compression system might lead to certain HSE concerns which have to be evaluated carefully in order to prevent harm to the people who work with it. When a new system is installed, modifications of the surface connection lines have to be made. This leads to the risk that operators are exposed to reservoir fluids, high pressures and high temperatures. To avoid any incidents by technical and operational measures, the installation has to be planned precisely, all possible risks have to be evaluated, and steps have to be introduced to make sure no harm comes to people or to the environment. As a personal measure, the use of special personal protection equipment (PPE) may be included.

7.4 Applied Plant Safety (SGU)

Wintershall developed its own system to apply a hazard and operability study (HAZOP), which is used for every facility and consists of 5 steps. HAZOP is an analysis of the possible hazards that occur during a process, using a simple risk matrix to evaluate the potential severity and likelihood of an event. [47]

The aim of SGU step 0 is to identify the fundamental risks of the discussed topics. In this early step of a project the type of process, the location of the facility and the logistics concept are discussed and a preliminary decision is made.

SGU step 1 and 2 are often combined, because they deal with the identification of the hazards within a process and the facility, the editing of the safety and environment concept, and the audit of the concept. After the completion of step 2 a document providing actualized actions to prevent all found risks, the identification of new risks and the decision on how to proceed further is compiled.

SGU step 3 audits the planned concept again, using a safety concept tool called HAZOP (Hazard and Operability Study). The outcome should be a very detailed documentation of all conceivable risks and the actions taken against them.

The final and fourth step of the SGU deals with the review of the implementation of the safety, health and environment concept prior to commissioning.

For the use of the GasJack compressors at Staffhorst Z9 following points were discussed in SGU step 1 and 2: facility safety, work and health protection, environment and further permits. Facility safety included a detailed investigation into all potential appearing hazards derived from physical effects (e.g. flowrate , concentration, temperature or pressure too high or too low), hazards appearing when energy systems fail, hazards regarding construction, explosion and fire protection regulations as well as external hazards (e.g. interference from unauthorized third parties). Work and health protection addressed the accessibility of the facility and noise protection, along with protection against accidental contact. The environmental evaluation deals with the possible hazard of various emissions in water or air and the waste management. SGU step 3 documented the hazards and their prevention or the measures taken in detail.

8 Results

8.1 Screening

To evaluate the potential of the chosen wells, the following screening criteria were used:

1. Production Benefits:

The reservoir engineering division of Wintershall provided MBAL™ or GAP™ models of the different reservoirs. The Petroleum Experts Integrated Production Modelling software MBAL™ uses the material balance equation and reservoir parameters to calculate the initial gas in place and does further simulations of the reservoir. The different tanks, displaying the compartments of the reservoir, are first fed with the available reservoir and production data to create a proper history match (see the details in Appendix B).

The software GAP™ combines the reservoir models created in MBAL™ and the well models of PROSPER™ to get a full field production forecast. Afterwards, forecasts of the fields were simulated from 2017 to 2036, where the manifold pressure was lowered to 3bar to observe the effect of a lowered wellhead pressure.

The reservoir Barrien was described with two MBAL™ tank models, which were developed, to be imported into GAP™ later. The GAP™ software also includes the PROSPER™ models of the wellbore. In this case the production forecast was evaluated using GAP™.

The other type of model uses only a MBAL™ simulation, which already includes wells. So for the reservoirs Staffhorst and Düste the calculation of additionally recoverable gas was directly carried out in MBAL™. See the example below for the calculations done for Barrien T2, Appendix C shows the detailed calculations and diagrams for all investigated wells.

Table 2: Overview of additional recoverable gas at Barrien T2

Year	Average Gas Rate without WHC [Sm³/h]	Average Gas Rate with WHC [Sm³/h]	Cumulative Gas Production without WHC [Mio Sm³]	Cumulative Gas Production with WHC [Mio Sm³]	Annual Production without WHC [Mio Sm³]	Annual Production with WHC [Mio Sm³]	Additional Production [Mio Sm³]
2017	412	631	4,30	11,33	4,30	11,33	7,03
2018	392	516	8,11	17,16	3,81	5,83	2,03
2019	376	476	11,73	21,93	3,62	4,77	1,15
2020	361	451	15,21	26,33	3,48	4,40	0,92
2021	348	430	18,55	30,51	3,35	4,18	0,83
2022	335	413	21,77	34,49	3,21	3,98	0,76
2023	322	397	24,86	38,31	3,09	3,82	0,73
2024	310	382	27,83	41,98	2,97	3,67	0,70
2025	299	367	30,70	45,51	2,87	3,54	0,67
2026	289	353	33,47	48,91	2,76	3,39	0,63
2027	279	341	36,13	52,17	2,67	3,27	0,60
2028	270	329	38,71	55,32	2,58	3,15	0,57
2029	261	318	41,21	58,37	2,50	3,05	0,55
2030	253	307	43,62	61,31	2,41	2,94	0,52
2031	0,00	296	43,62	64,14	0,00	2,83	2,83
2032	0,00	287	43,62	66,88	0,00	2,74	2,74
2033	0,00	278	43,62	69,54	0,00	2,66	2,66
2034	0,00	270	43,62	72,10	0,00	2,57	2,57
2035	0,00	262	43,62	74,60	0,00	2,49	2,49
2036	0,00	254	43,62	77,01	0,00	2,42	2,42
					Total Additional Production		**33,39**

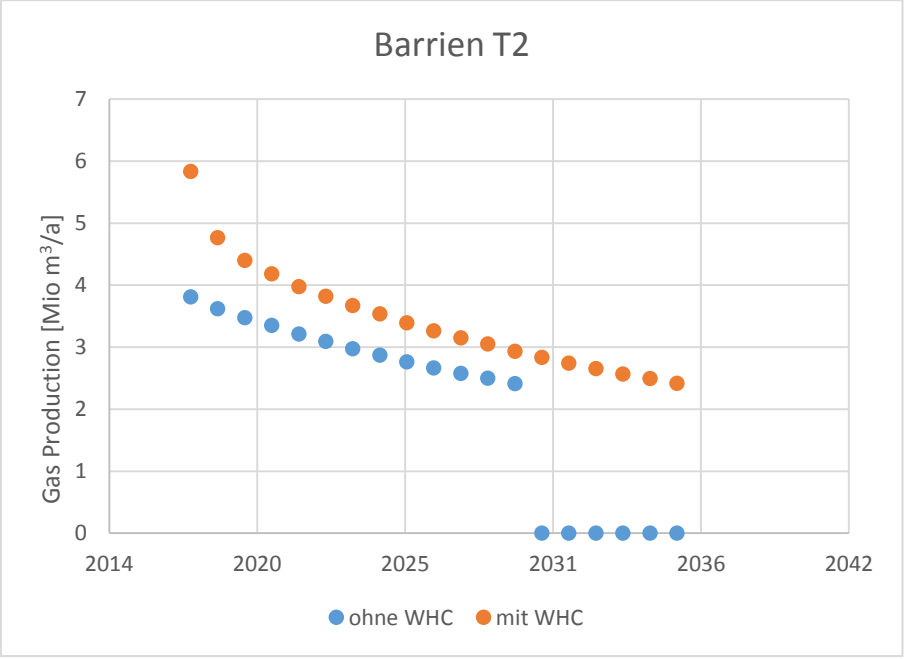

Figure 43: Predicted Gas Production of Barrien T2

Table 3: First ranking after simulating the production benefit when the wellhead pressure gets lowered down to 3 bar

Well	**Production Benefit Increment** [Mio Sm^3]
Barrien T5	119,91
Barrien T9	39,63
Barrien T2	33,39
Staffhorst Z9	20,35
Staffhorst Z4	15,05
Barrien T3	6,04
Düste Z7	3,39
Düste T3	2,30
Düste T1	0,70
Düste Z8	0,53
Düste T4	0,45

2. Liquid Loading:

In a second step the actual production data of the wells was analysed. The Turner model was used for the evaluation of the critical velocity hence flowrate, because the investigated wells are nearly vertical. Using data from the completion design and the current wellhead pressures, the critical flowrate was calculated for each well and compared with the actual average gas rate. To make the results more comparable, a flowrate ratio, being the actual flowrate divided by the critical rate was introduced. It helped ranking wells by the severity of liquid loading, given that it occurred. Table 4 below shows the results for the production with current wellhead pressures.

$$Flowrate\ Ratio = \frac{Actual\ flowrate}{Critical\ flowrate} \tag{38}$$

When FR > 1 → no liquid loading occurs, when FR < 1 → well suffers liquid loading

Table 4: Calculation of the Flowrate Ratio for the Current Production Scenario

Well	Average Gas Production [Sm³/d]	Critical Rate [Sm³/d]	Flowrate Ratio
Staffhorst Z4	22875	12522	1,83
Düste T3	9968	14219	0,70
Barrien T2	12246	17510	0,70
Barrien T5	25307	36223	0,70
Barrien T9	20469	31621	0,65
Düste Z7	9094	18068	0,50
Barrien T3	6898	15128	0,46
Barrien T12	18325	62475	0,29
Staffhorst Z9	4137	21453	0,19
Düste T1	2310	12067	0,19
Düste Z8	2654	20979	0,13
Düste T4	2320	27946	0,08

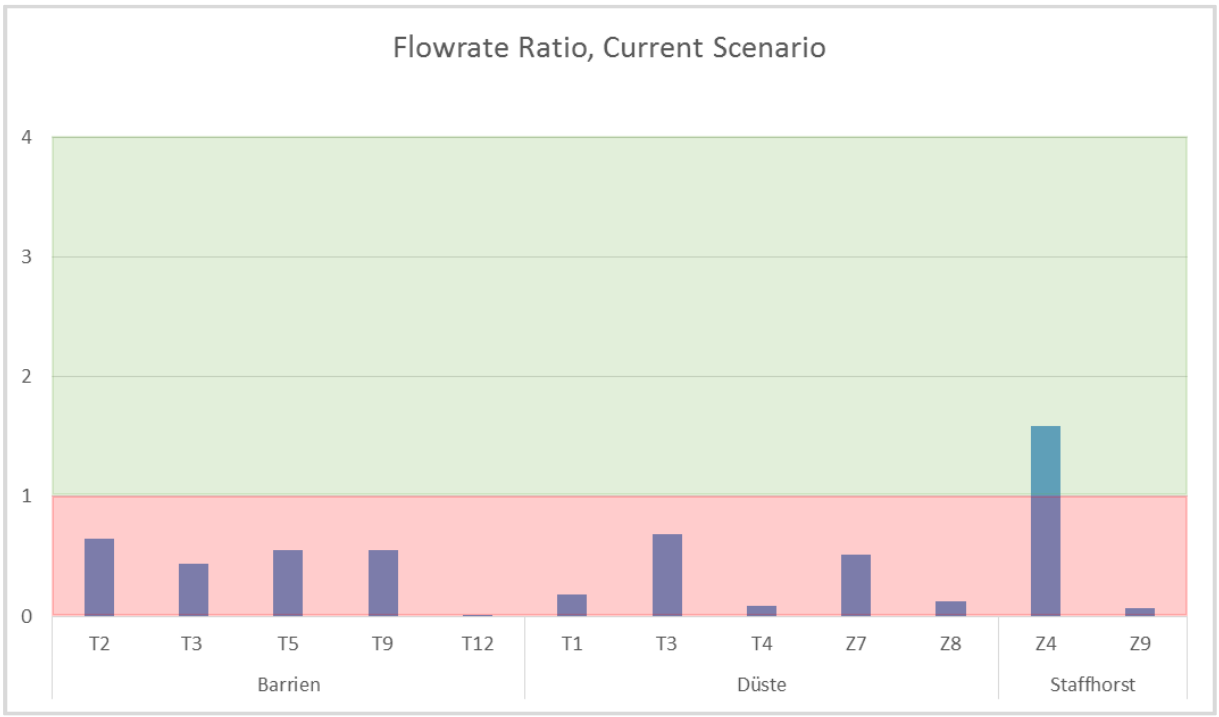

Figure 44: The diagram shows that most of the wells suffer from severe liquid loading (red area, below a flowrate ratio of 1). Only Staffhorst Z4 can overcome the critical flowrate and continuously produce liquid to the surface (green area, flowrate ratio above 1).

3. Effectiveness of reducing wellhead pressure:

With the Petroleum Experts IPM software PROSPER™, a realistic model of the wells was built. Using PVT data, deviation survey, equipment and inflow performance data for the model, VLP-IPR curves were generated. Carrying out a sensitivity analysis of the top node pressure (wellhead pressure), it was evaluated whether wellhead compression is a useful tool to increase the gas production rate. Figure 45 shows the result of the well Barrien T2. By decreasing the wellhead pressure down to 3 bar, the flowrate of all wells can be increased significantly.

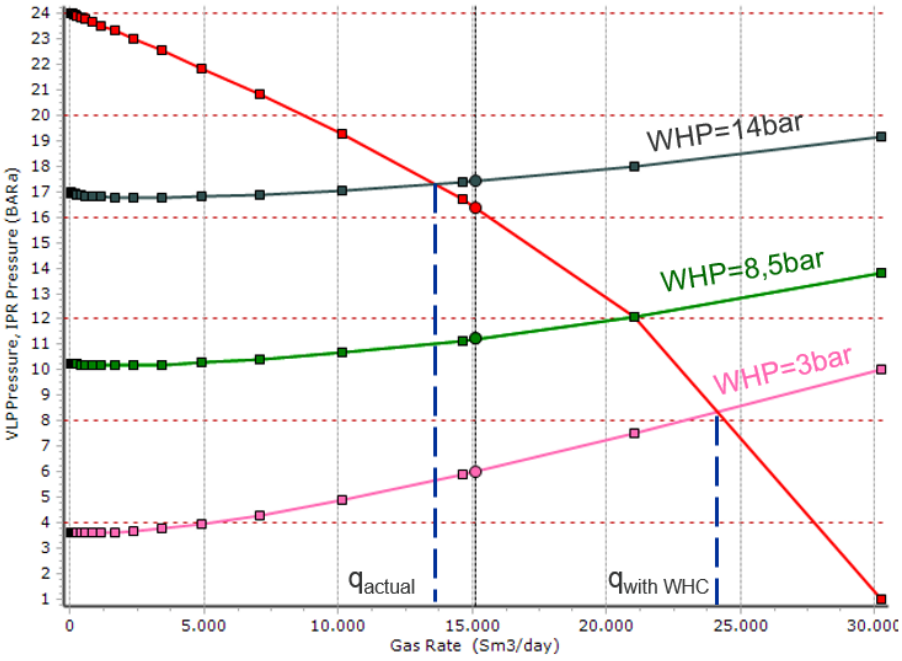

Figure 45: IPR/VLP analysis of Barrien T2 in PROSPER™. The gas rate is measured at standard conditions of 1 atm and 15,5 °C.

The achievable production rate with a lowered wellhead pressure ($q_{with\ WHC}$) was then used to calculate the new flowrate ratio, to verify that the new production rate is sufficient to overcome the critical rate, hence to avoid liquid loading.

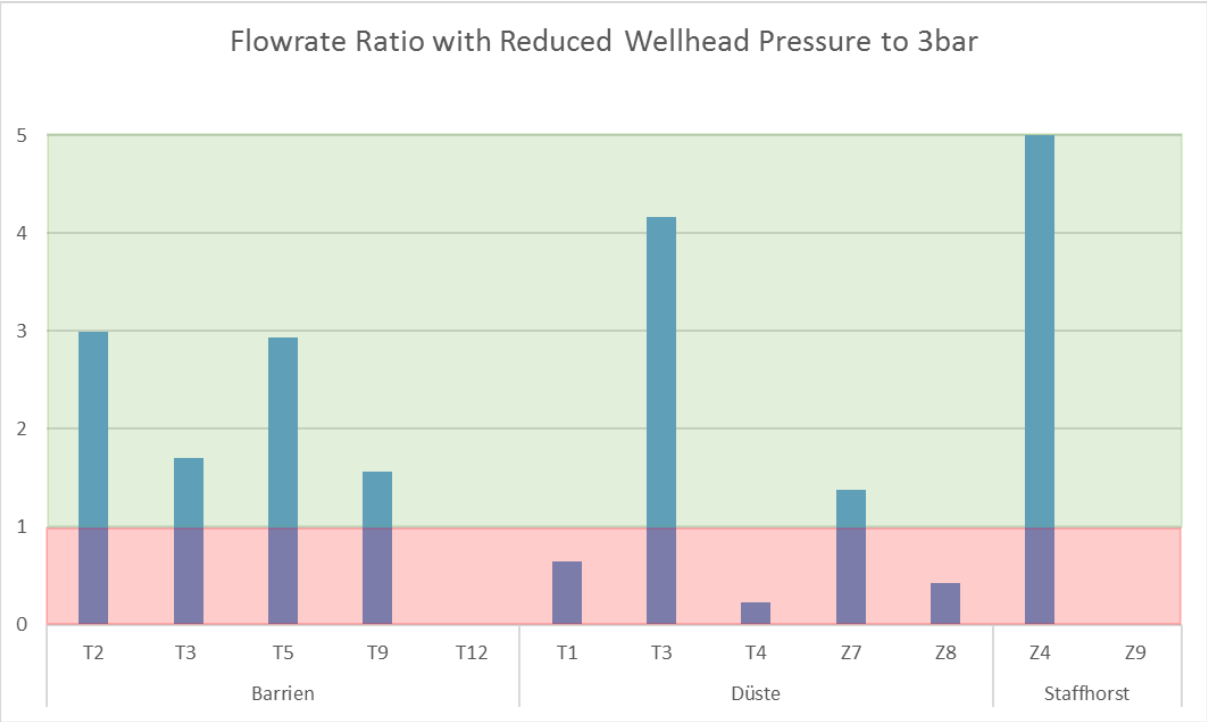

Figure 46: Analysis of the flowrate ratio when wellhead compression is used. As illustrated, the wells from the reservoir Barrien, Düste T3, Z7 and Staffhorst Z4 react well to a reduced wellhead pressure and their flowrate exceeds the critical flowrate, thus avoiding loading of the well (green area, flowrate ratio above 1). Whereas for the wells Düste T1, T4 and Z8 a decreased wellbore pressure does not help to increase the actual flowrate above the critical one (red area, flowrate ratio below 1).

Table 5: Calculation of the flowrate ratio takes wellhead compression down to 3 bar into account

Well	Gas Production Rate [Sm^3/d]	Critical Rate [Sm^3/d]	Flowrate Ratio
Staffhorst Z4	27779	5463	5,08
Düste T3	14566	3496	4,17
Barrien T2	23520	7867	2,99
Barrien T5	36000	12292	2,93
Barrien T3	9307	5463	1,70
Barrien T9	19272	12292	1,57
Düste Z7	10870	7867	1,38
Düste T1	3504	5463	0,64
Düste Z8	3339	7867	0,42
Düste T4	2784	12292	0,23

For the wells Barrien T12 and Staffhorst Z9 no sufficient PROSPER™ model could be created, therefore no reliable future production rate with a reduced wellhead pressure was provided and the wells were excluded from the further screening process.

4. Integrity of the completion

In order for wellhead compression to be successful, the tubing of the wellbore has to be completely tight, because if there are leaks along the tubing, the liquid which is lifted inside the tubing might enter the casing-tubing annulus and eventually flow back into the tubing, reducing the efficiency of the removal of liquids from the wellbore significantly. Therefore, the integrity of the completion was set as a knock- out criteria. For further screening purposes a proper integrity of the wells was assumed.

5. Summary of well screening

To make the different factors better comparable, the screened wells were ranked in the evaluated categories. The final ranking equals the arithmetic average of the individual rankings,also considering the flowrate ratio and reservoir potential equally with a weighting factor of 50%

Table 6: Final Ranking of the Well Screening

Well	Ranking Flowrate Ratio	Ranking Production Benefit	Final Ranking
Barrien T5	4	1	1
Staffhorst Z4	1	5	2
Barrien T2	3	3	2
Barrien T9	6	2	4
Düste T3	2	8	5
Barrien T3	5	6	6
Düste Z7	7	7	7
Düste T1	8	9	9
Düste Z8	9	10	10
Düste T4	10	11	11

It was decided to set a top 4 proposal of wells which are to be tested for wellhead compression to elongate their productive life. For further field tests Barrien T5, Barrien T2, Barrien T9 and Staffhorst Z4 are considered. Even though it was shown that the well Staffhorst Z4 would react positively to a reduced wellhead pressure, it will not be used for testing because currently it does not suffer from liquid loading.

8.2 Economic Analysis

An economic evaluation of the different compressor systems was conducted to determine the most favourable solution. The available compressor types were discussed in chapter 5.3.

It was assumed, that all compressors were installed at the production site Barrien T2 in the fourth quarter of 2016 and that production started in 2017 either until 2025 or until the economic cut-off (when the cash-flow turns negative) was reached.

The company which sells the reciprocating compressor offers two different operating options: a buy and a rent option. As the screw compressor can only be bought, also the buying option of the GasJack was included to better compare the results.

Table 7 shows the needed investments. It can be seen that the screw compressor has the highest initial investment costs of all compared systems. The installation of noise prevention measures was necessary, because the production sites are close to residential area where strict noise limits have to be maintained throughout production. The maintenance costs were estimated according to empirical knowledge.

Table 7: Cost Summary

		BUY: Reciprocating Compressor	RENT: Reciprocating Compressor	BUY: Screw Compressor	BUY: GasJack
Initial Investment					
- Compressor	T€	300	50	438	180
- Installation + Noise Prevention	T€	180	180	180	180
Rent [(1)]	T€/a		120		
Maintenance [(1)]	T€/a	20		20	20

[(1)] annual increase of 2,5%/a

Table 8: Summary of the economic analysis

Results		BUY: Reciprocating Compressor	RENT: Reciprocating Compressor	BUY: Screw Compressor	BUY: GasJack
Review Period		2016 - 2025	2016 - 2019	2016 - 2025	2016 - 2025
Revenue	T€	2222,5	1501,7	2579,3	2387,3
Expenses					
- Project Execution	T€	480,0	528,3	618,0	360,0
- Operating Costs, Royalties	T€	633,9	265,0	1439,6	710,0
- Taxes	T€	381,4	212,5	219,4	299,6
Cash-Flow after Tax	T€	727,2	495,9	302,3	1017,7

Net Present Value	T€	517,3	448,7	178,9	733,0
Internal Rate of Return	%	61,7	410,2	24,9	100,9
Payback Period	Years	1,9	1,2	2,7	1,6
Present Value Interest		2,1	1,9	1,3	3,0

Except for the rent option of the reciprocating compressor, the review periods are the obtainable 9 years. The trial duration of the rent option ends earlier, because it would generate a negative cash flow in 2020.

The expenses vary due to different initial costs and operating costs. Whereas the screw compressor is driven by an electrical motor, so the electrical power has to be bought in addition, the other compression systems are run with a gas engine, where prior produced gas can be used.

The net present value (NPV) was the first key performance indicator (KPI) analysed, it measures the profitability by discounting all future cash-flows to their present value. [39] When the NPV of the different options is compared, one sees that the GasJack has the highest value with 733T€, before the buy option of the reciprocating compressor (517,3T€), the rent option (448,7T€) and the screw compressor with the lowest value (178,9T€).

Another KPI is the internal rate of return (IRR), a percentage indicating the annual, average return. [40] The rent option shows an exceptionally high internal rate of return, with over 410%, which is due to the low initial project costs. The other options also have a significantly high IRR (GasJack 100,9% reciprocating buy: 61,7%), the lowest IRR has again the screw compressor (24,9%).

The payback period varies between 1,2 and 2,7 years, where the screw compressor shows the longest duration until the investment has paid off.

The findings of the conducted economic analysis show that all investment options are feasible. According to the KPIs, the top ranked option is the GasJack buy option, followed by the reciprocating compressor buy option. The reciprocating compressor rent option is ranked third, and the screw compressor on the other hand is ranked last. Even though the GasJack compressor shows the best KPIs, due to the negative experiences, which emerged when it was used the last time (see chapter 6.1 for details), one suggests to prefer the buy option of the reciprocating compressor.

9 Conclusion/ Interpretation

This thesis has shown, that wellhead compression can be a useful tool to extend the productive life and postpone the economic limit. Hence, it increases the recovery factor of Wintershall's gas wells, even whole fields in the Detfurth formation.

To find the problems and challenges, which have to be overcome to be able to challenge the economic – off of the gas fields, an extensive literature study was conducted.

Liquid loading was diagnosed to be one of the main challenges when operating mature gas fields. It is described as the process, when liquids start to accumulate at the bottom of the wellbore, leading to a decreased production. In the worst case, the reservoir pressure is too low to overcome the hydrostatic column and the well eventually dies.

There are various ways to recognize, predict and prevent liquid loading. This thesis focuses on the use of wellhead compression. The physical principle of compression as well as commonly used compression systems were discussed. A market study was conducted to detect compression systems which could be used to lower the wellhead pressure in the low productivity, low pressure sweet gas wells of Wintershall in the Detfurth formation.

A well screening was introduced, intending to find appropriate well candidates for a future field trial of wellhead compression. The well screening applied specified criteria. The first screening criteria was the production benefit, which was forecasted using reservoir models. By lowering the wellhead pressure most of the wells reacted with a significantly higher gas production. As a result, the gas flowrates increased, and also the recoverable reserves rose, due to the decreased abandonment pressure of the wells.

The second screening criteria evaluated, whether a reduction of the wellhead pressure would avoid liquid loading. A flowrate ratio was introduced to be able to rank the severity of appearing liquid loading. The ratio was calculated with the current operation conditions and with the forecasted conditions with a lowered wellhead pressure. The screening proposed four wells to be the best suited candidates for future field trials.

Especially in the first years of deployment, a significantly higher gas production can be achieved when the wellhead pressure is lowered. So it might prove successful to use a mobile wellhead compression system which can be easily moved from one production site to another to increase the gas production of a well for two to three years, where the major additional gas production can be achieved. This approach has proved to be successful for a variety of mature gas fields in Europe operated by different E&P companies. [51]

For further evaluation of the wellhead compression systems, it is suggested to perform a field study at the chosen wells candidates to prove the shown theoretical positive effects of compression on the gas production. The analysed and suggested reciprocating compressor system could be tested in the scope of a conducted technology project.

Furthermore, a new technology, which uses downhole gas compression systems was found, which might also be an option to boost gas production and elongate the wells life in the future. [49] Instead of mounting the compressor to the wellhead, the compressor is positioned downhole, in the region of the perforations of the wellbore. This brings the advantage that the bottomhole flowing pressure can be reduced even further when compared to conventional wellhead compression.

To sum up, wellhead compression proves to be an effective gas well deliquification method. The conducted screening of possible well and compressor systems, which are applicable for the gas fields of Wintershall in the Detfurth formation in northern Germany showed promising results. To successfully use wellhead compression in the field, further carefully carried out research is suggested, to ensure that the field trials become successful.

10 Registers

10.1 Reference List

[1] T. Ahmed, Reservoir Engineering Handbook, Amserdam: Elsevier, 2006, p. p.855 .

[2] F. Jahn, M. Cook and M. Graham, Hydrocarbon Exploration and Production, 2. ed., Amsterdam: Elsevier, 2008, p. p.120 .

[3] V. MacKay, Determination of Oil and Gas Reservoirs, The Petroleum Society of the Canadian Institute of Mining, Metallurgy and Petroleum, 2004, pp. p.146-147 .

[4] A. Sattler, G. M. Iqbal and J. L. Buchwalter, Practical Enhanced Reservoir Engineering: Assisted with Simulation Software, 2007, pp. p.356-357.

[5] M. Kelkar, Natural Gas Production Engineering, Tulsa: PennWell Corporation, 2007.

[6] L. P. Dake, Fundamentals of Reservoir Engineering, Amsterdam: Elsevier, 1998, p. p. 27.

[7] “Mature Fields,” Society of Petroleum Engineers, 5 October 2015. [Online]. Available: http://petrowiki.org/Mature_fields.

[8] M. J. Economides, D. A. Hill and C. Ehlig-Economides, Petroleum Production Systems, USA: PTR Pretice Hall, 2010, p. p.148 .

[9] J. F. Lea, H. V. Nickens and M. R. Wells, Gas Well Deliquification, 2. ed., Gulf Professional Publishing, 2008.

[10] R. G. Turner, M. G. Hubbard and A. E. Dukler, “Analysis and Prediction of Minimum Flowrate for the Continuous Removal of Liquids from Gas Wells,” *Journal of Petroleum Technology,* 1969.

[11] J. Li, F. Almudairis and H. Zhang, “Prediction of Critical Gas Velocity of Liquid Unloading for Entire Well Deviation,” in *IPTC 17846*, Kuala Lumpur, 2014.

[12] R. P. Sutton, S. A. Cox, J. F. Lea and O. Lynn, “Guidelines for Proper Application of Critical Velocity Calculations,” in *SPE 120625*, Oklahoma, 2009.

[13] O. J. Hinze, “Critical Speeds and Sizes of Liquid Globules,” *Applied Scientific Research,* p. 273-288, 1949.

[14] S. B. Coleman, H. B. Clay, D. G. McCurdy and H. L. Norris III, "A New Look at Predicting Cas-Well Load-Up," *Journal of Petroleum Technology,* 9. February 1990.

[15] M. Li, S. L. Li and L. T. Sun, “New View on Contiuous- Removal Liquids from Gas Wells,” *SPE Production & Facilities,* pp. 42-46, February 2002.

[16] G. Yuan, Liquid Loading of Gas Wells, Tulsa: The University of Tulsa, 2011.

[17] T. R. Neves and R. M. Brimhall, "Elimination of Liquid Loading in Low-Productivity Gas Wells," in *SPE 18833*, Oklahoma, 1989.

[18] J. F. Lea and H. V. Nickens, “Solving Gas-Well Liquid-Liading Problems,” *JPT,* p. 30-36, April 2004.

[19] Y. Nallaparaju, “Prediction of Liquid Loading,” in *9th Biennial International Conference & Exposition on Petroleum Geophysics*, Hyderabad, 2012.

[20] A. Joseph, C. M. Sand and J. A. Ajienka, “Classification and Management of Liquid Loading in Gas Wells,” in *SPE 167603*, Lagos, 2013.

[21] C. H. Whitson, S. D. Rahmawati and A. Juell, “Cyclic Shut-in Eliminates Liquid- Loading in Gas Wells,” in *SPE 153073*, Vienna, 2012.

[22] G. J. Koperna Jr., “Review and Selection of Velocity Tubing Strings for Efficient Liquid Lifting in Stripper Gas Wells,” Advanced Resources International, Inc., Arlington, 2004.

[23] J. Quintana, E. Duque, J. D. Diaz, J. Eras, J. Rodas, E. Vergara and W. Prieto, “Coiled Tubing Velocity String Hang-Off Solves and Prevents Liquid- Loading Problems in Gas Well: Case Study in the Gulf of Guayaqull, Equador,” in *SPE 177264*, Quito, 2015.

[24] G. Schwaiger, Modelling of Critical Gas Velocities based on the Entrained Droplet Model for Gas Wells and the Effect of Heat Loss on Gas Production, Leoben: Montanuniversität Leoben, 2016.

[25] G. Stephenson, R. Rouen and M. Rosenzweig, “Gas-Well Dewatering: A Coordinated Approach,” in *SPE 58984*, Vilahemosa, 2000.

[26] R. W. Donnelly, Oil and Gas Production - Artificial Lift, Austin: Petroleum Extension Service Division of Continuing Education,The UNiversity of Texas at Austin, 1985.

[27] K. Veeken, “Basics of Gas Well Deliquification,” in *7th European Gas Well Deliquification Conference*, Groningen, 2012.

[28] C. Passucci, O. Imbo and M. Pelucchi, “Downhole Injection of Foaming Agents with Capillary String in a Mediterranean Offshore Gas Well,” in *OMC 2011-182*, Ravenna, 2011.

[29] S. Peyton, Investigation of Batch Foamer Efficiency and Optimisation in North Sea Gas Condensate Wells, London: Imperial College London, 2013.

[30] L. K. Harms, “Installing Low-Cost, Low-Pressure Wellhead Compression on Tight Lobo Wilcox Wells in South Texas: A Case History,” in *SPE 90550*, Texas, 2004.

[31] W. C. Lyons and G. J. Plisga, Standard Handbook of Petroleum and Natural Gas Engineering, Amsterdam: Elsevier, 2005, pp. p.3-48.

[32] J. R. Fanchi, Petroleum Engineering Handbook, Vol. 3, Texas: Society of Petroleum Engineers, 2006, pp. p. III-261-262.

[33] P. C. Hanlon, Compressor Handbook, New York: McGraw-Hill, 2001, p. p. 5.6.1.

[34] J. M. Campbell, Gas Conditioning and Processing. Vol. 2: The Equipment Modules, Oklahoma: PetroSkills, 2014, p. p. 157.

[35] D. H. Robison and P. J. Beaty, “Compressor Types, Classifications and Applications,” in *Proceedings of the Twenty-First Turbomachinery Symposium*, Delaware, 1992.

[36] W. E. Forsthoffer, Forsthoffer's Rotating Equipment Handbooks. Vol. 3: Compressors, Amsterdam: Elsevier, 2005, pp. p. 4, 115.

[37] “AtlasCopco,” [Online]. Available: http://www.atlascopco.com/classzerode/download/imagedownloads/classzerocomp/. [Accessed 12 2016].

[38] R. Salimat, “Quora,” [Online]. Available: https://www.quora.com/Which-mechanism-is-preferable-for-reciprocating-compressors. [Accessed 23 January 2017].

[39] “CSI Compressco,” [Online]. Available: http://www.csicompressco.com/products-and-services/compression-services/production-enhancement/gasjack-compressors/. [Accessed 20 January 2017].

[40] K. E. Arnold and L. W. Lake, Petroleum Engineering Handbook, Vol.3: Facilities and Construction Engineering, Richardson: Society of Petroleum Engineers, 2007, pp. p. III-396 .

[41] T. Dr. Boyle, Health and Safety: Risk Management, Abingdon: Routledge, 2015.

[42] “NORM (LSA) Management,” Sureclean, [Online]. Available: http://www.sureclean.com/services/norm-management. [Accessed 23 November 2016].

[43] S. Salchenegger, “Disposalkapazitäten der Gasbetriebe Nord- Aktueller Stand und Ausblick,” Wintershall Holding GmbH, Barnstorf, 2015.

[44] “Sechste Allgemeine Verwaltungsvorschrift zum Bundes-Immissionsschutzgesetz (Technische Anleitung zum Schutz gegen Lärm – TA Lärm),” 26 August 1998. [Online]. Available: http://www.verwaltungsvorschriften-im-internet.de/bsvwvbund_26081998_IG19980826.htm. [Accessed 5 December 2016].

[45] E. P. u. Rat, *Verordnung (EG) Nr. 1272/2008 (CLP) über die Einstufung. Kennzeichnung und Verpackung von Stoffen und Gemischen,* Brüssel: EU, 2008.

[46] D. Bjerketvedt, J. R. Bakke and K. van Wingerden, Gas Explosion Handbook, Gexcon, 1992, p. p.124 .

[47] D. G. Unfallversicherung, *DGUV Regel 113-001: Explosionsschutz - Regeln,* DGUV, 2016, p. p. 37.

[48] C. Joerges, “Explosionsschutzdokument für den Erdgasförderbetrieb Staffhorst (DEP/N-Sh),” Wintershall Holding GmbH, Barnstorf, 2016.

[49] H. Duhon and J. Cronin, “Risk Assessment in HAZOPs,” in *SPE 173544*, Denver, 2015.

[50] H.-U. Krause and D. Arora, Controlling - Kennzahlen - Key Performance Indicators, Oldenbourg: De Gruyter Oldenbourg, 2008, p. p.141 .

[51] B. J. Feibel, Investment Performance Measurement, Frank J. Fabozzi Series, 2003.

[52] M. Seywald, “RAG Deliquification Experience, Scope and Strategy,” in *Gas Well Deliquification Conference*, Groningen, 2011.

[53] M. D. Tullio, S. Fomasari, D. Ravaglia, N. Bernatt and J. Liley, “Downhole Gas Compression: World's First Installation of a New Artificial Lifting System for Gas Wells,” in *SPE 121815*, Amsterdam, 2009.

[54] T. O. Allen and A. P. Roberts, Production Operations, Well Completion, Workover, and Stimulation Volume 2, Tulsa, Oklahoma: OGCI,Inc.,PetroSkills,LLC., 2008.

[55] Edwin C. Moritz and Natalie Barron, “Wattenberg Field Unconventional Reservoir Case Study,” in *SPE Middel East Unconventional Gas Conference*, Abu Dhabi, 2012.

[56] S. B. Coleman, H. B. Clay, D. G. McCurdy and H. L. Norris III, “Understanding Gas-Well Load-Up Behavior,” *Journal of Petroleum Technology,* March 1991.

[57] “Petrowiki,” SPE, [Online]. Available: http://petrowiki.org/Mature_fields. [Accessed 2016].

[58] S. Belfroid, W. Schiferli and J. Veltin, “Liquid Loading Experiments with Tube Wall Modifications,” BHR Group, The Netherlands, 2011.

[59] R. Schmitz and G. Steele, “Combining Plunger Lift and Compression to Lift Liquids in Low Rate Gas Wells,” in *PETSOC 2006-159*, Calgary, 2006.

10.2 List of Tables

10.3 List of Figures

10.4 Abbreviations

CIL	Chemical injection line
DGUV	German Statutory Accident Insurance (Deutsche gesetzliche Unfallversicherung)
EC	European community
E&P	Exploration and Production
ESP	Electric submersible pump
FWKO	Free water knock out
GAP™	General allocation package
GLR	Gas-liquid ratio
GWC	Gas water contact
HAZOP	Hazard and operability study
ID	Inner diameter
IGIP	Initial gas in place
IPM	Integrated production modelling
MBAL™	Material balance
MD	Measured depth
Mio m^3, Mm^3	Million cubic meter
NORM	Naturally occurring radioactive material
IPR	Inflow performance relationship
PCP	Progressing cavity pump
PPP	Petroleum Production and Processing
PROSPER™	Production and Performance
PVT	Pressure, volume, temperature
Sm^3	Standard m^3 (volume at standard conditions)
SGU	Applied plant safety (Sicherheits-, Gesundheits- und Umweltschutz)
SRP	Sucker rod pump
TPC	Tubing performance curve
T€	Thousand Euro
VLP	Vertical lift performance

10.5 List of Symbols

A	flow area	[in^2]
A_D	area droplet	[in^2]
B_g, B_w	formation volume factor for gas and water at a given pressure	[m^3/Sm^3]
B_{gi}	formation volume factor for gas at initial pressure	[m^3/Sm^3]
C	performance coefficient	
C_D	drag coefficient	[ ]
c_f	formation compressibility	[1/Pa]
c_w	water compressibility	[1/Pa]
d	diameter of droplet	[in]
d_{ti}	tubing inside diameter	[in^2]
F_D	drag force	[lbf], [N]
F_G	gravitational force	[lbf], [N]
g	gravitational constant	[ft/s^2]
g_c	gravitational conversion constant	[$lbm*ft/lbf*s^2$]

G_i	initial gas in place	[Sm^3]
G_P, W_P	produced gas, water	[Sm^3]
k	specific heat ratio	[ ]
M	molecular mass air	[g/mol]
n	deliverability exponent	[ ]
n_p	polytropic index	[ ]
N_{WE}	Weber number	[ ]
p	pressure	[kPa], [psi]
$\overline{p_r}$	average reservoir pressure	[kPa]
p_{wf}	well flowing pressure	[kPa]
Δp	change in pressure	[kPa]
PV	pore volume	[m^3]
q	gas flowrate	[m^3/d]
q_t	critical flowrate	[Mio scf/d], [Mio m^3/d]
R	universal gas constant	[psi*ft^3/(lb*mol*°R)]
S_w	water saturation	[ ]
S_{wc}	connate water saturation	[ ]
T	temperature	[°K], [°F], [°R]
V	volume	[m3]
v_D	droplet velocity	[ft/s]
v_t	critical velocity	[ft/s],[m/s]
W_e	cumulative water influx	[Sm^3]
z	compressibility factor,	[ ]
γ_G	gas gravity	[ ]
ρ_l, ρ_g	density of liquid or gas	[lbm/ft^3]
σ	surface tension	[dynes/cm]

Appendices

Appendix A

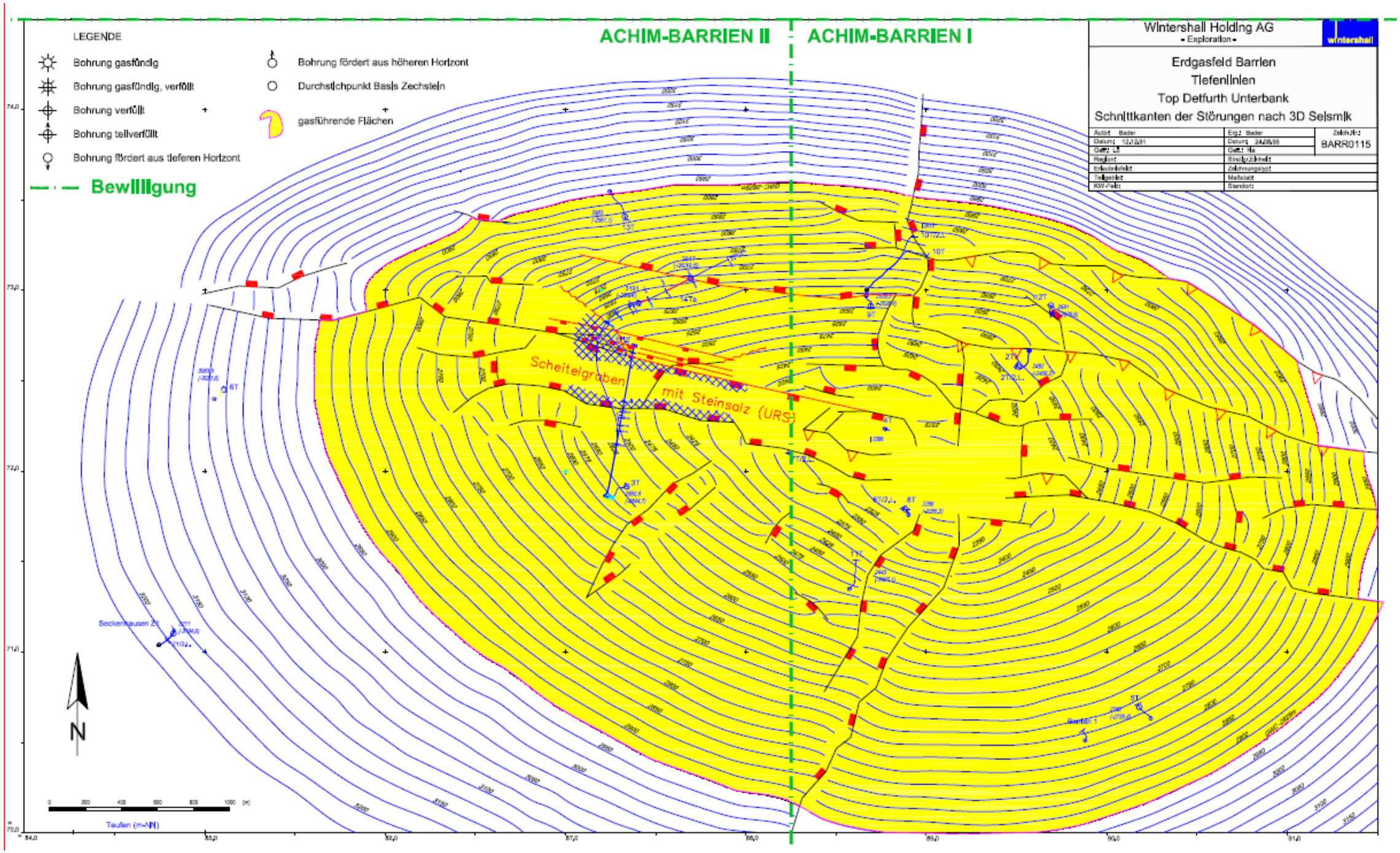

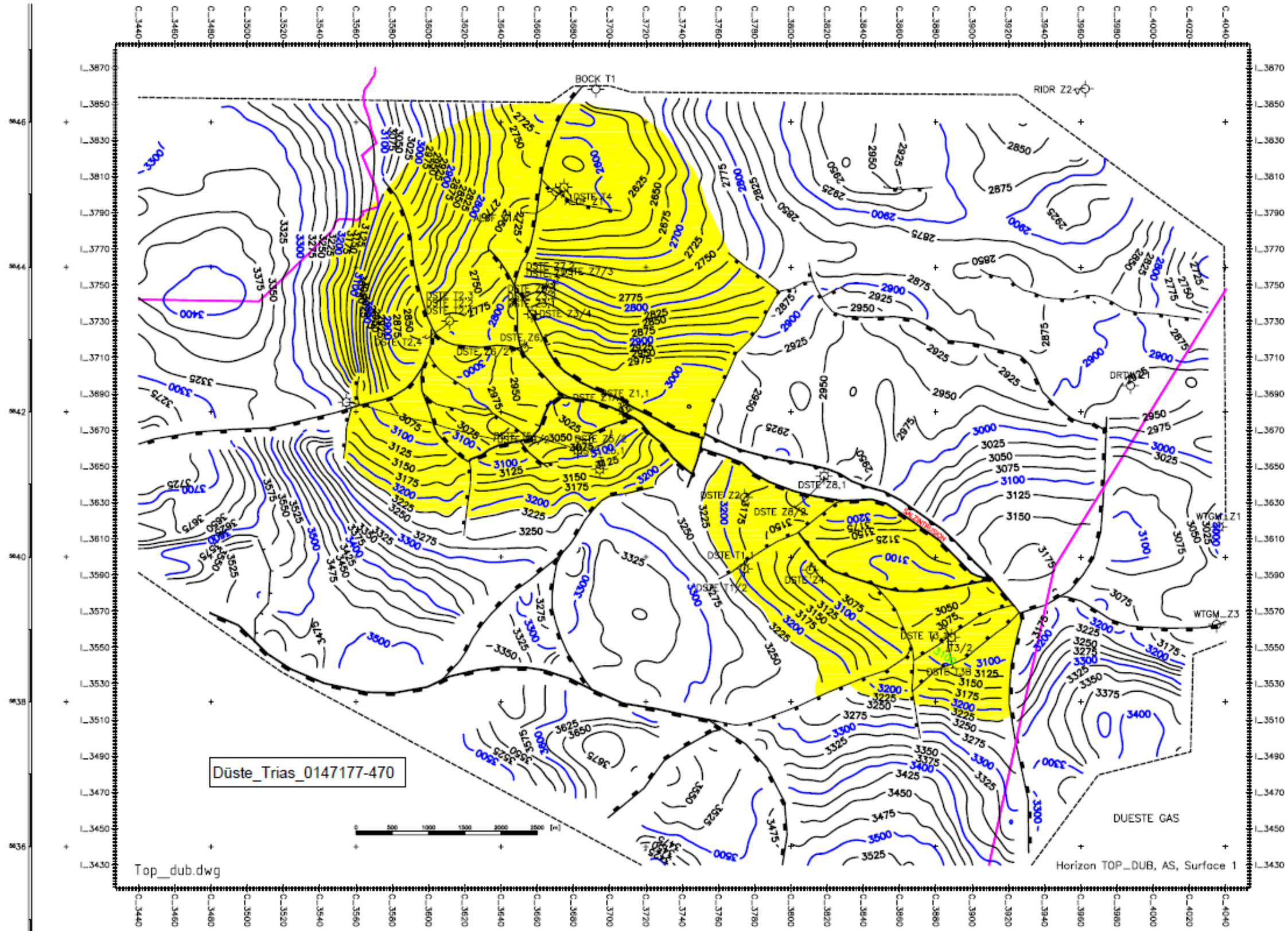
BOCK T1
RIDR Z2
DSTE T4
DSTE Z7,2
DSTE Z7,3
DSTE Z7,5
DSTE T2,3
DSTE T2,2
DSTE Z3/4
DSTE Z6,1
DSTE Z6/2
DSTE Z1,1
DSTE Z8,1
DSTE Z2,1
DSTE Z8/4
DSTE T1,1
DSTE T2,4
DSTE T1,1/2
DSTE Z3/2
DSTE T3,8
DRTM_Z1
WTGM_Z1
WTGM_Z3
DUESTE GAS
Düste_Trias_0147177-470
Top_dub.dwg
Horizon TOP_DUB, AS, Surface 1

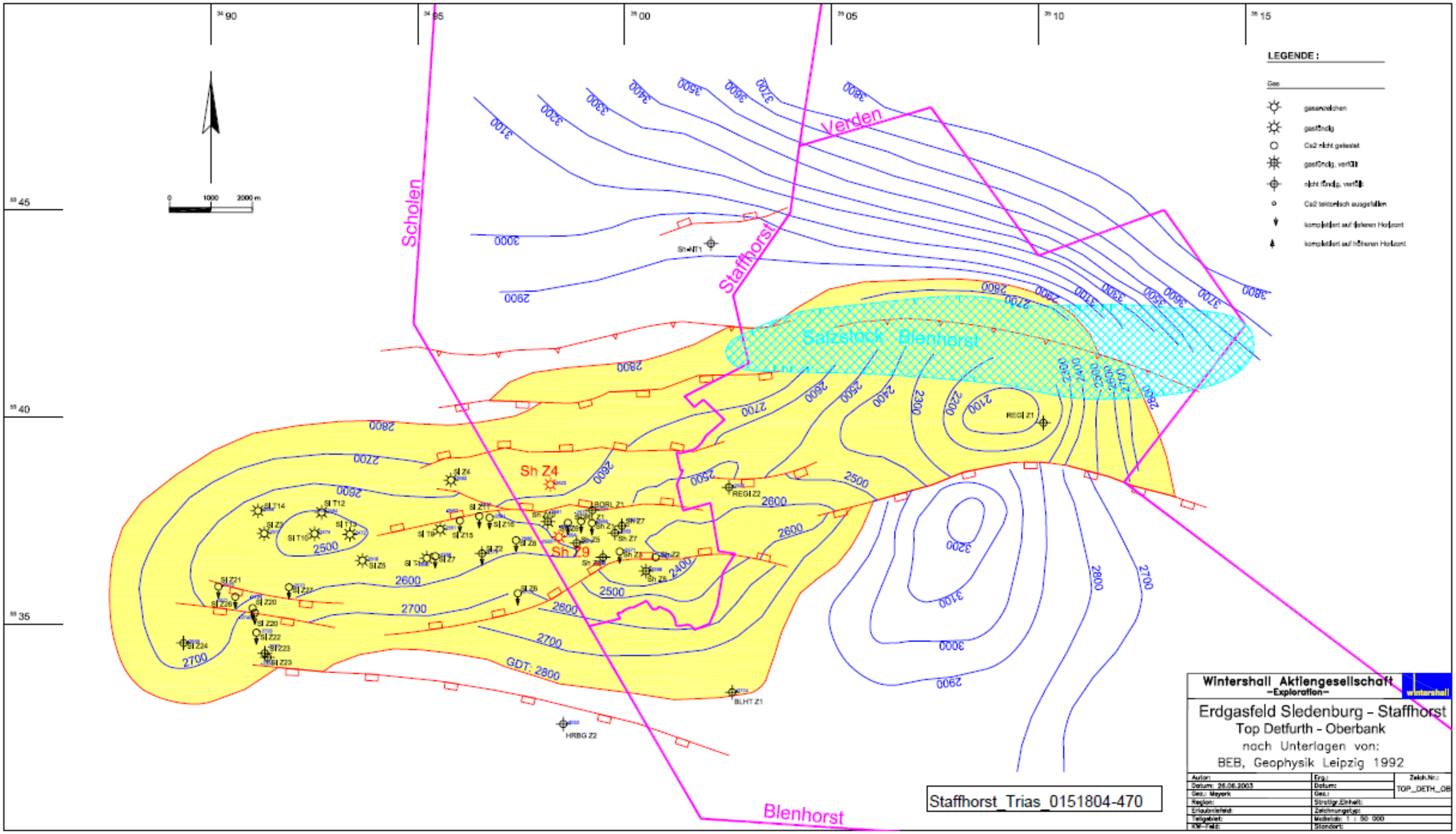
34 90
34 95
35 00
35 05
35 10
35 15
55 45
55 40
55 35
0 1000 2000 m
Scholen
Staffhorst
Verden
Blenhorst
Salzstock Blenhorst
Sh Z4
Sh Z9
SHENT1
REGI Z1
REGI Z2
BORL Z1
BLHT Z1
HRBG Z2
GDT: 2800
LEGENDE :
Gas
gasanzeichen
gasführdig
Co2 nicht getestet
gasführdig, verfüllt
nicht führdig, verfüllt
Co2 teilweise ausgefallen
komplettiert auf tieferen Horizont
komplettiert auf höheren Horizont
Staffhorst_Trias_0151804-470
Wintershall Aktiengesellschaft
-Exploration-
Erdgasfeld Sledenburg - Staffhorst
Top Detfurth - Oberbank
nach Unterlagen von:
BEB, Geophysik Leipzig 1992
Autor:
Datum: 26.06.2003
Ges.: Mayerk
Region:
Erlaubnisfeld:
Teilgebiet:
KW-Feld:
Erg.:
Datum:
Ges.:
Zeich.Nr.:
TOP_DETH_OB
Stratigr.Einheit:
Zeichnungstyp:
Maßstab: 1 : 50 000
Standort:

Appendix B

Table 9: Tank details used for the MBAL™ models for the reservoirs Barrien, Staffhorst and Düste.

	Temperature	Initial Pressure	Porosity	Connate Water Saturation	IGIP	Start of Production
	[°C]	[bar]	[ ]	[ ]	[Mio m^3]	[YYYY]
Barrien						
T11	106	407	0,15	0,28	2190	1964
T12	106	404	0,15	0,25	450	1964
T12a	106	407	0,15	0,25	80	1964
T13	106	404	0,15	0,25	200	1964
T15	106	407	0,15	0,28	1300	1964
T2	106	404	0,15	0,25	300	1964
T2a	106	407	0,15	0,25	200	1964
T3	106	407	0,15	0,28	3610	1964
T5	106	407	0,15	0,28	2420	1964
T8	106	407	0,15	0,28	1995	1964
T9T14	106	404	0,15	0,25	2265	1964
Staffhorst						
Staffhorst	116	356	0,07	0,35	1650	1963
Sta-dicht	116	356	0,07	0,35	300	1963
Siedenburg	116	356	0,1	0,3	10000	1963
Sie-dicht	116	356	0,1	0,3	5600	1963
Düste						
T1a	136	447	0,1	0,2	52	1966
T1a-a	136	447	0,1	0,2	80	1966
T3b	137	448	0,1	0,2	130	1965
T4	124	459	0,1	0,2	40	1990
Z5	133	461	0,1	0,2	350	1962
Z5-T5	133	461	0,1	0,2	40	1962
Z7	124	432	0,1	0,25	380	1965
Z7a	124	432	0,1	0,25	115	1965
Z8a	133	455	0,1	0,25	62	1986
Z9	123	438	0,1	0,2	117	1996

Appendix C

The tables and figures below show the detailed analysis of the additional reservoir potential. The wellhead pressure was lowered from 16 bar to 3 bar, and the change in the gas production rate and the cumulative gas production was calculated using MBAL™ /GAP™ models.

Table 10: Minimum Gas Rates used for the MBAL™ models. When the simulation of the wells forecast rates below the minimum gas rate, the well is shut and abandoned.

Well	**Minimum Gas Rate** [m^3/h]
Barrien T2	250
Barrien T3	150
Barrien T5	500
Barrien T9	500
Barrien T12	-
Düste T1	50
Düste T3	-
Düste T4	50
Düste Z7	50
Düste Z8	50
Staffhorst Z4	200
Staffhorst Z9	200

Table 11: Calculation of the Z-factor according to the Beggs&Brill model

Z Factor	(Beggs & Brill)
p_{pcf}	46,39
T_{pcf}	200,57
p_{prf}	0,32
T_{prf}	1,44
a	0,38
b	0,10
c	0,08
d	0,94
Z	**0,97**

Table 12: Overview of the relevant completion data for the investigated wells

Well	Casing @ Perforation Depth [in]	Tubing OD [in]	Tubing ID [in]
Barrien T2	5	2 7/8	2 2/5
Barrien T3	7	2 3/8	2
Barrien T5	7	3 1/2	3
Barrien T9	7	3 1/2	3
Barrien T12	7	3 1/2	3
Düste T1	7	2 3/8	2
Düste T3	4 1/2	2	1 3/5
Düste T4	7	3 1/2	3
Düste Z7	5	2 7/8	2 2/5
Düste Z8	7	2 7/8	2 2/5
Staffhorst Z4	5	2 3/8	2
Staffhorst Z9	9 5/8	2 7/8	2 2/5

Table 13: Annual Rates and Production for Barrien T3

Year	Average Gas Rate without WHC [Sm³/h]	Average Gas Rate with WHC [Sm³/h]	Cumulative Gas Production without WHC [Mio Sm³]	Cumulative Gas Production with WHC [Mio Sm³]	Annual Production without WHC [Mio Sm³]	Annual Production with WHC [Mio Sm³]	Additional Production [Mio Sm³]
2017	247	371	2,47	3,86	2,47	3,86	1,38
2018	229	316	4,76	7,29	2,28	3,43	1,15
2019	212	272	6,88	10,21	2,12	2,92	0,81
2020	197	236	8,84	12,72	1,96	2,51	0,55
2021	183	206	10,67	14,91	1,83	2,18	0,36
2022	169	181	12,36	16,81	1,69	1,90	0,21
2023	0	160	13,92	18,48	1,56	1,67	0,11
2024	0	0	13,92	19,95	0,00	1,48	1,48
2025	0	0	13,92	19,95	0,00	0,00	0,00
						Total Additional Production	**6,04**

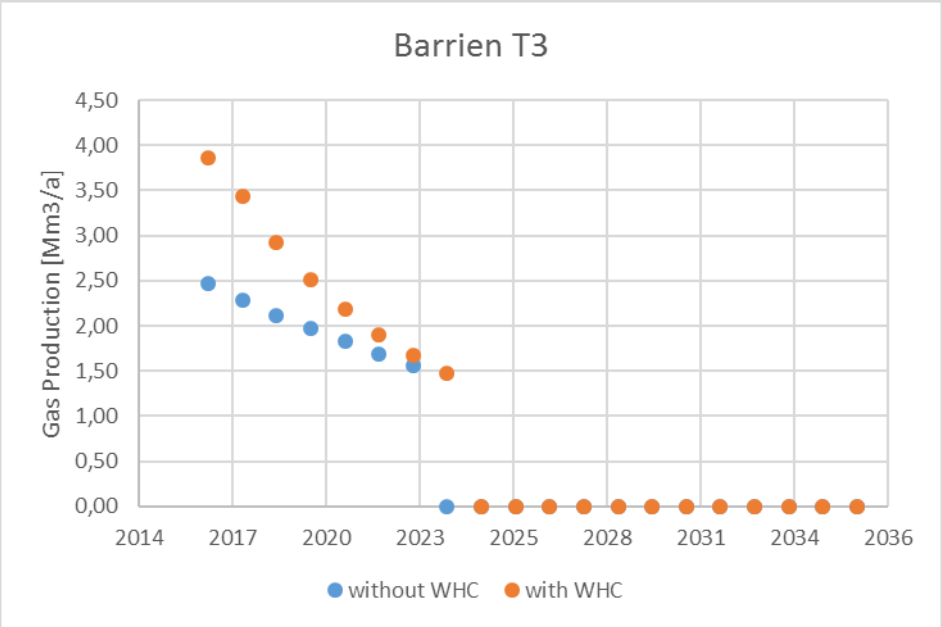

Figure 47: Annual Gas Production Forecast

Table 14: Annual Rates and Production for Barrien T5

Year	Average Gas Rate without WHC [Sm³/h]	Average Gas Rate with WHC [Sm³/h]	Cumulative Gas Production without WHC [Mio Sm³]	Cumulative Gas Production with WHC [Mio Sm³]	Annual Production without WHC [Mio Sm³]	Annual Production with WHC [Mio Sm³]	Additional Production [Mio Sm³]
2017	788	1843	7,49	18,00	7,49	18,00	10,51
2018	769	1751	14,78	35,04	7,29	17,04	9,75
2019	751	1668	21,88	51,22	7,11	16,18	9,08
2020	734	1591	28,83	66,63	6,94	15,41	8,47
2021	718	1520	35,63	81,38	6,80	14,75	7,95
2022	702	1454	42,27	95,43	6,64	14,05	7,42
2023	687	1392	48,75	108,87	6,49	13,44	6,95
2024	672	1335	55,10	121,73	6,35	12,87	6,52
2025	658	1280	61,33	134,10	6,23	12,37	6,14
2026	645	1228	67,41	145,93	6,08	11,83	5,75
2027	631	1180	73,36	157,28	5,96	11,35	5,39
2028	619	1134	79,20	168,19	5,83	10,91	5,07
2029	607	1091	84,93	178,70	5,74	10,51	4,78
2030	595	1050	90,54	188,78	5,61	10,08	4,47
2031	584	1011	96,04	198,49	5,50	9,70	4,20
2032	574	974	101,44	207,83	5,40	9,35	3,95
2033	563	939	106,76	216,86	5,31	9,03	3,72
2034	553	906	111,96	225,54	5,20	8,68	3,48
2035	543	875	117,07	233,91	5,11	8,37	3,26
2036	534	844	122,09	242,00	5,02	8,08	3,06
					Total Additional Production		**119,91**

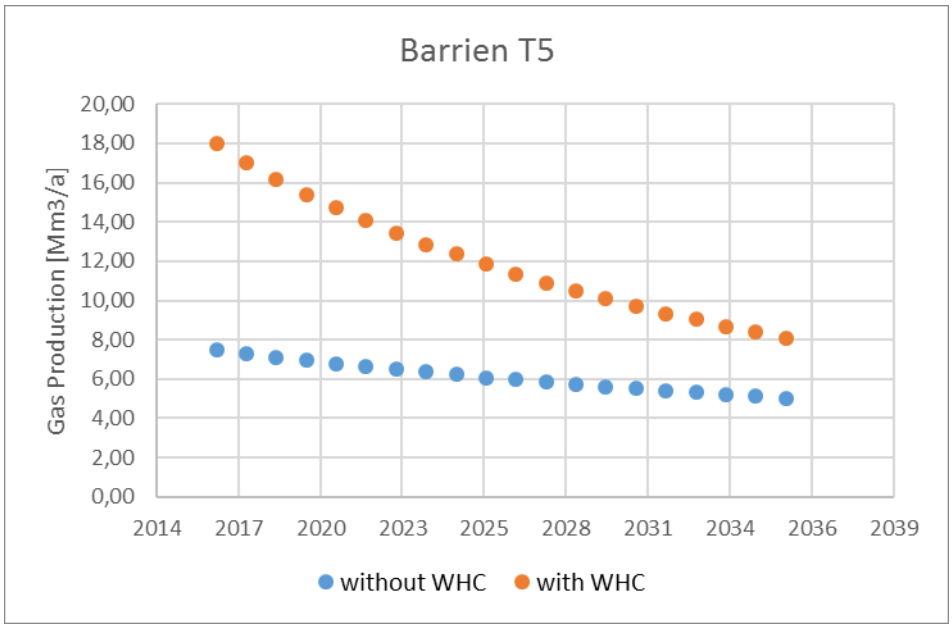

Figure 48: Annual Gas Production Forecast

Table 15: Annual Rates and Production for Barrien T9

Year	Average Gas Rate without WHC [Sm³/h]	Average Gas Rate with WHC [Sm³/h]	Cumulative Gas Production without WHC [Mio Sm³]	Cumulative Gas Production with WHC [Mio Sm³]	Annual Production without WHC [Mio Sm³]	Annual Production with WHC [Mio Sm³]	Additional Production [Mio Sm³]
2017	662	780	6,346	7,438	6,35	7,44	1,09
2018	640	758	12,461	14,644	6,12	7,21	1,09
2019	619	737	18,373	21,651	5,91	7,01	1,10
2020	598	717	24,09	28,464	5,72	6,81	1,10
2021	575	698	29,633	35,107	5,54	6,64	1,10
2022	554	679	34,95	41,553	5,32	6,45	1,13
2023	533	661	40,068	47,827	5,12	6,27	1,16
2024	512	643	44,992	53,933	4,92	6,11	1,18
2025	493	627	49,74	59,896	4,75	5,96	1,22
2026	474	611	54,293	65,689	4,55	5,79	1,24
2027	450	595	58,675	71,332	4,38	5,64	1,26
2028	423	580	62,834	76,832	4,16	5,50	1,34
2029	397	565	66,756	82,208	3,92	5,38	1,45
2030	371	551	70,424	87,433	3,67	5,23	1,56
2031	296	538	73,849	92,527	3,43	5,09	1,67
2032	0	525	76,584	97,496	2,74	4,97	2,23
2033	0	512	76,584	102,358	0,00	4,86	4,86
2034	0	499	76,584	107,089	0,00	4,73	4,73
2035	0	488	76,584	111,705	0,00	4,62	4,62
2036	0	476	76,584	116,212	0,00	4,51	4,51
					Total Additional Production		**39,63**

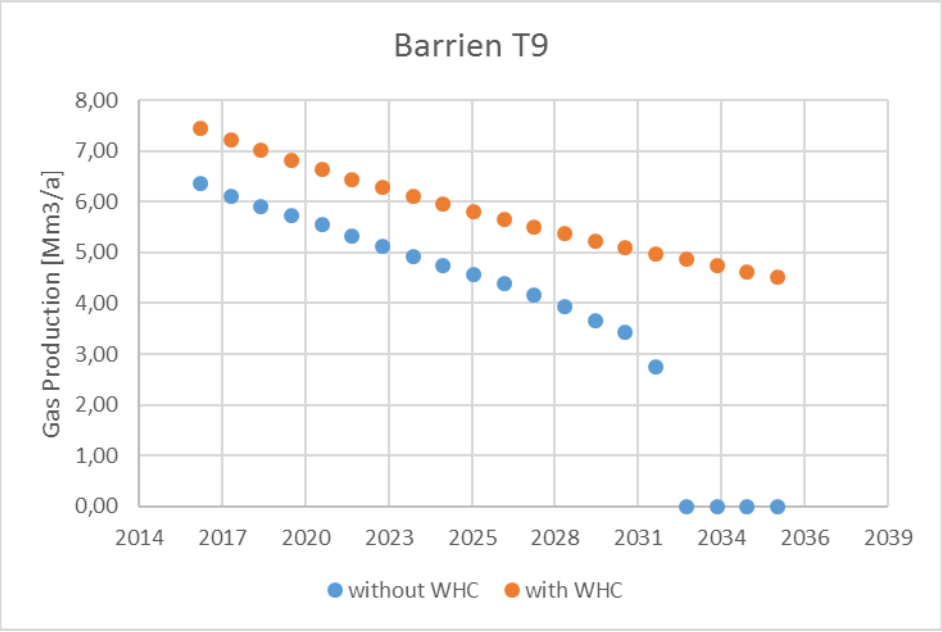

Figure 49: Annual Gas Production Forecast

Table 16: Annual Rates and Production for Düste T1

Year	Average Gas Rate without WHC [Sm³/h]	Average Gas Rate with WHC [Sm³/h]	Cumulative Gas Production without WHC [Mio Sm³]	Cumulative Gas Production with WHC [Mio Sm³]	Annual Production without WHC [Mio Sm³]	Annual Production with WHC [Mio Sm³]	Additional Production [Mio Sm³]
2017	139	146	4,75	4,81	3,54	3,54	0,00
2018	130	136	5,87	5,98	1,21	1,27	0,06
2019	121	127	6,91	7,08	1,12	1,18	0,06
2020	114	119	7,89	8,11	1,04	1,10	0,05
2021	107	112	8,81	9,07	0,98	1,03	0,05
2022	102	106	9,68	9,98	0,92	0,96	0,04
2023	97	101	10,51	10,85	0,87	0,91	0,04
2024	92	97	11,30	11,67	0,83	0,87	0,04
2025	88	92	12,05	12,46	0,79	0,83	0,04
2026	85	89	12,77	13,21	0,75	0,79	0,03
2027	81	85	13,46	13,93	0,72	0,75	0,03
2028	78	82	14,13	14,63	0,69	0,72	0,03
2029	75	79	14,76	15,30	0,67	0,70	0,03
2030	73	76	15,38	15,95	0,64	0,67	0,03
2031	70	74	15,98	16,57	0,62	0,65	0,03
2032	68	71	16,56	17,18	0,60	0,62	0,03
2033	66	69	17,11	17,76	0,58	0,60	0,03
2034	64	67	17,66	18,33	0,56	0,59	0,03
2035	62	65	18,18	18,88	0,54	0,57	0,03
2036	60	63	18,69	19,41	0,52	0,55	0,03
						Total Additional Production	**0,70**

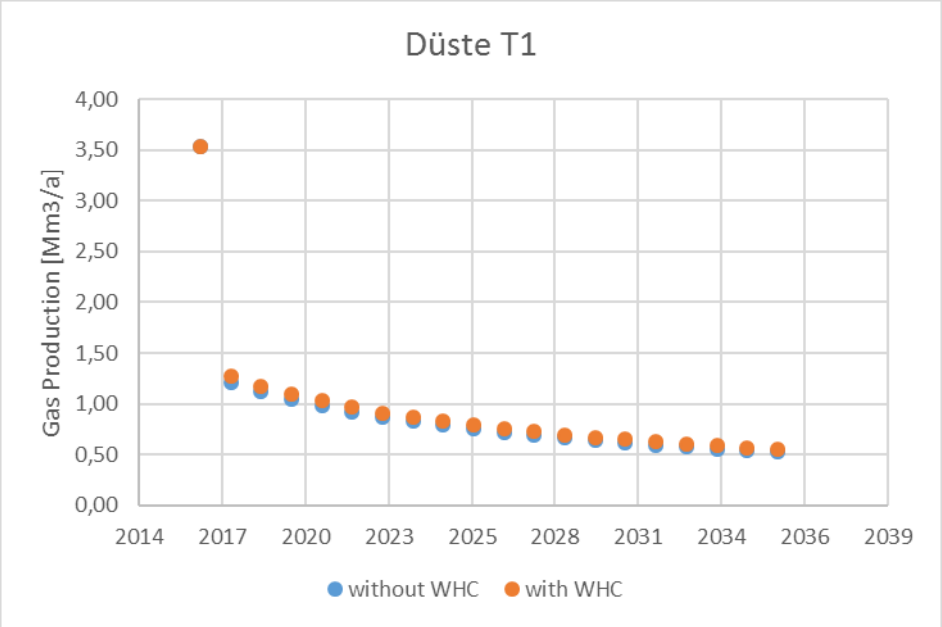

Figure 50: Annual Gas Production Forecast

Table 17: Annual Rates and Production for Düste T3

Year	Average Gas Rate without WHC [Sm³/h]	Average Gas Rate with WHC [Sm³/h]	Cumulative Gas Production without WHC [Mio Sm³]	Cumulative Gas Production with WHC [Mio Sm³]	Annual Production without WHC [Mio Sm³]	Annual Production with WHC [Mio Sm³]	Additional Production [Mio Sm³]
2017	36	58	1,26	1,45	0,95	0,95	0,00
2018	33	54	1,55	1,92	0,32	0,51	0,19
2019	30	49	1,81	2,35	0,29	0,47	0,18
2020	27	46	2,05	2,75	0,26	0,43	0,17
2021	25	42	2,27	3,11	0,24	0,40	0,16
2022	23	39	2,47	3,45	0,22	0,37	0,15
2023	21	36	2,65	3,76	0,20	0,34	0,14
2024	19	34	2,82	4,05	0,18	0,31	0,13
2025	18	31	2,97	4,33	0,17	0,29	0,13
2026	16	29	3,11	4,58	0,15	0,27	0,12
2027	15	27	3,24	4,82	0,14	0,25	0,11
2028	14	26	3,36	5,04	0,13	0,24	0,11
2029	12	24	3,47	5,24	0,12	0,22	0,10
2030	11	23	3,57	5,44	0,11	0,21	0,10
2031	11	21	3,66	5,62	0,10	0,20	0,10
2032	10	20	3,75	5,80	0,09	0,18	0,09
2033	9	19	3,82	5,96	0,09	0,17	0,09
2034	8	18	3,89	6,11	0,08	0,16	0,09
2035	8	17	3,96	6,26	0,07	0,15	0,08
2036	7	16	4,02	6,40	0,07	0,15	0,08
					Total Additional Production		**2,30**

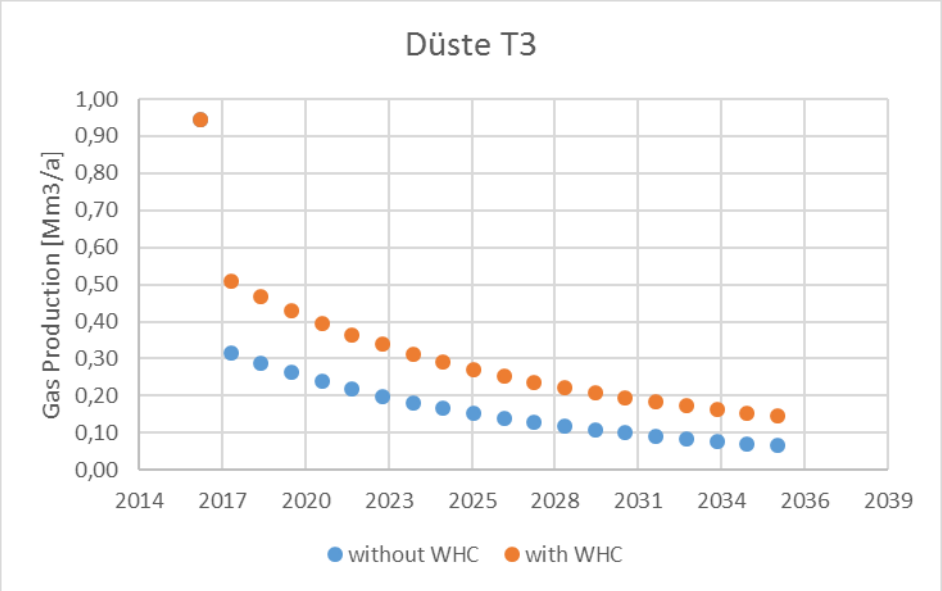

Figure 51: Annual Gas Production Forecast

Table 18: Annual Rates and Production for Düste T4

Year	Average Gas Rate without WHC [Sm³/h]	Average Gas Rate with WHC [Sm³/h]	Cumulative Gas Production without WHC [Mio Sm³]	Cumulative Gas Production with WHC [Mio Sm³]	Annual Production without WHC [Mio Sm³]	Annual Production with WHC [Mio Sm³]	Additional Production [Mio Sm³]
2017	97	99	3,08	3,10	2,26	2,26	0,00
2018	93	94	3,87	3,90	0,83	0,84	0,01
2019	88	90	4,63	4,66	0,79	0,80	0,01
2020	84	86	5,35	5,40	0,75	0,77	0,01
2021	81	82	6,03	6,10	0,72	0,73	0,01
2022	77	78	6,69	6,76	0,69	0,70	0,01
2023	73	75	7,32	7,40	0,65	0,67	0,01
2024	70	72	7,91	8,01	0,63	0,64	0,01
2025	67	68	8,49	8,60	0,60	0,61	0,01
2026	64	66	9,03	9,16	0,57	0,58	0,01
2027	61	63	9,56	9,69	0,55	0,56	0,01
2028	59	60	10,06	10,20	0,52	0,53	0,01
2029	56	57	10,53	10,69	0,50	0,51	0,01
2030	54	55	10,99	11,16	0,48	0,49	0,01
2031	51	53	11,43	11,61	0,46	0,47	0,01
2032	0	51	11,69	12,04	0,44	0,45	0,01
2033	0	0	11,69	12,14	0,26	0,43	0,17
						Total Additional Production	**0,35**

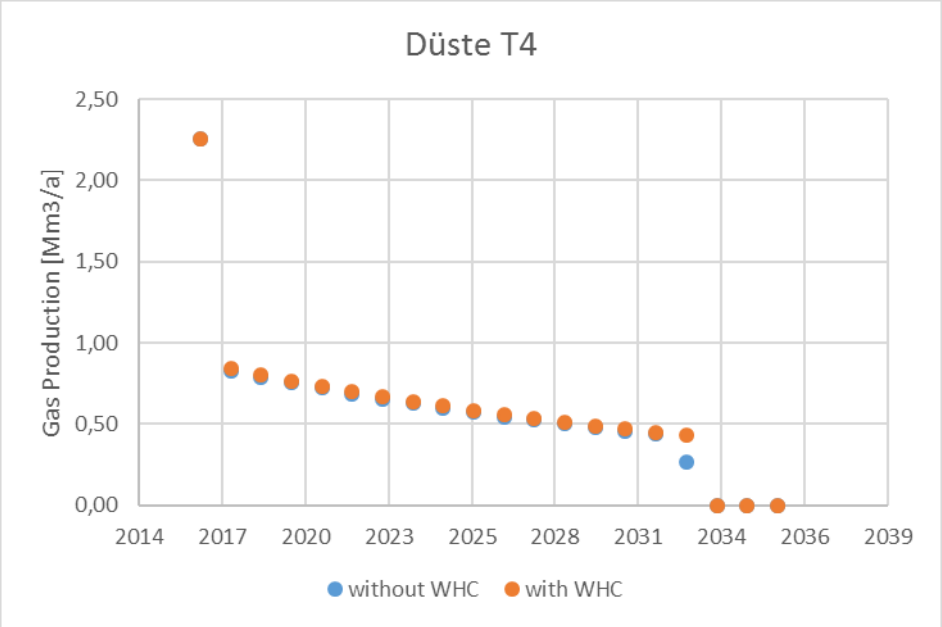

Figure 52: Annual Gas Production Forecast

Table 19: Annual Rates and Production for Düste Z7

Year	Average Gas Rate without WHC	Average Gas Rate with WHC	Cumulative Gas Production without WHC	Cumulative Gas Production with WHC	Annual Production without WHC	Annual Production with WHC	Additional Production
	[Sm³/h]	[Sm³/h]	[Mio Sm³]	[Mio Sm³]	[Mio Sm³]	[Mio Sm³]	[Mio Sm³]
2017	375	398	11,55	11,75	8,38	8,38	0,00
2018	363	386	14,62	15,01	3,17	3,36	0,19
2019	352	375	17,60	18,18	3,07	3,27	0,19
2020	342	364	20,50	21,27	2,98	3,17	0,19
2021	331	353	23,30	24,25	2,90	3,09	0,19
2022	321	343	26,02	27,15	2,80	2,99	0,18
2023	311	333	28,65	29,97	2,72	2,90	0,18
2024	302	323	31,21	32,71	2,63	2,82	0,18
2025	293	314	33,69	35,36	2,56	2,74	0,18
2026	284	305	36,09	37,94	2,48	2,65	0,18
2027	275	296	38,42	40,44	2,40	2,58	0,18
2028	267	288	40,68	42,88	2,33	2,50	0,18
2029	259	279	42,86	45,24	2,26	2,44	0,18
2030	251	271	44,98	47,53	2,19	2,36	0,17
2031	243	263	47,04	49,76	2,12	2,29	0,17
2032	236	256	49,04	51,93	2,06	2,23	0,17
2033	229	249	50,97	54,03	2,00	2,17	0,17
2034	222	242	52,84	56,07	1,93	2,10	0,17
2035	215	235	54,66	58,05	1,87	2,04	0,17
2036	208	228	56,43	59,98	1,82	1,98	0,17
						Total Additional Production	**3,39**

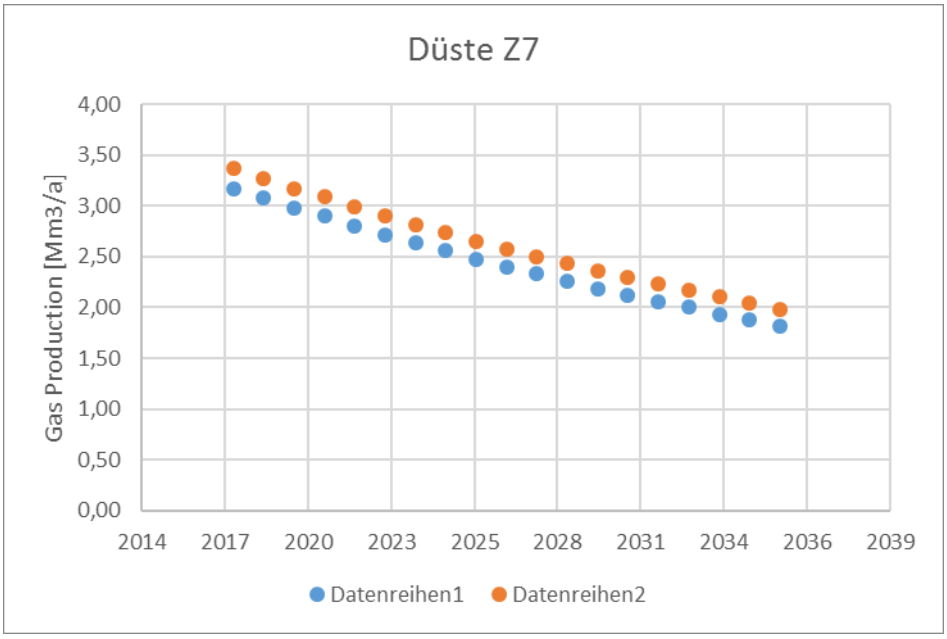

Figure 53: Annual Gas Production Forecast

Table 20: Annual Rates and Production for Düste Z8

Year	Average Gas Rate without WHC [Sm³/h]	Average Gas Rate with WHC [Sm³/h]	Cumulative Gas Production without WHC [Mio Sm³]	Cumulative Gas Production with WHC [Mio Sm³]	Annual Production without WHC [Mio Sm³]	Annual Production with WHC [Mio Sm³]	Additional Production [Mio Sm³]
2017	128	130	4,15	4,17	3,06	3,06	0,00
2018	121	123	5,19	5,22	1,10	1,12	0,02
2019	114	116	6,17	6,22	1,04	1,05	0,02
2020	108	110	7,10	7,16	0,98	1,00	0,02
2021	102	104	7,97	8,05	0,93	0,94	0,01
2022	96	98	8,79	8,89	0,87	0,89	0,02
2023	91	93	9,57	9,68	0,82	0,84	0,02
2024	86	88	10,30	10,43	0,78	0,79	0,02
2025	81	83	11,00	11,14	0,74	0,75	0,01
2026	77	78	11,66	11,81	0,70	0,71	0,01
2027	73	74	12,28	12,45	0,66	0,67	0,01
2028	69	70	12,87	13,05	0,62	0,64	0,02
2029	65	67	13,43	13,63	0,59	0,61	0,01
2030	62	63	13,96	14,17	0,56	0,57	0,01
2031	59	60	14,46	14,68	0,53	0,54	0,01
2032	56	57	14,93	15,17	0,50	0,52	0,01
2033	53	54	15,39	15,64	0,48	0,49	0,01
2034	50	52	15,81	16,08	0,45	0,46	0,01
2035	0	0	15,83	16,36	0,43	0,44	0,01
2036	0	0	15,83	16,36	0,02	0,28	0,27
						Total Additional Production	**0,53**

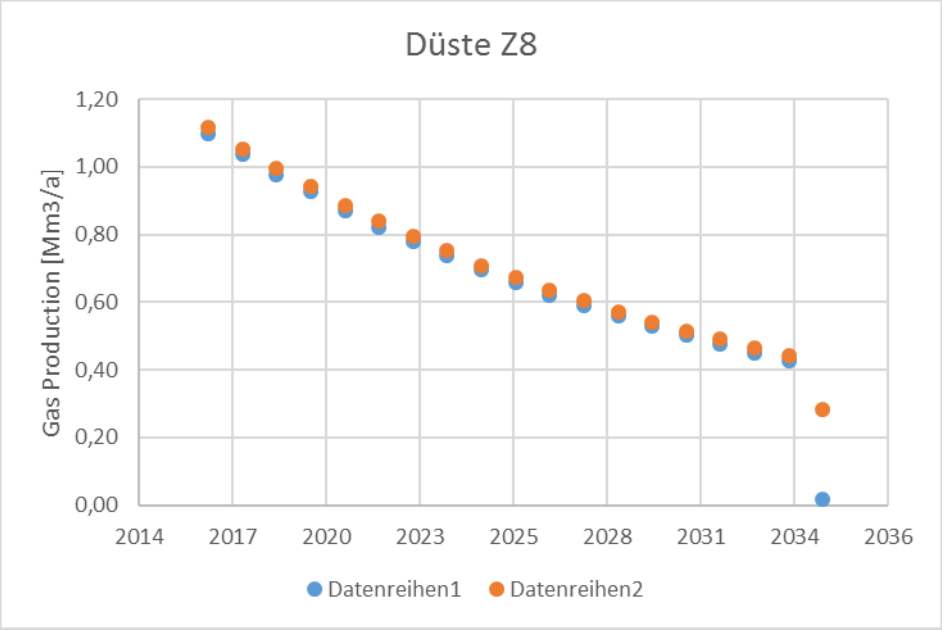

Figure 54: Annual Gas Production Forecast

Table 21: Annual Rates and Production for Staffhorst Z4

Year	Average Gas Rate without WHC [Sm³/h]	Average Gas Rate with WHC [Sm³/h]	Cumulative Gas Production without WHC [Mio Sm³]	Cumulative Gas Production with WHC [Mio Sm³]	Annual Production without WHC [Mio Sm³]	Annual Production with WHC [Mio Sm³]	Additional Production [Mio Sm³]
2017	477	635	5,16	6,79	4,04	5,34	1,29
2018	415	562	8,68	11,51	3,52	4,72	1,20
2019	363	498	11,75	15,69	3,07	4,18	1,11
2020	317	443	14,44	19,41	2,69	3,72	1,03
2021	279	395	16,79	22,72	2,35	3,31	0,96
2022	245	354	18,86	25,68	2,07	2,96	0,89
2023	224	319	20,70	28,34	1,84	2,66	0,82
2024	208	288	22,41	30,74	1,71	2,40	0,69
2025	0	262	23,21	32,91	0,80	2,17	1,37
2026	0	238	23,21	34,88	0,00	1,97	1,97
2027	0	218	23,21	36,68	0,00	1,80	1,80
2028	0	201	23,21	38,34	0,00	1,66	1,66
2029	0	0	23,21	38,60	0,00	0,26	0,26
2030	0	0	23,21	38,60	0,00	0,00	0,00
						Total Additional Production	**15,05**

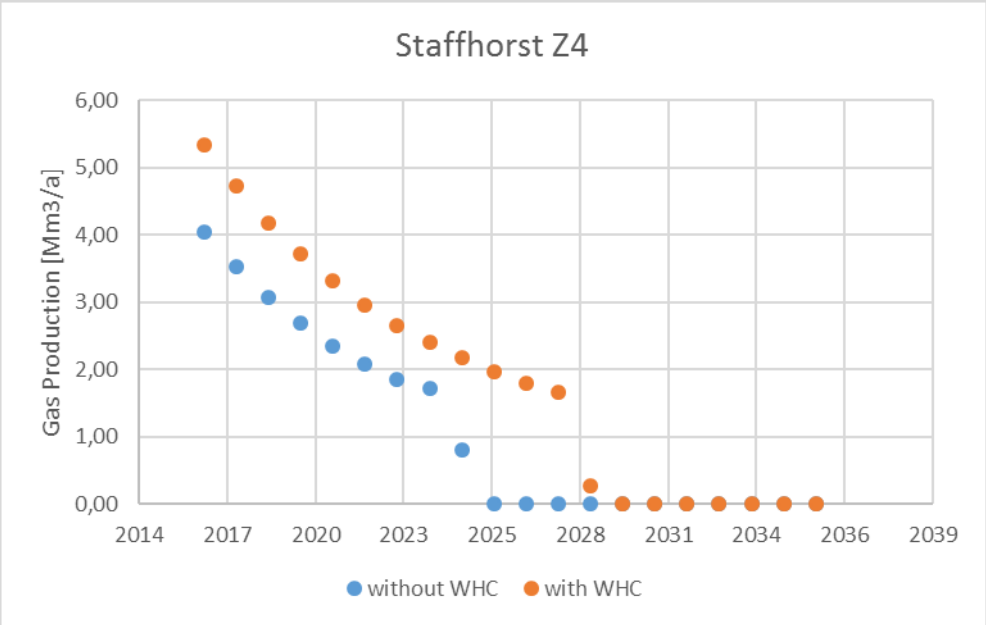

Figure 55: Annual Gas Production Forecast

Table 22: Annual Rates and Production for Staffhorst Z9

Year	Average Gas Rate without WHC [Sm³/h]	Average Gas Rate with WHC [Sm³/h]	Cumulative Gas Production without WHC [Mio Sm³]	Cumulative Gas Production with WHC [Mio Sm³]	Annual Production without WHC [Mio Sm³]	Annual Production with WHC [Mio Sm³]	Additional Production [Mio Sm³]
2017	460	658	5,04	7,06	3,94	5,55	1,61
2018	393	578	8,40	11,94	3,37	4,88	1,51
2019	336	510	11,28	16,23	2,88	4,29	1,42
2020	287	451	13,75	20,03	2,47	3,80	1,33
2021	246	400	15,85	23,38	2,11	3,35	1,25
2022	211	356	17,65	26,37	1,80	2,98	1,18
2023	0	319	18,26	29,03	0,61	2,67	2,06
2024	0	287	18,26	31,43	0,00	2,40	2,40
2025	0	259	18,26	33,59	0,00	2,16	2,16
2026	0	235	18,26	35,54	0,00	1,95	1,95
2027	0	214	18,26	37,31	0,00	1,77	1,77
2028	0	0	18,26	38,61	0,00	1,30	1,30
2029	0	0	18,26	38,61	0,00	0,00	0,00
						Total Additional Production	**19,93**

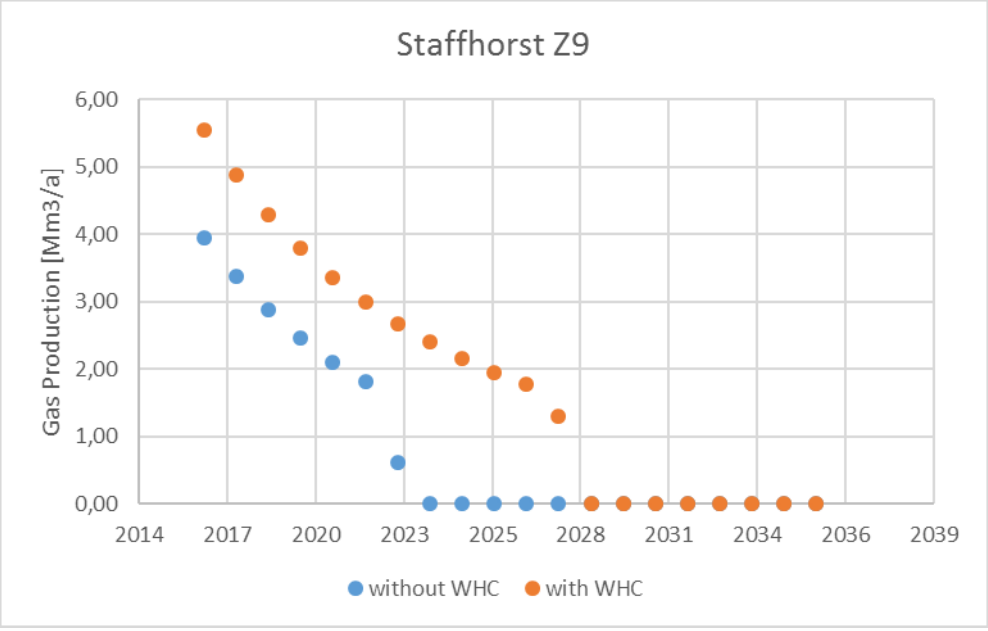

Figure 56: Annual Gas Production Forecast

Appendix D

Figure 57 shows the Ex-zone classification of the production site Staffhorst Z4.

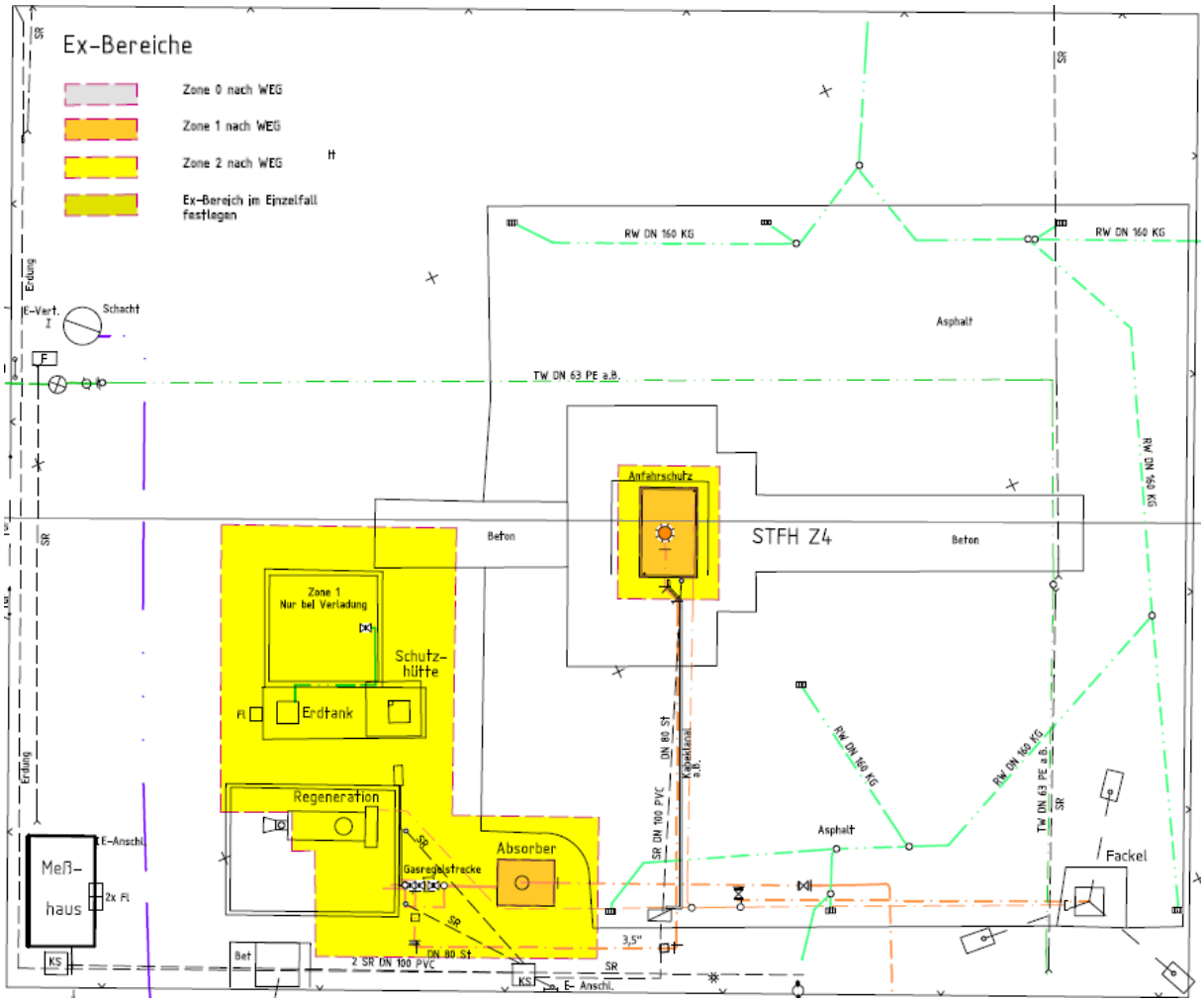

Figure 57: Ex- zones